NACA RM A55J11

NACA

RESEARCH MEMORANDUM

A STUDY OF LOCAL-PRESSURE FLUCTUATIONS RELATIVE TO STATIC-PRESSURE DISTRIBUTIONS ON TWO-DIMENSIONAL AIRFOILS AT HIGH SUBSONIC MACH NUMBERS

By Charles F. Coe

Ames Aeronautical Laboratory
Moffett Field, Calif.

NATIONAL ADVISORY COMMITTEE
FOR AERONAUTICS
WASHINGTON

December 21, 1955
Declassified October 14, 1957

NATIONAL ADVISORY COMMITTEE FOR AERONAUTICS

RESEARCH MEMORANDUM

A STUDY OF LOCAL-PRESSURE FLUCTUATIONS RELATIVE TO STATIC-PRESSURE DISTRIBUTIONS ON TWO-DIMENSIONAL AIRFOILS AT HIGH SUBSONIC MACH NUMBERS

By Charles F. Coe

SUMMARY

A study has been made relating local-pressure fluctuations to static-pressure distributions on six two-dimensional airfoils. Total-pressure fluctuations and the total-pressure loss in the wake of an NACA 65A008 airfoil have also been compared. Data were obtained for Mach numbers between about 0.59 and 0.90, with corresponding Reynolds numbers varying from about 6.3 million to 8.0 million.

The results of the study showed that certain relationships existed between the local-pressure fluctuations and the static-pressure distributions on two-dimensional airfoils and also between the total-pressure fluctuations and the total-pressure loss in the wake.

In general, it appears that the largest fluctuations of pressure coefficient on an airfoil occurred at the lower Mach numbers due to an intermittent building up and dropping of the pressure peak near the leading edge. Fluctuations of this type began and increased rapidly in magnitude when the peak static pressure stopped decreasing with increasing angle of attack. Since at the lowest test Mach number the pulsations over the entire chord approached the static pressures on the upper surface at the highest test angles of attack, it is suggested that the upper-surface static pressure could possibly serve as a rough estimate of the maximum fluctuations at high angles of attack.

The results show that when a strong normal shock wave was present, the maximum fluctuations occurred at the location of the shock wave due to its fore-and-aft motion, while fluctuations of pressure well ahead of and behind the shock wave were considerably less intense. The maximum fluctuations were generally approximately equal to but could be less than the static-pressure rise at the shock wave.

The maximum total-pressure fluctuations in the wake occurred where the pressure gradients were largest due, apparently, to the vertical movement of the wake. The results indicate that the maximum intensities of the pulsations may be approximately equal to the maximum time-average total-pressure loss.

INTRODUCTION

A study of local-pressure fluctuations on airfoils is of importance in determining or understanding the nature of the lift fluctuations which buffet airplanes. In previous investigations, studies have been made on two-dimensional airfoils of the effects of airfoil geometry on local-pressure fluctuations (refs. 1 and 2) and on fluctuations of section normal force and pitching moment (refs. 3, 4, and 5). Work has also been done to study total-pressure fluctuations in the wakes of airfoils (ref. 6).

In reference 3, it was noted that two principal types of pressure pulsations were apparent which can be associated with buffeting: pulsations which arise from intermittent building up and dropping of the leading-edge pressure peak, and pulsations which are attributable to shock-wave motion and unsteady air flow following the shock wave. The present investigation, which was conducted in conjunction with the work reported in reference 3, is concerned primarily with a detailed study of the possible relationship between local-pressure fluctuations and static-pressure distributions and, secondarily, with an analysis of total-pressure fluctuations in the wake of an airfoil relative to the total-pressure loss.

SYMBOLS

P time-average static-pressure coefficient, $\frac{p-p_o}{q_o}$

P_{cr} critical pressure coefficient

P_d differential-pressure coefficient between upper and lower surface at the same chordwise station

ΔP_d coefficient of the fluctuation of differential pressure determined from an average of the largest three peak-to-peak measurements

δP_d coefficient of the average change in differential-pressure measurements taken between the limits of time which bracket Δc_n and ΔP_d measurements

c_n section normal-force coefficient

Δc_n one-half the average of the largest three peak-to-peak fluctuations of section normal-force coefficient

$\frac{h}{q_o}$ time-average total-pressure coefficient

$\frac{\Delta h}{q_o}$ average of the largest three peak-to-peak fluctuations of total-pressure coefficient

$\frac{\delta h}{q_o}$ average of the differences of total-pressure coefficient measured between limits of time which bracket maximum $\Delta h/q_o$ measurements

M free-stream Mach number

c airfoil chord

h total-pressure loss in the wake

p local static pressure

p_o free-stream static pressure

q_o free-stream dynamic pressure

α angle of attack

APPARATUS AND INSTRUMENTATION

Wind Tunnel

The tests were conducted in a two-dimensional channel in the Ames 16-foot high-speed wind tunnel. A description of the channel, which was formed by two walls 18.5 inches apart, may be found in reference 6. Figure 1 shows the channel, a model, and the rake installation.

Models

Sketches of the section profiles investigated are shown in figure 2. The airfoils used were the same as those of reference 3, and had 2-foot chords and approximately 18-1/4-inch spans. Spaces between the models and the mounting walls were sealed with felt on one side and with a spring-loaded seal on the other. The models were of rigid construction. Those having thickness ratios of 12 percent and 8 percent were wood with steel reinforcing, while the thinner models were aluminum.

Instrumentation

The installation of flush-diaphragm-type electrical pressure cells in the models was the same as described in reference 3. The pressure cells and related electrical equipment are described in reference 7. A sketch of a typical model showing the arrangement of pressure cells and orifices from which time-average static pressures were measured is given in figure 3. Thirty cells and static-pressure orifices were distributed over both the upper and lower surfaces at 15 chordwise stations. The upper- and lower-surface pressure cells were mounted in matched pairs and were connected electrically so that only the fluctuations of differential pressure were recorded at each station. The reference pressure at the back of each pressure cell in the models was the static pressure at the adjacent orifice.

To measure fluctuations of total pressure in the wake of the NACA 65A008 airfoil, a rake of 1/4-inch-diameter pressure cells was constructed. The cells were installed in 5/16-inch-diameter tubing with the diaphragms recessed approximately 1/16 inch back from the opening. Photographs showing details of the rake are presented in figure 4. Near the center of the rake the tubes containing pressure cells were spaced at intervals equal to 2-1/2 percent of the airfoil chord. In addition to the pressure cells, open-ended tubes were also installed with a spacing of 0.025c for measuring the time-average total-pressure loss in the wake. The rake was mounted 0.75c behind the trailing edge of the airfoil on a sting support which could be adjusted vertically so that the center of the rake could be positioned near the center of the wake. The reference pressure for the cells in the rake was free-stream total pressure.

Time-average pressures, that is, the indicated static pressures on the airfoils and the total pressures in the wake, were recorded photographically from mercury-in-glass manometers.

Electrical responses from each pair of pressure cells in the models and from each cell in the rake were recorded on oscillographs. For the pressure cells in the models the amplitude response of the galvanometer elements used was flat to about 60 cycles per second, then dropped to about 50 percent of that amplitude at 170 cps. The response of the elements used for the wake survey was flat to approximately 500 cps. Although the frequency response of the elements used for the models was rather limited, it is believed that it was adequate. Good agreement was obtained for the chordwise distribution of pressure fluctuations for a few duplicate tests using the 500 cps elements from the wake survey.

PROCEDURE

Range of Test Variables

For this investigation, which was conducted in conjunction with the work reported in reference 3, data were analyzed over a Mach number range from about 0.59 to 0.90. The Reynolds number based on the airfoil chord varied with increasing Mach number from about 6.3 million to 8.0 million. The angle-of-attack range was from near 0° to the maximum that was within the strength limits of each model.

Reduction of Data

Static calibrations of each pair of pressure cells on the models and of each cell on the rake were made before and after each run.

The intensity of the maximum fluctuations of pressure on the airfoils and of the total pressures in the wake was computed from a record of approximately 1-second duration by averaging the three largest measurements of peak-to-peak heights on the corresponding oscillograph trace (see fig. 5). In addition, to check for possible phase relationships, the pressure change was determined for each trace from the average of the displacements between the same limits of time which bracketed each of the three peak-to-peak measurements of the trace for Δc_n, or the three peak-to-peak measurements of a trace for ΔP_d. For the wake, measurements of the pressure change were made between the limits of time which bracketed each of the three measurements on a trace for $\Delta h/q_o$.

Mach numbers were corrected for constriction effects by the methods of reference 8. Since the airfoils were symmetrical, a correction was applied to the angles of attack at each Mach number so that the faired normal-force curve passed through $c_n = 0$ at $\alpha = 0$. No other corrections were applied to the data.

RESULTS AND DISCUSSION

Local-Pressure Fluctuations on the Models

Figures 6 through 11 show the local fluctuations of pressure and the time-average static-pressure distributions at various Mach numbers and angles of attack. Two principal types of pressure pulsations which are associated with buffeting forces are evident as indicated in reference 3. These are pulsations which arise from intermittent building up and dropping of the pressure peak near the leading edge, and pulsations which are

attributable to shock-wave motion and to unsteady air flow following the shock wave. The net effect of the local pulsations is the fluctuations of normal-force coefficient shown in figure 12, which is reproduced, in part, from reference 3.

Pulsations of the pressure peak near the leading edge.- Examination of the local-pressure fluctuations (figs. 6 to 11) shows that the largest pulsations occurred near the leading edge at the lower test Mach numbers. The angles of attack at which these large pulsations occurred varied with the profile. Generally the pulsations occurred at lower angles as the leading-edge radius was reduced. It may also be noted at the lower Mach numbers that as the highest test angles of attack were reached the pulsation intensities increased to about 50 or 100 percent of the upper-surface time-average pressure over most of the airfoil chord. (See figs. 6(a), 7(a), 8(a), 8(b), 9(a), and 10(a).) The fact that the variation of the intensities along the chord appears to have become similar to the variation of the static pressure suggests that the upper-surface static pressure could possibly serve as a rough estimate of the maximum fluctuations near maximum lift.

Figure 13 was prepared to determine whether relationships exist between the pressure pulsations and the variations of the time-average pressures with angle of attack. This figure presents the differential-pressure fluctuations and the upper-surface static-pressure coefficient at each station as a function of angle of attack for one Mach number near 0.6 for each airfoil. Since the variation with angle of attack of static pressure on the lower surface was small (see figs. 6 to 11), the fluctuations of pressure would also have a similar relationship to the variations of the local load with positive angle of attack.

Examination of figure 13 discloses that the pulsations near the leading edge generally began and increased rapidly when the time-average pressure stopped decreasing with increasing angle of attack. The maximum local intensities on the NACA $65_{(06)}$A004 and 877A008 airfoils reached magnitudes which were higher than the measured time-average pressures at the same stations. It is interesting to note in figures 13(a), (b), (c), and (e) that after the maximum intensity was reached the intensities of the fluctuations decreased with further increase in angle of attack. Also, as previously pointed out in connection with figures 6 to 11, the intensities of the pulsations over the entire airfoil chord generally approached the time-average pressures on the upper surface at the highest test angles of attack.

Figure 13 also shows that the large pulsations near the leading edge may have caused disturbances that passed other stations downstream and which bore no apparent relationship to the upper-surface time-average static pressures at these other stations. For example, for the $65_{(06)}$A004 airfoil (fig. 13(c)), a rise in intensity took place at $\alpha = 5.7^{\circ}$ at

stations downstream from 1.25-percent chord where the time-average pressure was still decreasing with increasing angle of attack.

Pressure pulsations at the shock wave.- In figures 6 through 11 it can be seen that at the higher speeds, relationships also existed between the pressure pulsations and the time-average pressures. The most significant pulsations at the higher speeds occurred at the locations of the shock waves, while the pulsations ahead of and behind the shock waves were considerably less intense. Typical examples are shown in figures 6(d), 7(e), 8(f), 9(e), 10(e), and 11(e). For some conditions where the shock waves occurred at different stations on both upper and lower surfaces, large fluctuations usually occurred at both stations (see figs. 6(e), 9(e), and 10(f)).

Since it is considered that the primary pulsations at a shock wave were due to its fore-and-aft motion and the consequent shifting of the pressure rise, it can be noted, as in figures 6(d), 7(e), 8(g), 9(e), 10(f), and 11(e), that when the limits of the pressure rise were well defined and the shock wave crossed a pressure cell, the maximum pressure fluctuations were approximately equal to the time-average static-pressure rise. When the shock wave was between pressure cells and did not cross one (such as in figs. 6(b), 9(d), and 10(e)), the maximum fluctuation intensity on the airfoil may not have been measured.[1] It also appears from the results that, for the type of pressure distribution shown in figures 7(c) and 8(d), the maximum fluctuations may have actually been smaller than the static-pressure rise through the shock wave, although the pressure-cell spacing may account for part of the lower measured maximum fluctuations. Where these lower maximum fluctuations occurred the pressure distributions are generally characterized by a large expansion at the leading edge followed by a compression region ahead of the primary shock wave.

Effect of peak pressure fluctuations on fluctuations of normal-force coefficient.- Since the largest fluctuations of pressure generally occurred in peaks near the leading edge or at the shock wave, the oscillograph records were examined to determine whether there was a consistent influence of the intensity at the peaks on the summed fluctuations of normal-force coefficient. Figure 14 shows how the average change in differential-pressure coefficient, δP_d, varied along the chord for a few selected cases which are representative of the variety and extremes of the influences that were observed. Where large pressure fluctuations occurred at two different stations due to shock waves on both upper and lower surfaces, curves are shown for both peaks. Examination of figure 14 shows that the influence of the peak local fluctuation on the summed result was inconsistent. For example, on the NACA 65A012 airfoil (fig. 14(a)) at $M = 0.79$

[1]This indicates the importance of pressure-cell spacing for this type of instrumentation. Scatter in the measurements of Δc_n could result if unmeasured fluctuations happened to represent a significant portion of the unsteady force.

the maximum normal-force fluctuations were due almost entirely to the pressure changes which were apparently in phase with the shock-wave motion. On the other hand, for the NACA 65A008 airfoil, the maximum normal-force fluctuations resulted primarily from small pressure changes along the chord which were not in phase with the shock-wave motion (fig. 14(b)). Where a shock wave occurred on both the upper and lower surfaces (figs. 14(a), (d), and (e)) it appears that the pressure change due to the shock-wave motion on the upper surface (peak closest to the leading edge) had the larger influence on Δc_n.

Total-Pressure Fluctuations in the Wake of an NACA 65A008 Airfoil

Fluctuations of the total pressure and the average total-pressure loss in the wake of the NACA 65A008 airfoil are shown in figure 15. Examination of figure 15 shows that there was a tendency toward the occurrence of double peaks in the variation of $\Delta h/q_o$ above and below the extended wing-chord plane similar to the results shown in reference 6. Where the two peaks were clearly measured, they appeared on each side of the maximum total-pressure loss in the regions where the total-pressure gradients were large. It is also interesting to note in figure 15 that significant fluctuations of the total pressure occurred even at the lower angles of attack where the normal-force fluctuations were negligible as shown by figure 12.

Since it is believed that the maximum intensities of $\Delta h/q_o$ were not always measured and that peaks may have occurred between cell stations, the need for closer pressure-cell spacing in the region of the maximum total-pressure gradients is indicated. For example, in figures 15(a) and 15(d) possible variations from the original fairing have been sketched with dashed lines.

Comparison of the intensities of the double peaks that were measured and the maximum total-pressure losses in the wakes suggests that, in addition to showing the relative locations of the peaks, the maximum total pressure may possibly serve as a reasonable approximation of the maximum fluctuation intensities. If the wake is fluctuating vertically, reasoning similar to that involving the pressure changes due to shock-wave motion may be used. Thus, the maximum pressure fluctuations would occur where the pressure gradients are largest and, if the motion was sufficient, the fluctuations could be approximately equal to the maximum time-average total-pressure loss.

In an effort to determine whether the wake was fluctuating vertically, figure 16 was prepared to show how the total pressure was varying at each station between the limits of time for the readings of the fluctuations at each of the two peaks. The measurements indicate only the difference

in total pressure at two instants of time, with the positive or negative signs corresponding to an increase or decrease in pressure. The fact that the values of $\delta h/q_o$ pass through zero does not indicate that the pressure was steady, but that at the two instants of time selected the total pressure returned to the same value. Results are presented for only the Mach numbers and angles of attack at which the most outstanding double peaks were measured. The subscripts in the symbol legend for the two curves showing $\delta h/q_o$ indicate the $\Delta h/q_o$ measurements from which the time limits were established.

Figure 16 shows that the pressure changes measured between the limits of time established by the two peaks were not in phase with one another. Generally, when the pressure was increasing to its maximum intensity at the location of one peak, it was decreasing at the location of the other peaks, a fact which suggests that the instantaneous wake was fluctuating vertically.

CONCLUSIONS

A study has been made relating local-pressure fluctuations and time-average pressure distributions on two-dimensional airfoils at high subsonic speeds. Total-pressure fluctuations and total-pressure loss in the wake of an NACA 65A008 airfoil have also been compared. The results of the study have indicated that the following relationships existed for the test Mach number range of about 0.59 to 0.90.

1. In general, the largest fluctuations of pressure coefficient occurred at the lower Mach numbers due to an intermittent building up and dropping of the pressure peak near the leading edge. They began and increased rapidly in magnitude when the static pressure on the upper surface stopped decreasing with increasing angle of attack.

2. Since at the lowest test Mach number the pulsations over the entire chord approached the static pressures on the upper surface at the highest test angles of attack, it is suggested that the upper-surface static pressure could possibly serve as a rough estimate of the maximum fluctuations at high angles of attack.

3. When a strong normal shock wave was present the maximum fluctuations occurred at the location of the shock wave due to its fore-and-aft motion, while the fluctuations ahead of and behind the shock wave were considerably less intense.

4. The maximum intensity of the fluctuations at the shock wave was, in general, approximately equal to the static-pressure rise. The intensity of the fluctuations could be lower than the static-pressure rise, however,

when the static-pressure distribution showed a negative-pressure peak near the leading edge with a compression region ahead of the shock wave.

5. The maximum total-pressure fluctuations in the wake occurred where the pressure gradients were largest, due to apparent vertical movement of the wake. The results indicate that the maximum intensities of the pulsations may be approximately equal to the maximum time-average total-pressure loss.

Ames Aeronautical Laboratory
National Advisory Committee for Aeronautics
Moffett Field, Calif., Oct. 11, 1955

REFERENCES

1. Humphreys, Milton D.: Pressure Pulsations on Rigid Airfoils at Transonic Speeds. NACA RM L51I12, 1951.

2. Humphreys, Milton D., and Kent, John D.: The Effects of Camber and Leading-Edge-Flap Deflection on the Pressure Pulsations on Thin Rigid Airfoils at Transonic Speeds. NACA RM L52G22, 1952.

3. Coe, Charles F., and Mellenthin, Jack A.: Buffeting Forces on Two-Dimensional Airfoils as Affected by Thickness and Thickness Distribution. NACA RM A53K24, 1954.

4. Polentz, Perry P., Page, William A., and Levy, Jr., Lionel L.: The Unsteady Normal-Force Characteristics of Selected NACA Profiles at High Subsonic Mach Numbers. NACA RM A55C02, 1955.

5. Humphreys, Milton D.: Measurements of Normal-Force-Coefficient Fluctuation on Four 9-Percent-Thick Airfoils Having Different Locations of Maximum Thickness. NACA RM L54B22, 1954.

6. Sorenson, Robert M., Wyss, John A., Kyle, James C.: Preliminary Investigation of the Pressure Fluctuations in the Wakes of Two-Dimensional Wings at Low Angles of Attack. NACA RM A51G10, 1951.

7. Erickson, Albert L., and Robinson, Robert C.: Some Preliminary Results in the Determination of Aerodynamic Derivatives of Control Surfaces in the Transonic Speed Range by Means of a Flush-Type Electrical Pressure Cell. NACA RM A8H03, 1948.

8. Allen, H. Julian, and Vincenti, Walter G.: Wall Interference in a Two-Dimensional-Flow Wind Tunnel, With Consideration of the Effect of Compressibility. NACA Rep. 782, 1944.

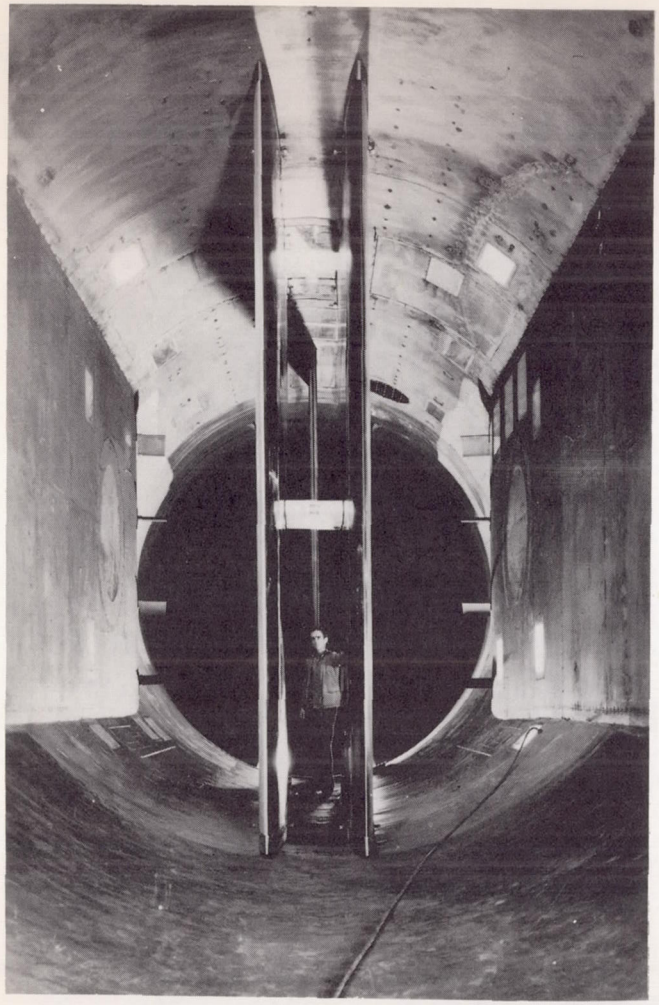

A-14566

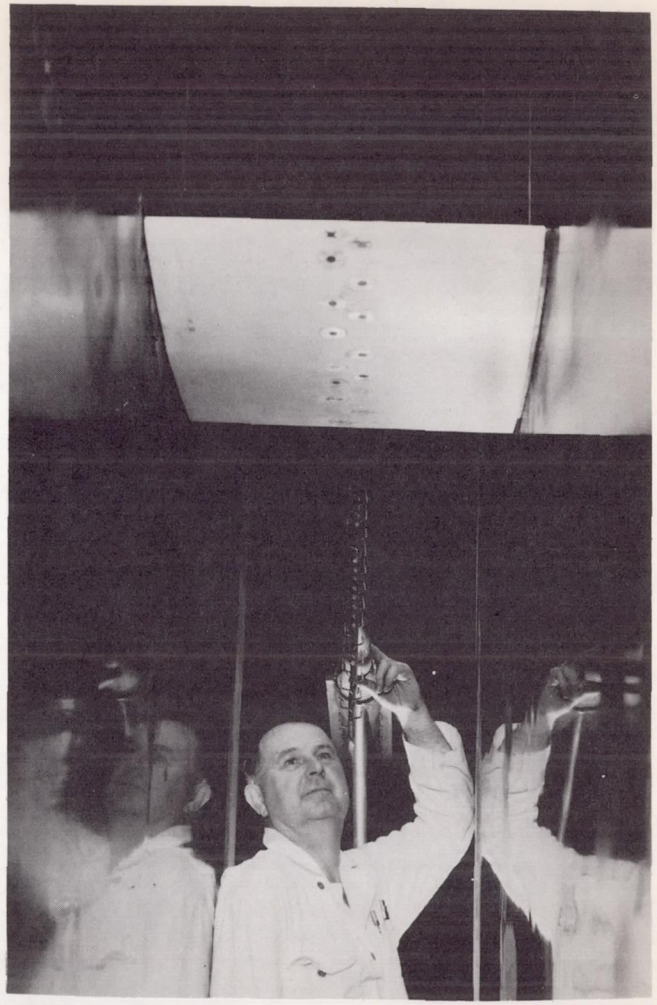

A-17210

Figure 1.- Views of the two-dimensional channel in the 16-foot high-speed wind tunnel showing a model and the rake installation.

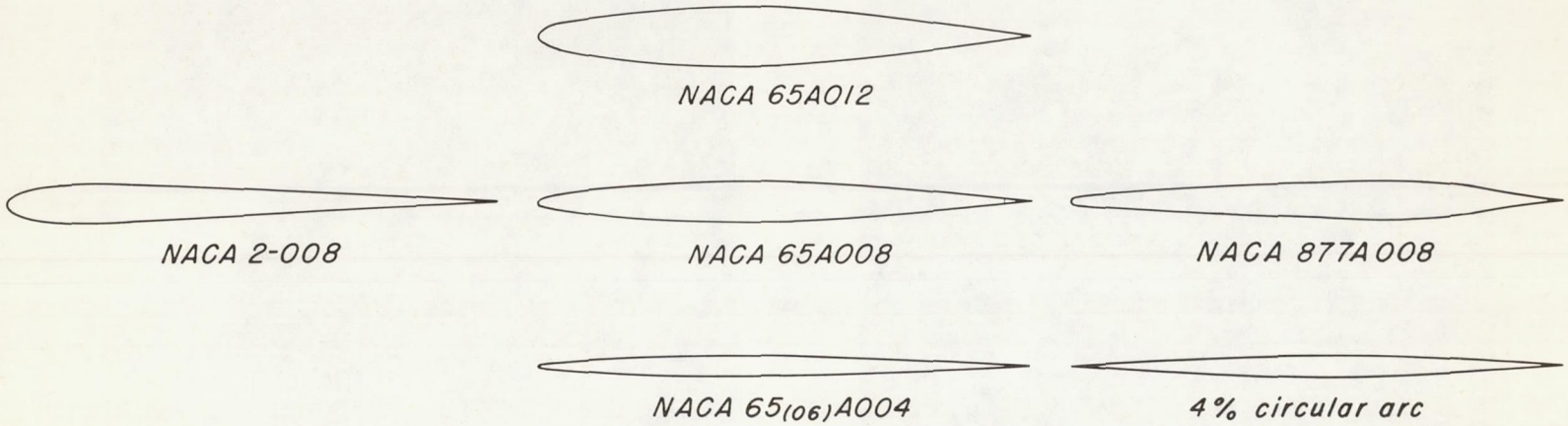

Figure 2.- Section profiles of the models investigated.

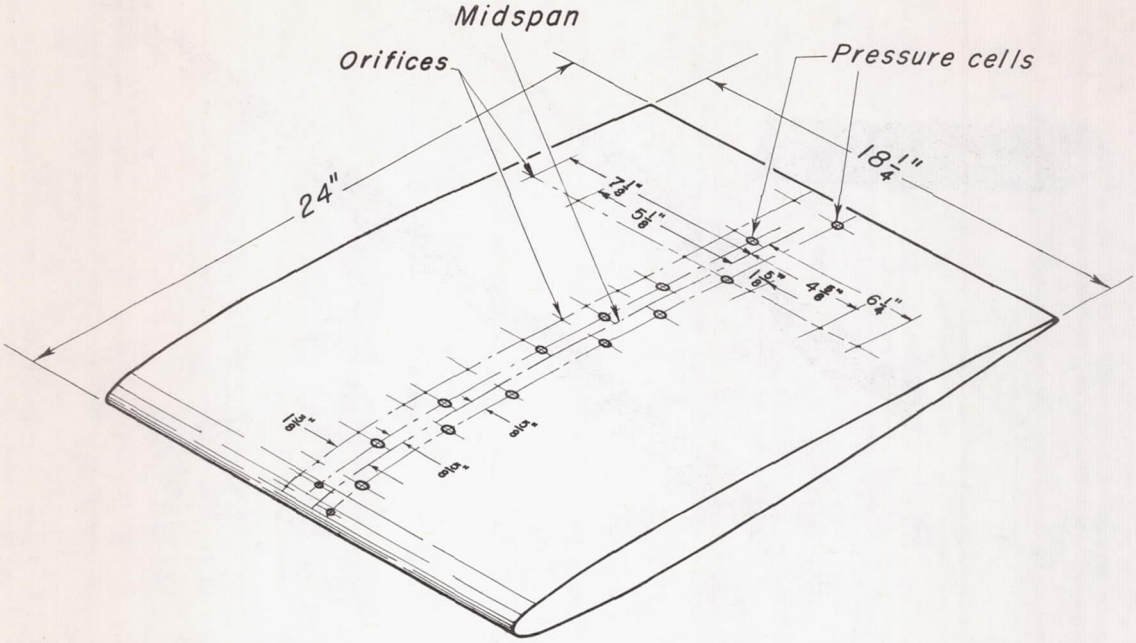

MODEL PRESSURE-CELL AND ORIFICE LOCATIONS
[In percent of model chord]

Cell and orifice number	65A012 and 65A008	65(06)A004 2-008 877A008	4-percent circular arc
1	1.25	1.25	5
2	3.75	3.75	10
3	7.5	7.5	15
4	15	15	22.5
5	22.5	22.5	27.5
6	27.5	27.5	35
7	35	35	45
8	45	45	52.5
9	52.5	52.5	57.5
10	57.5	57.5	62.5
11	62.5	62.5	67.5
12	67.5	67.5	75
13	75	75	85
14	85	85	90
15	95	90	95

Figure 3.- Sketch of a typical model with a table of the pressure-cell and orifice locations for all the models.

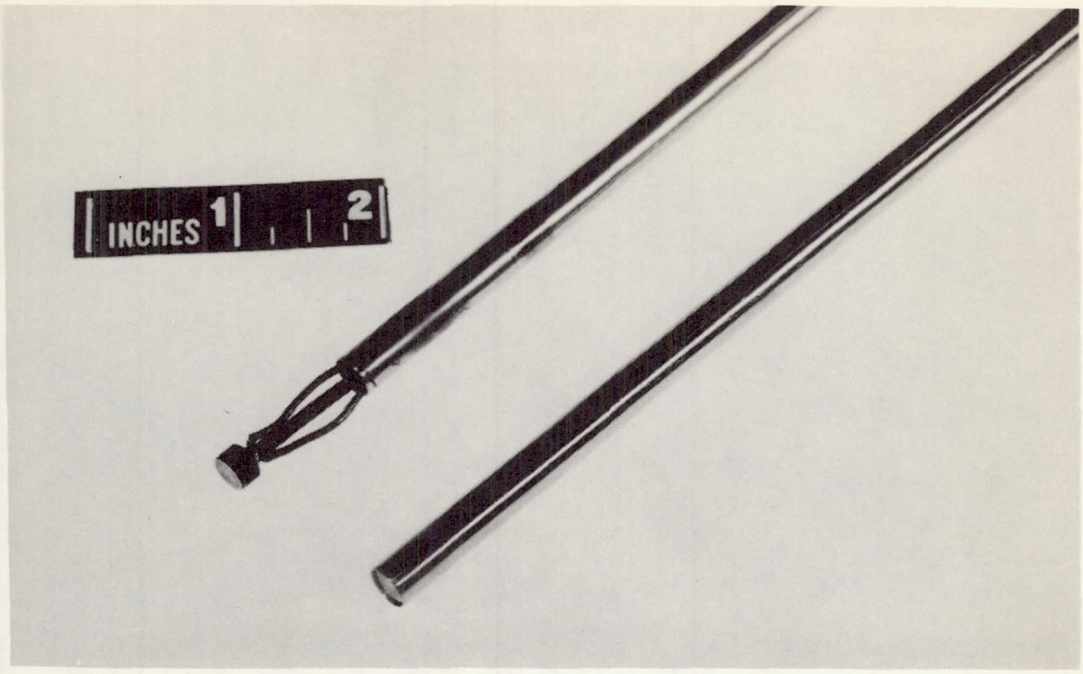

(a) Pressure-cell installation. A-17237

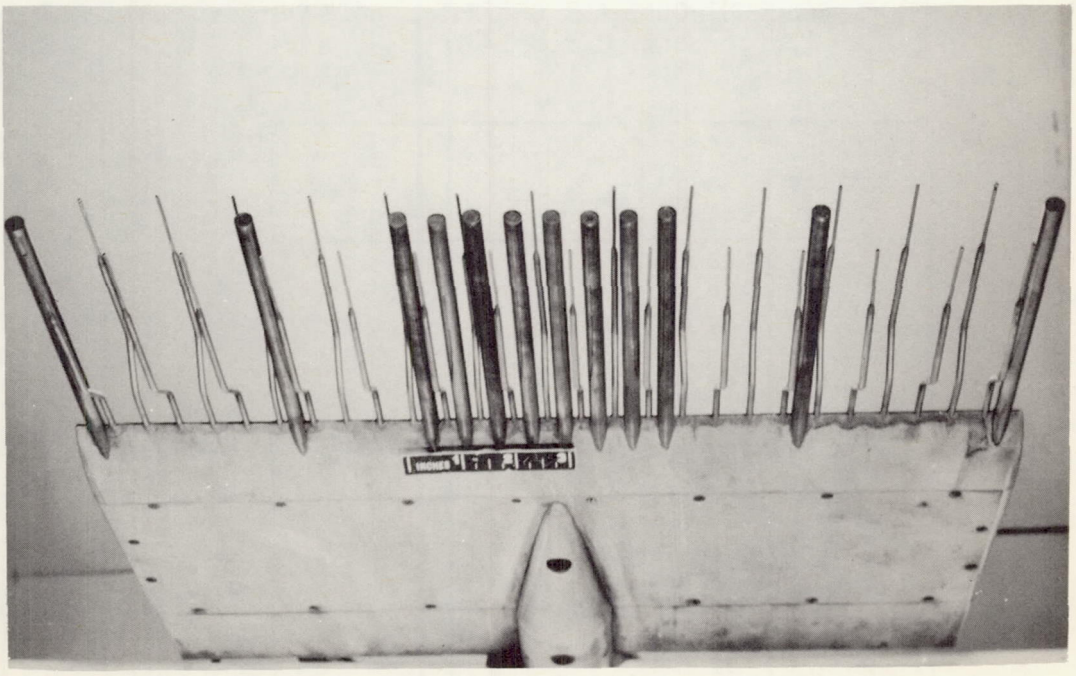

(b) Rake. A-19653

Figure 4.- Photographs showing details of the rake and pressure-cell installation.

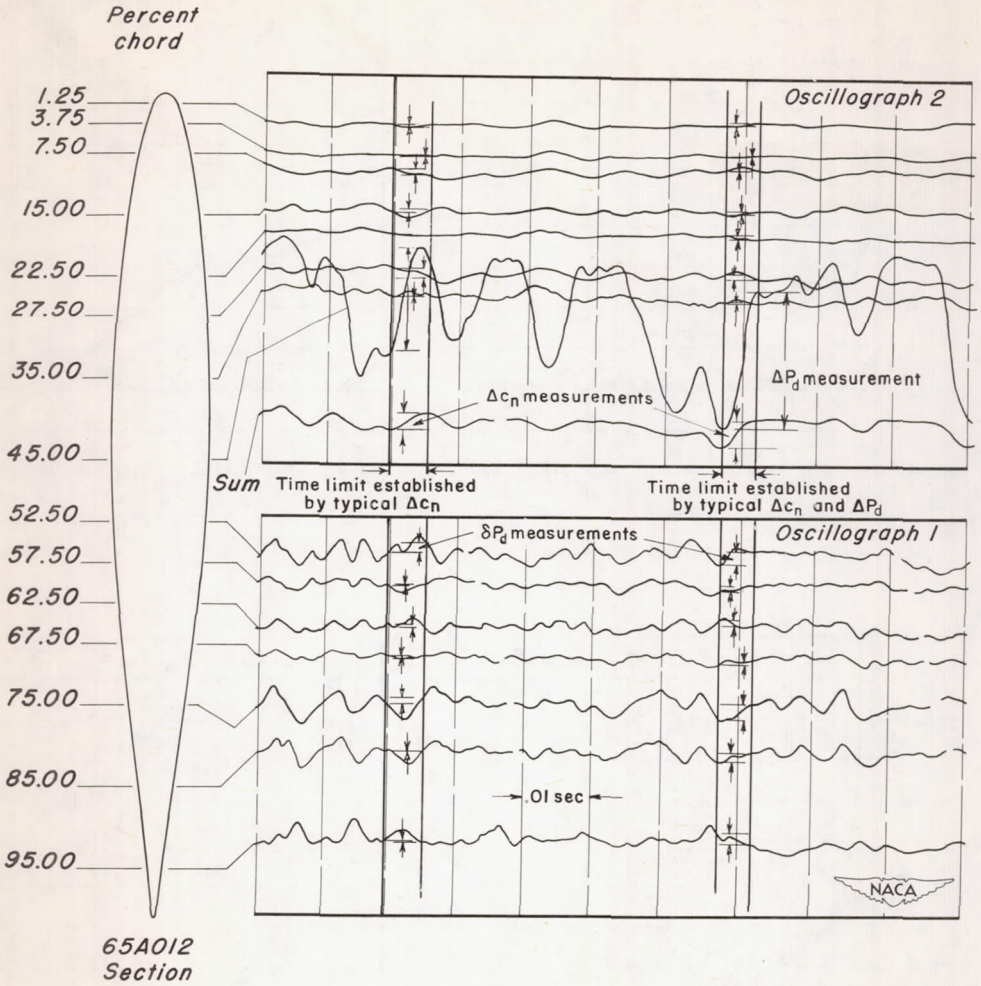

NACA 65A012; M, 0.79; α, 4.2.

Figure 5.- Sample oscillograph record illustrating methods of analyzing measurements.

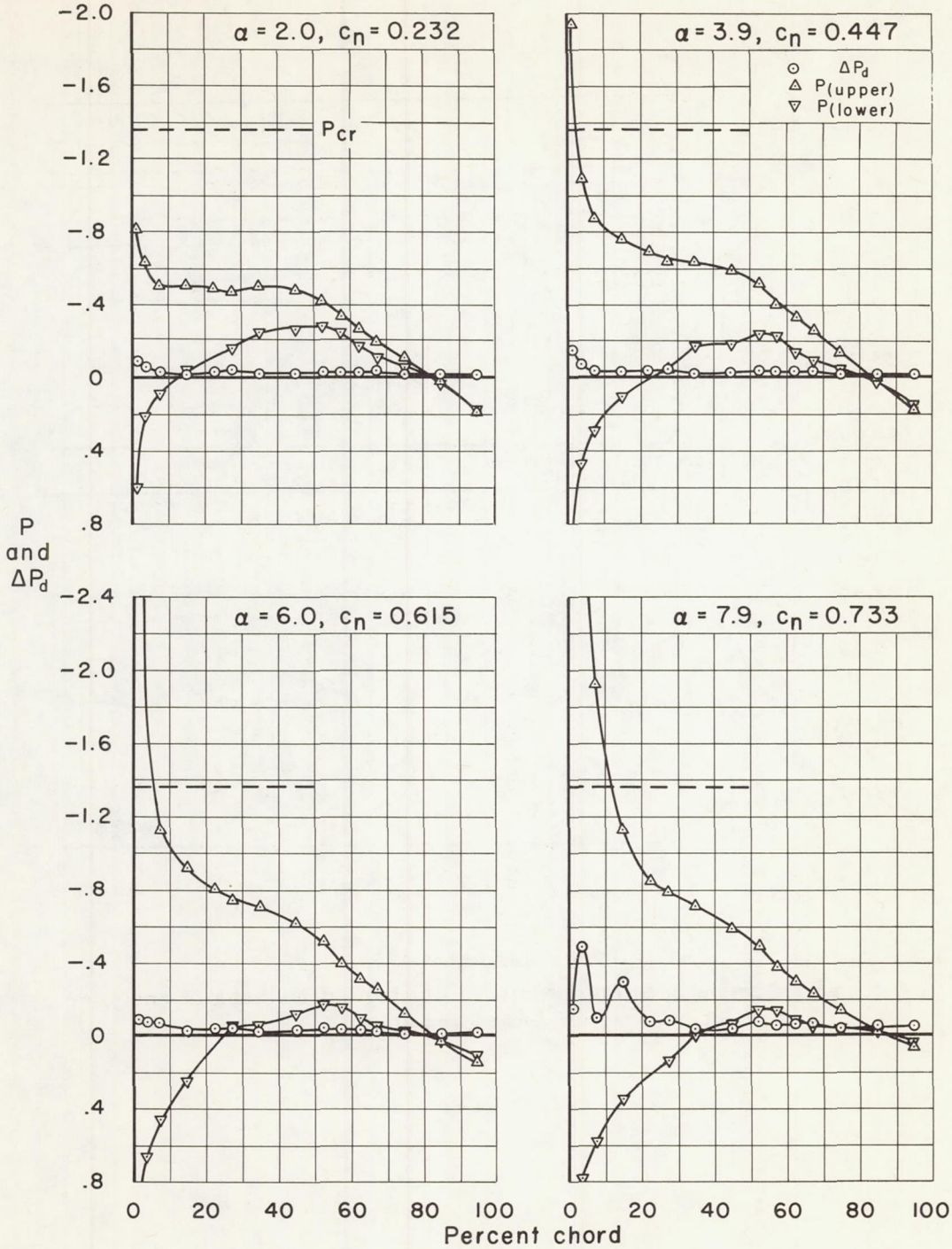

(a) M = 0.59.

Figure 6.- Local-pressure fluctuations and time-average static-pressure distributions for the NACA 65A012 airfoil.

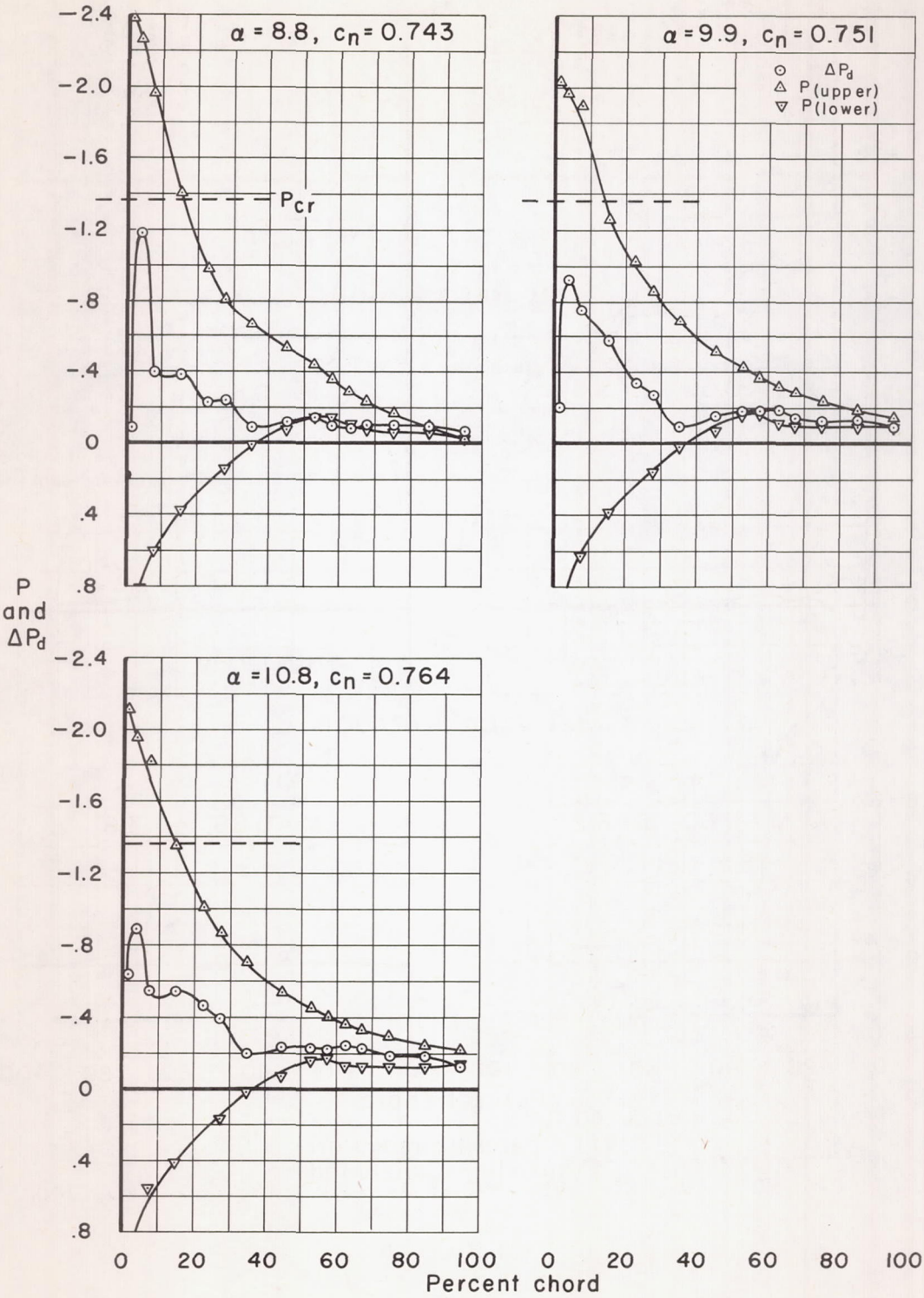

(a) M = 0.59 concluded.
Figure 6.- Continued.

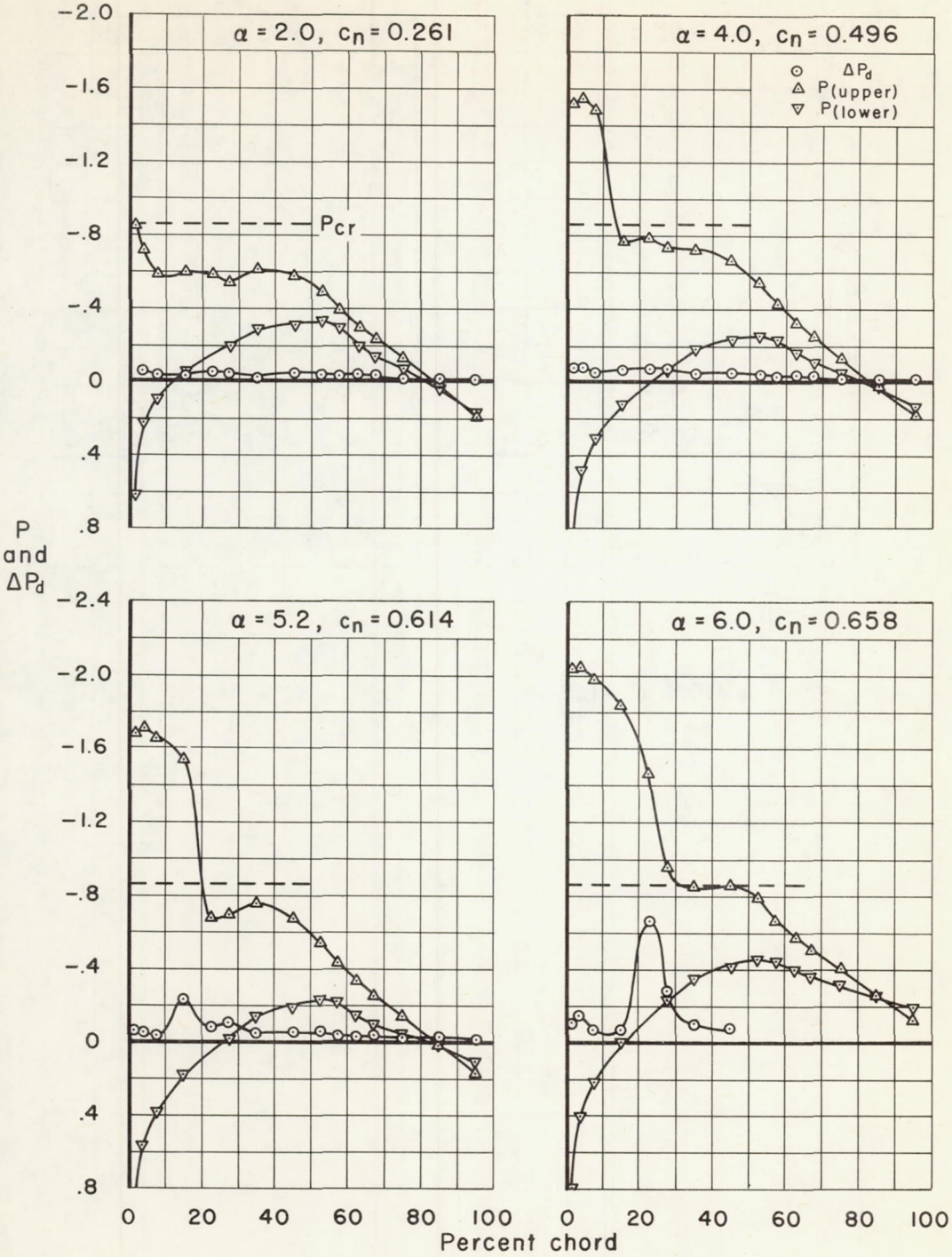

(b) M = 0.68.
Figure 6.- Continued.

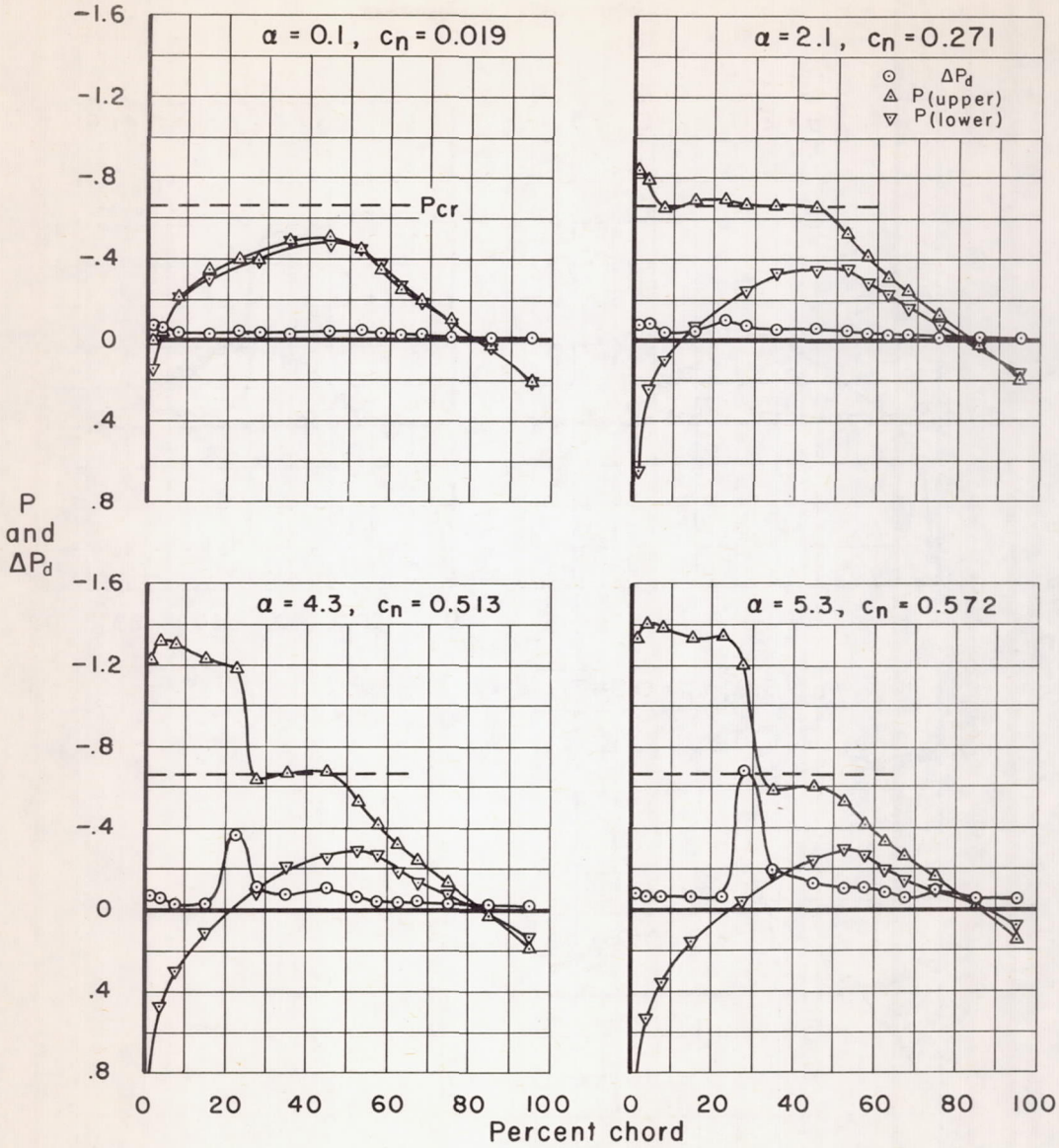

(c) M = 0.73.

Figure 6.- Continued.

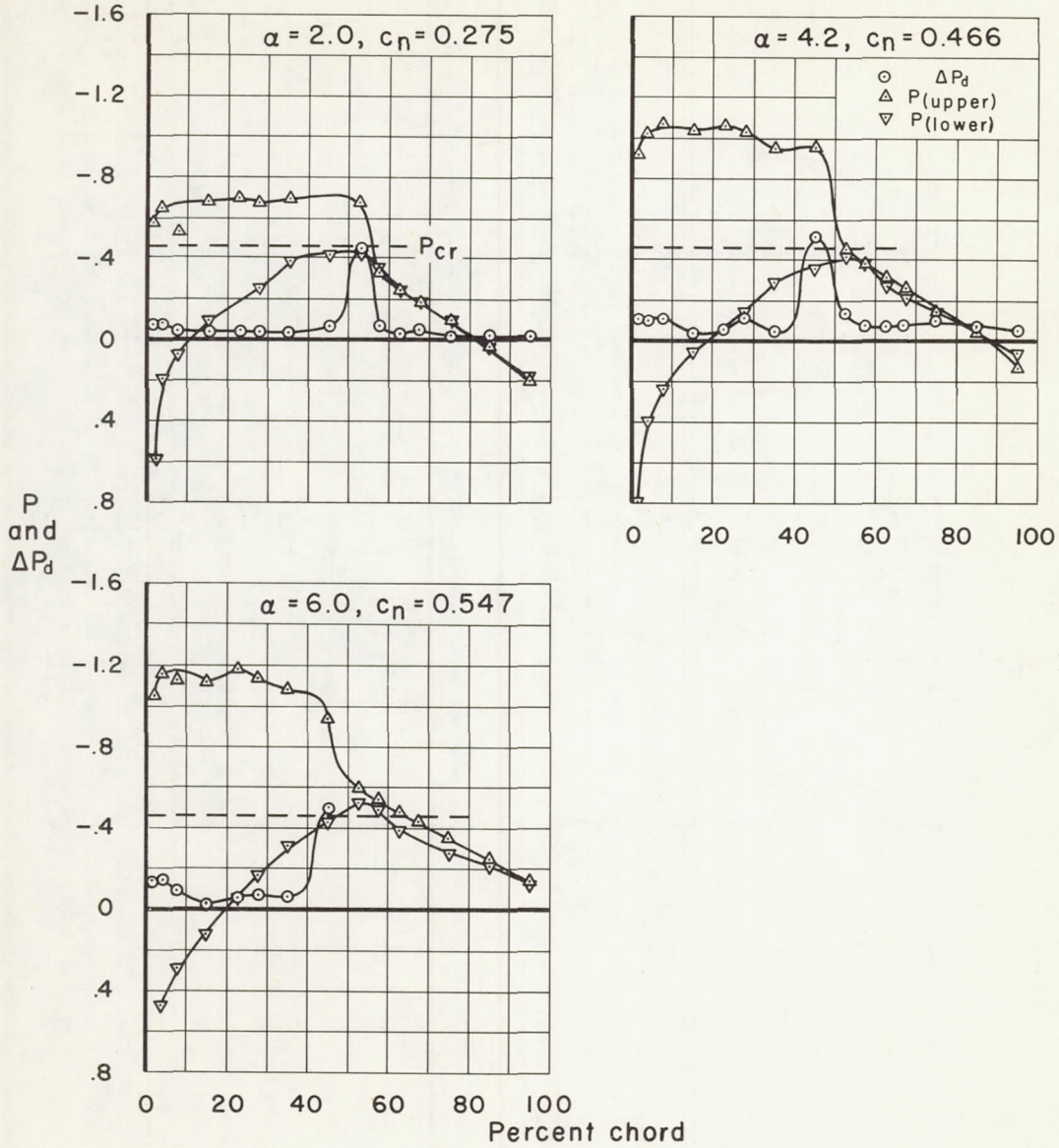

(d) M = 0.79.

Figure 6.- Continued.

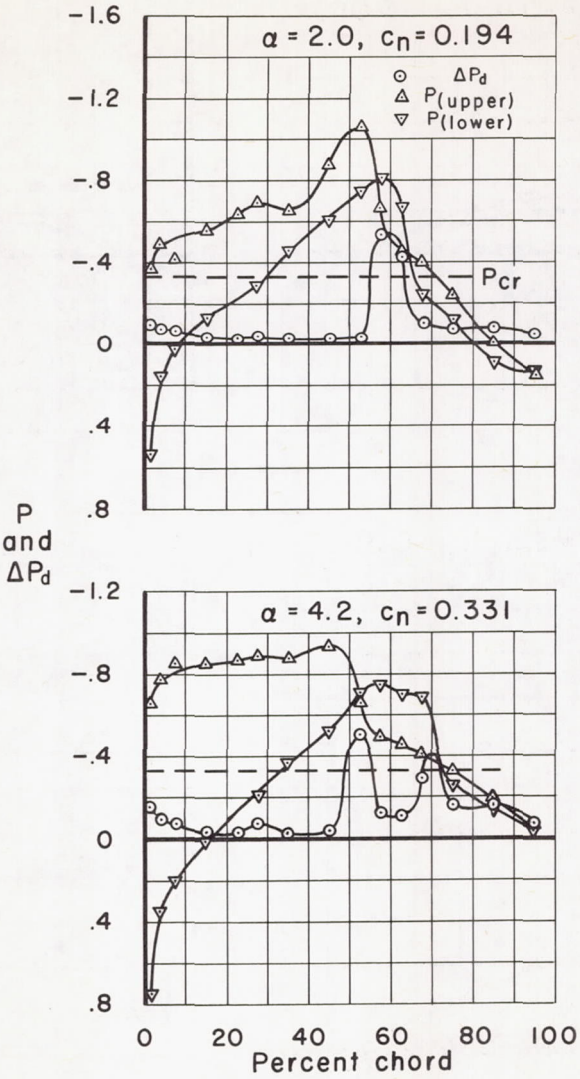

(e) M = 0.84.
Figure 6.- Concluded.

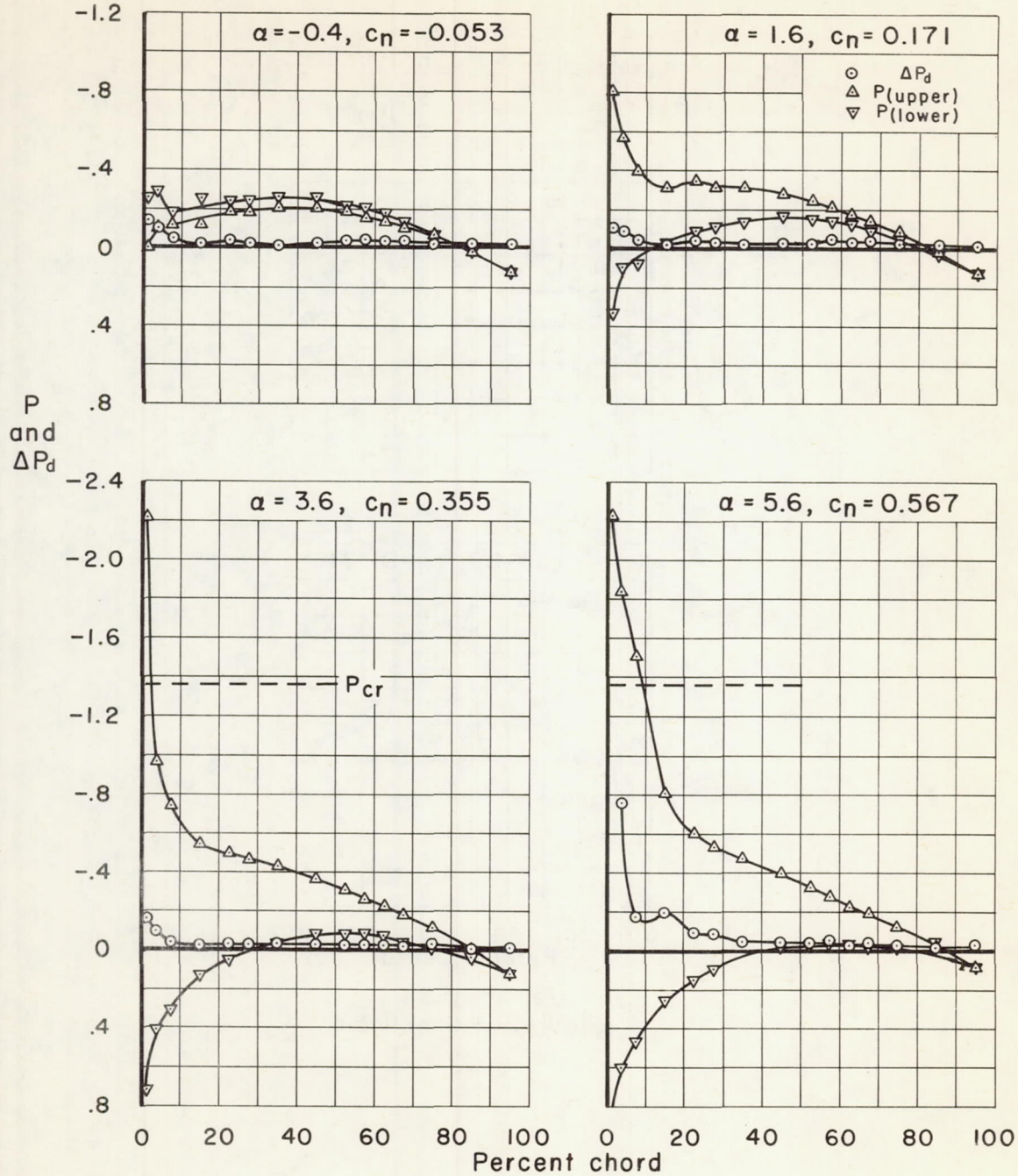

(a) M = 0.59.

Figure 7.- Local-pressure fluctuations and time-average static-pressure distributions for the NACA 65A008 airfoil.

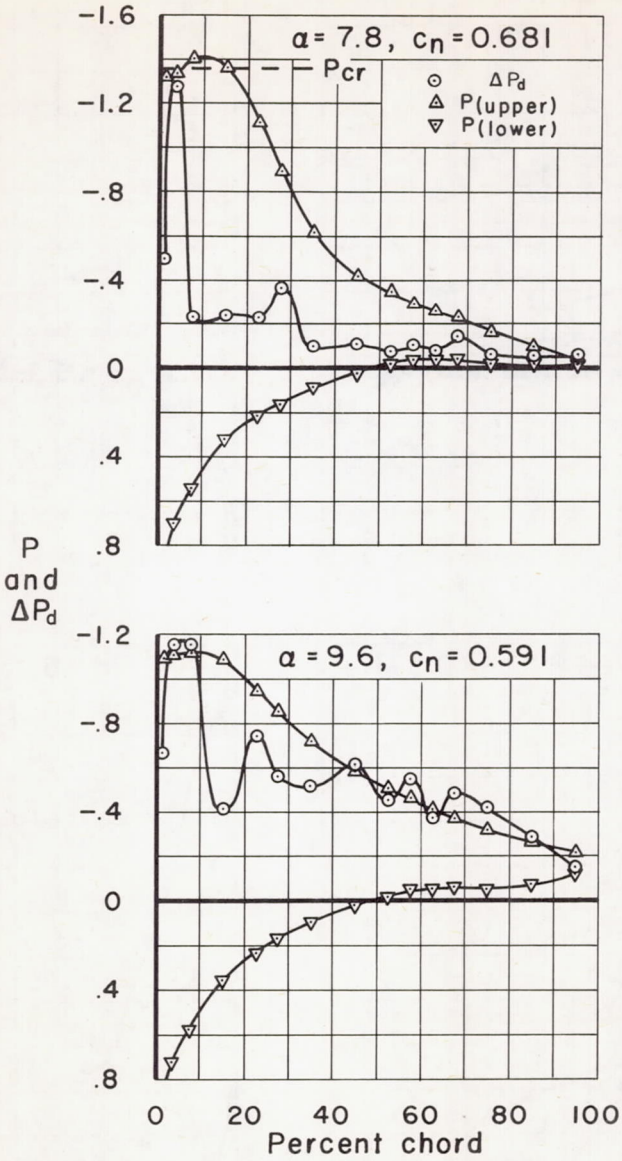

(a) M = 0.59 concluded.
Figure 7.- Continued.

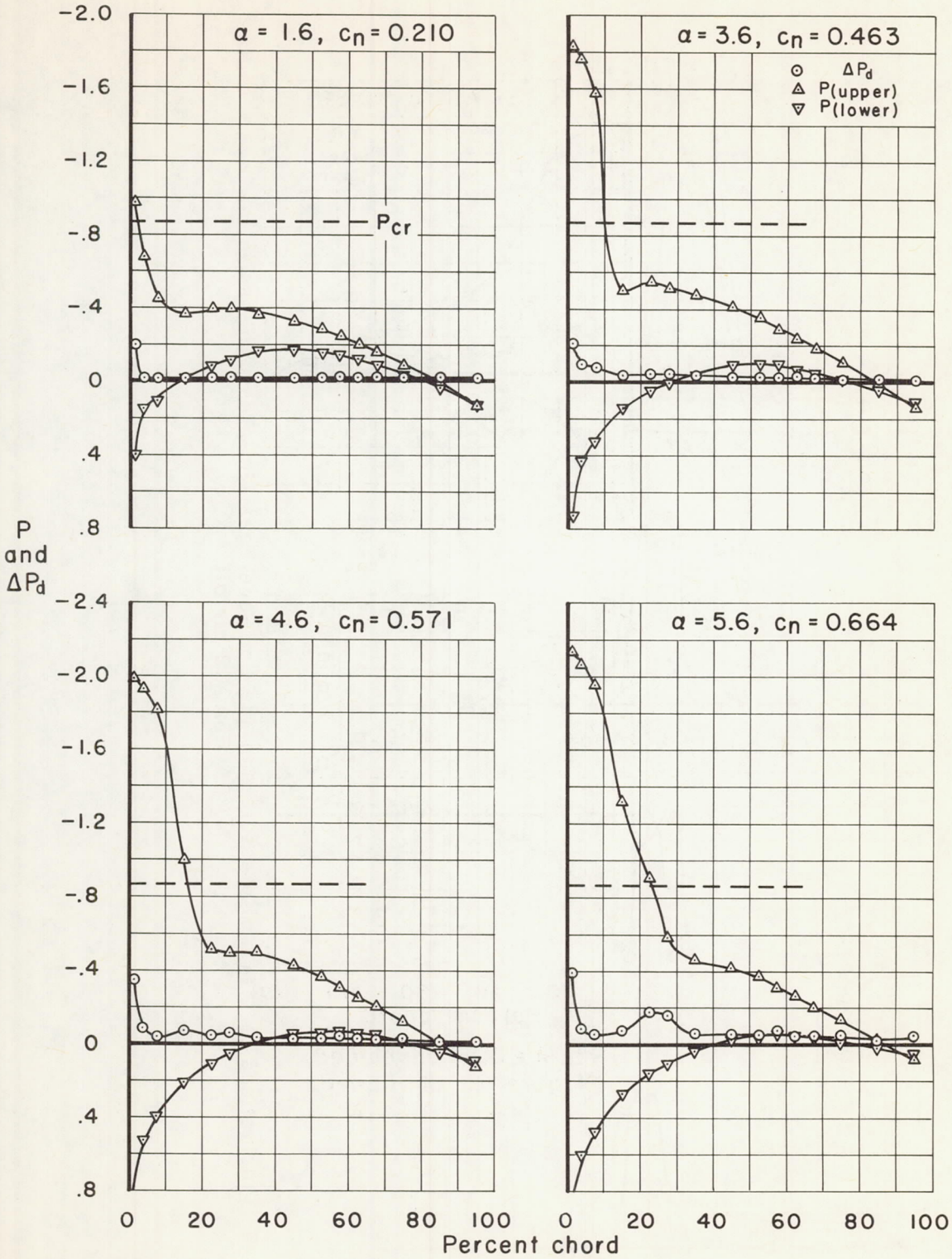

(b) M = 0.68.

Figure 7.- Continued.

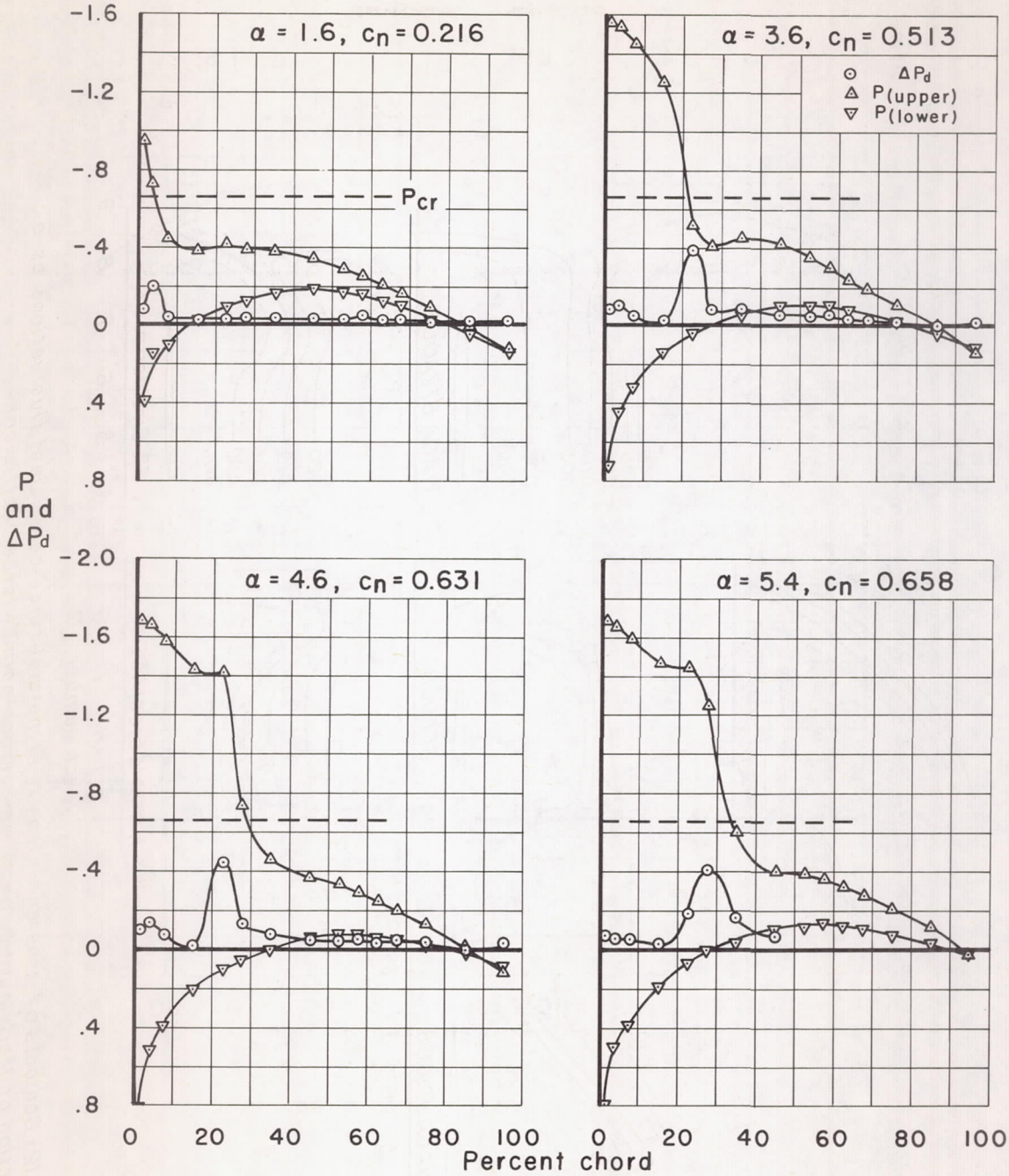

(c) M = 0.73.
Figure 7.- Continued.

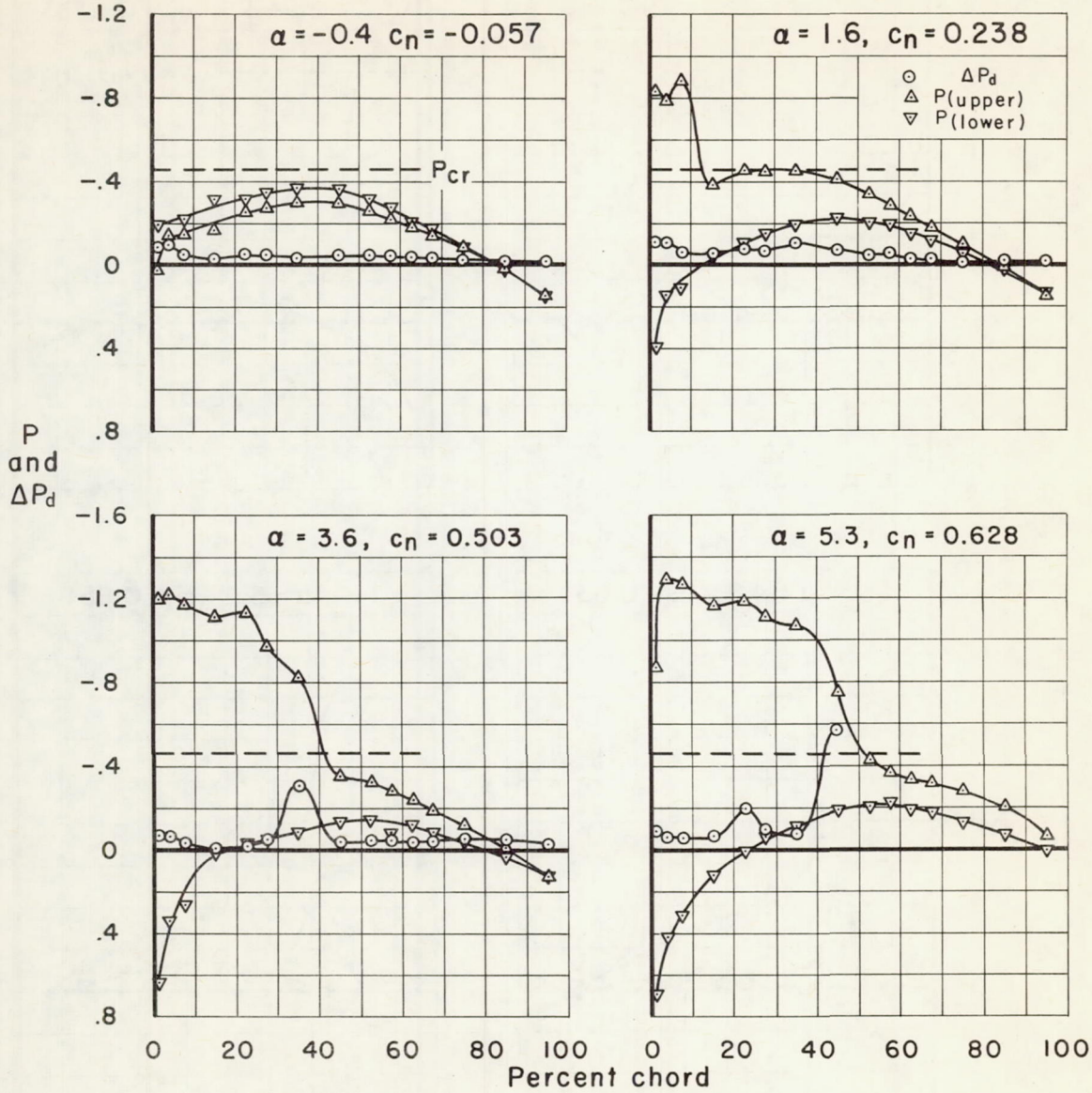

(d) M = 0.79.

Figure 7.- Continued.

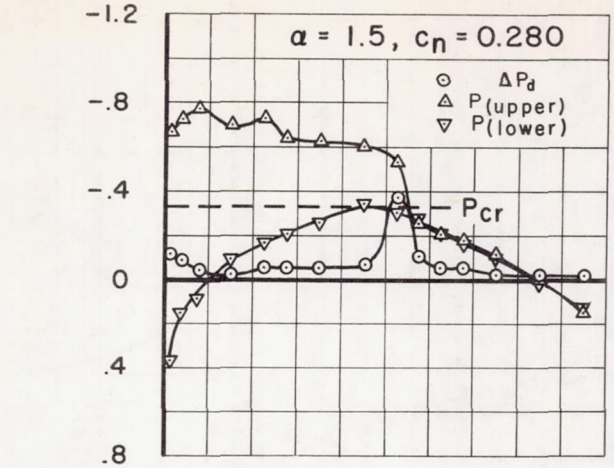

(e) M = 0.84.

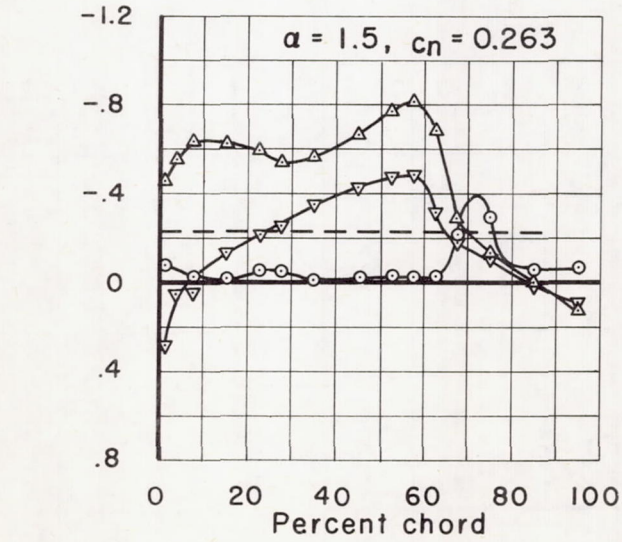

(f) M = 0.88.

Figure 7.- Concluded.

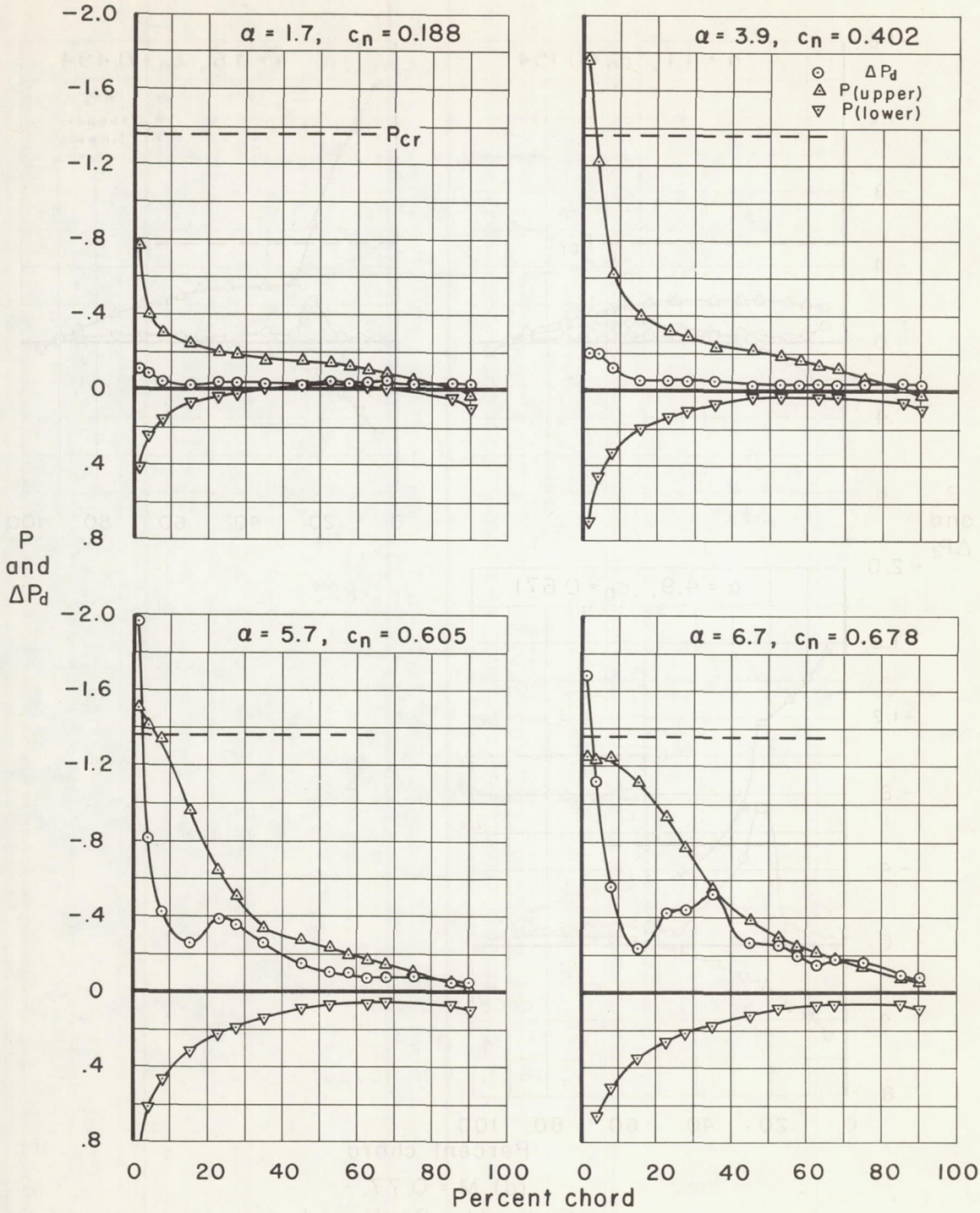

(a) M = 0.59.

Figure 8.-Local-pressure fluctuations and time-average static-pressure distributions for the NACA $65A_{(06)}004$ airfoil.

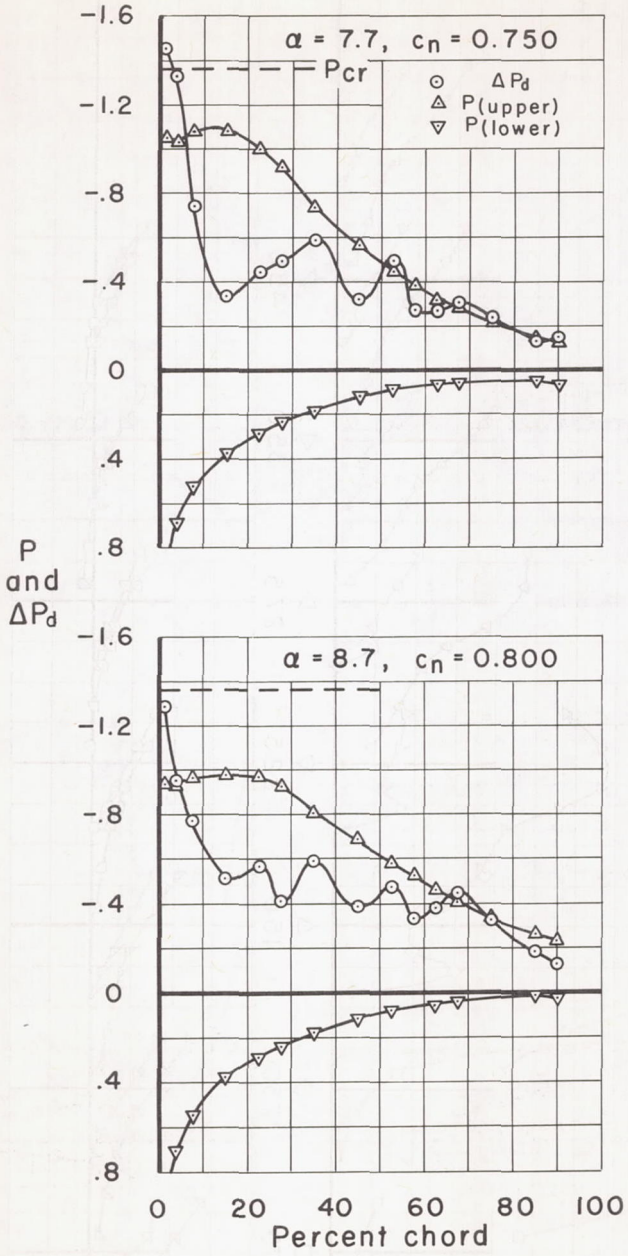

(a) M = 0.59 concluded.
Figure 8.- Continued.

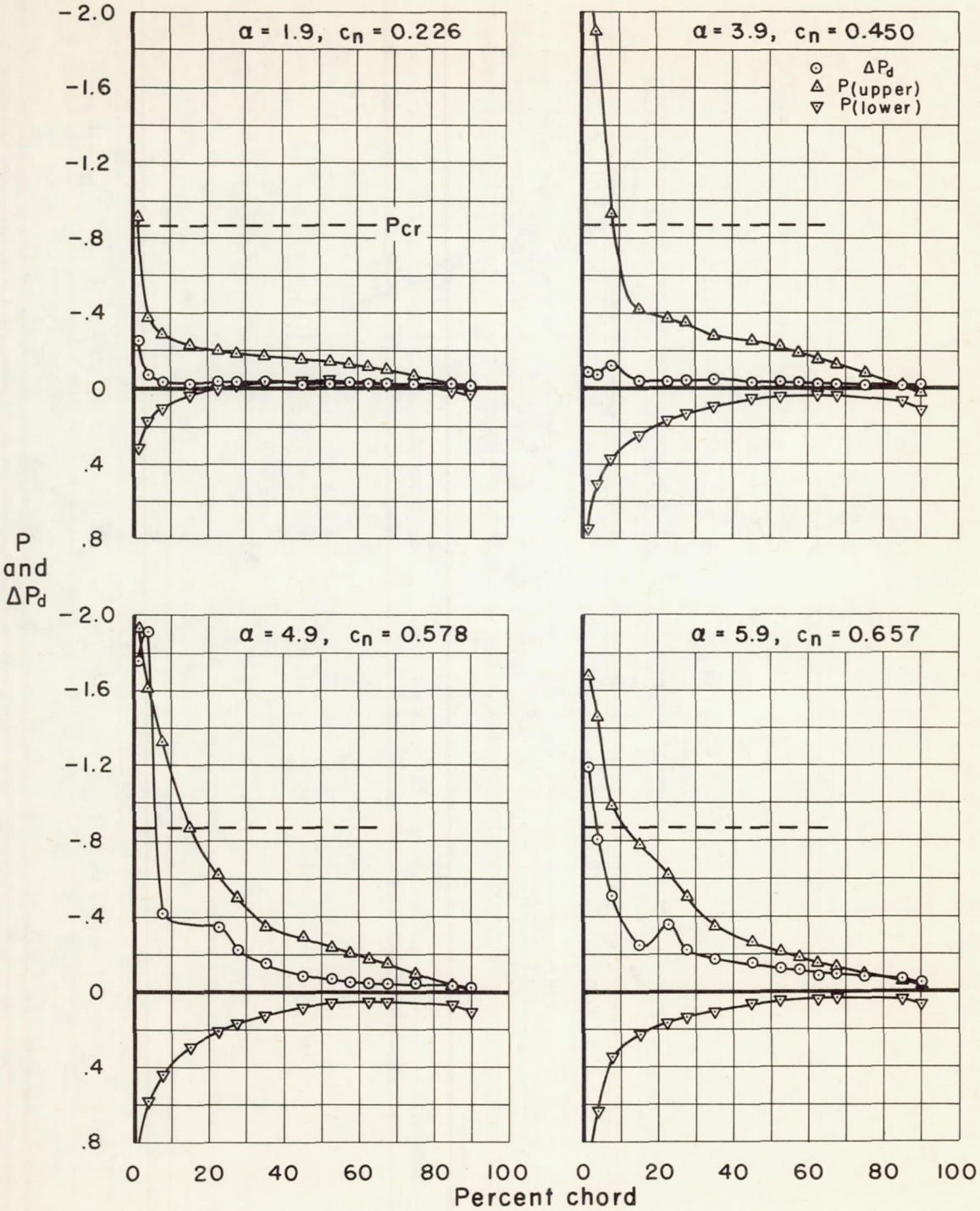

(b) M = 0.68.

Figure 8.- Continued.

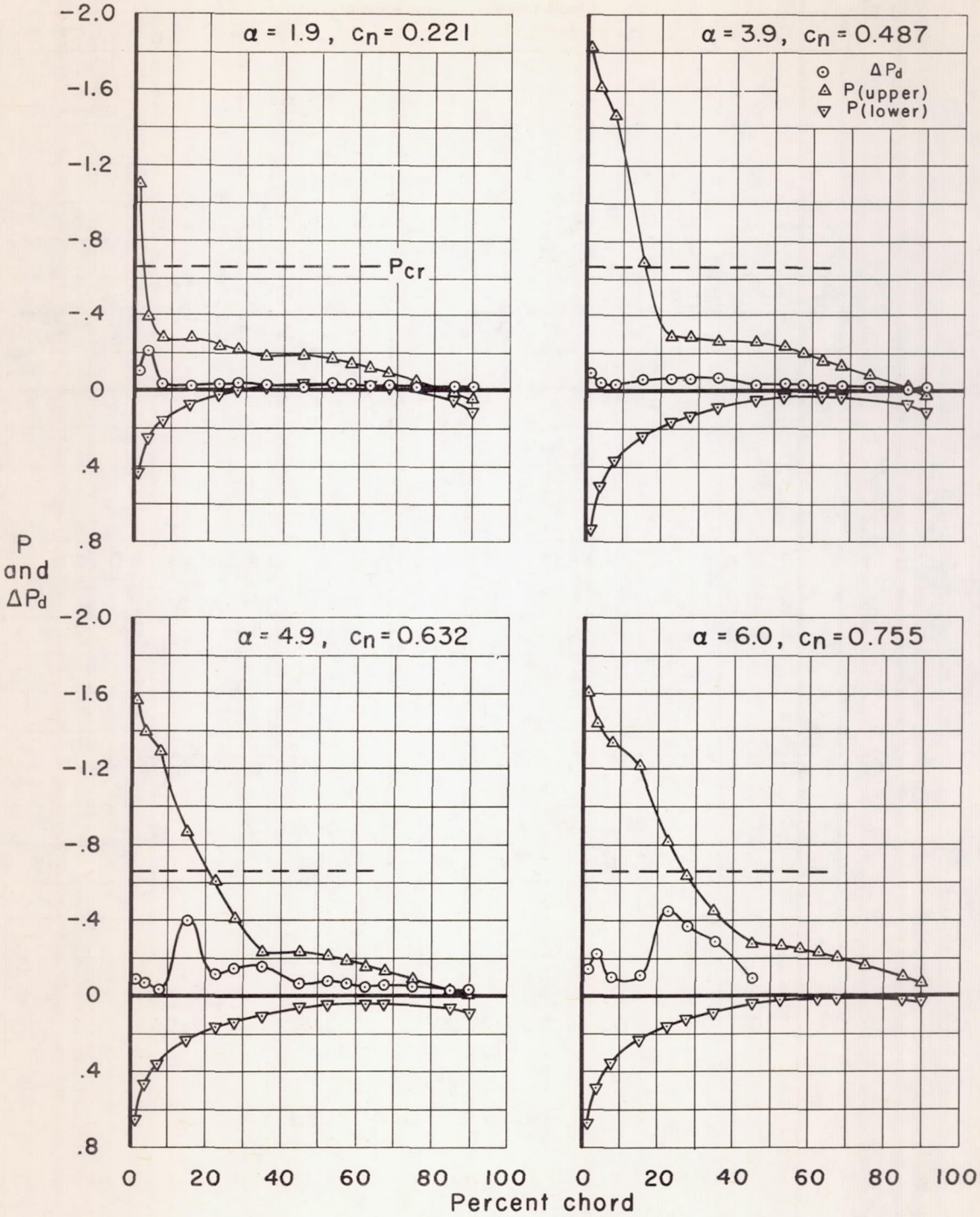

(c) M = 0.73.

Figure 8.- Continued.

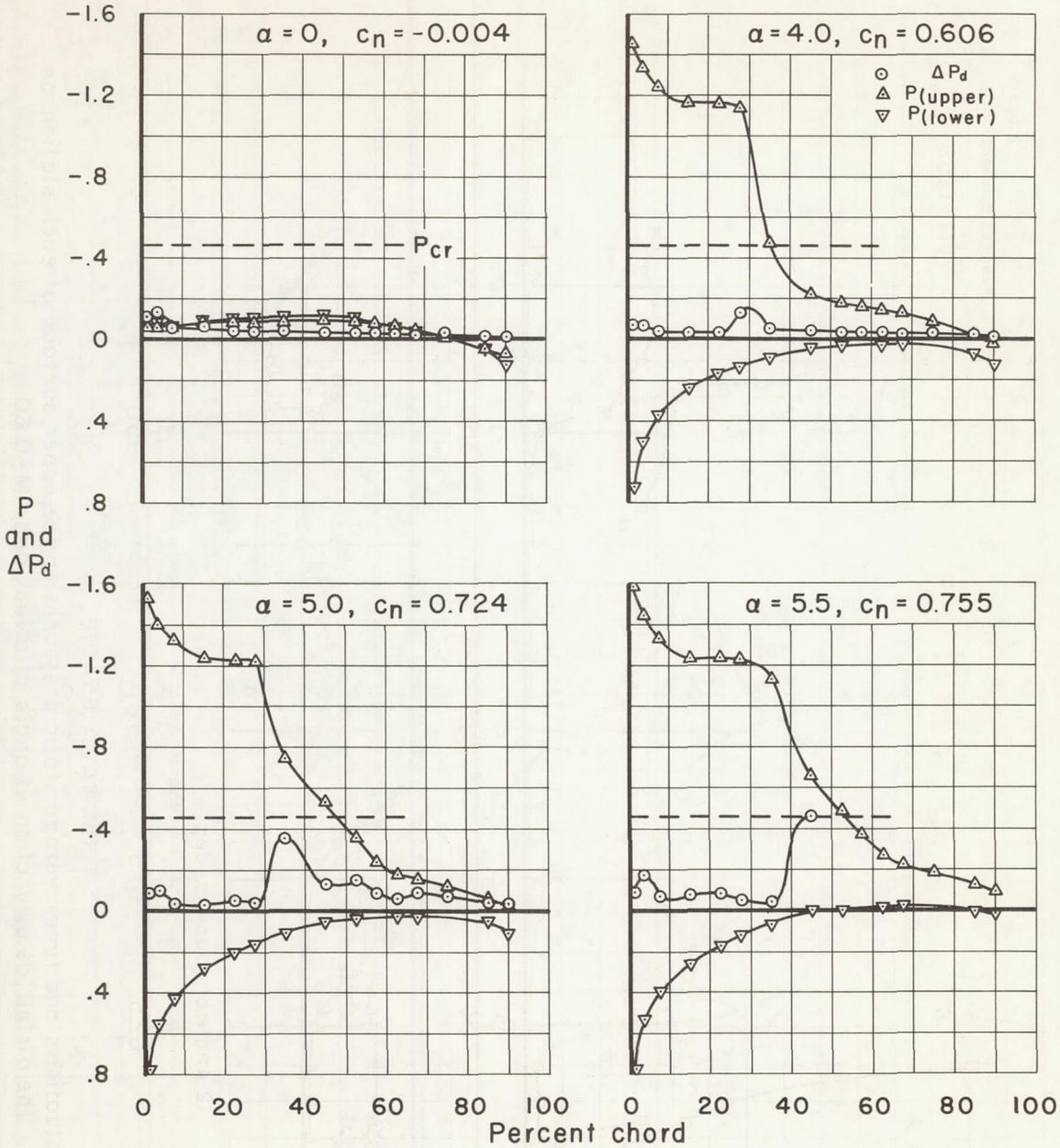

(d) M = 0.78.

Figure 8.- Continued.

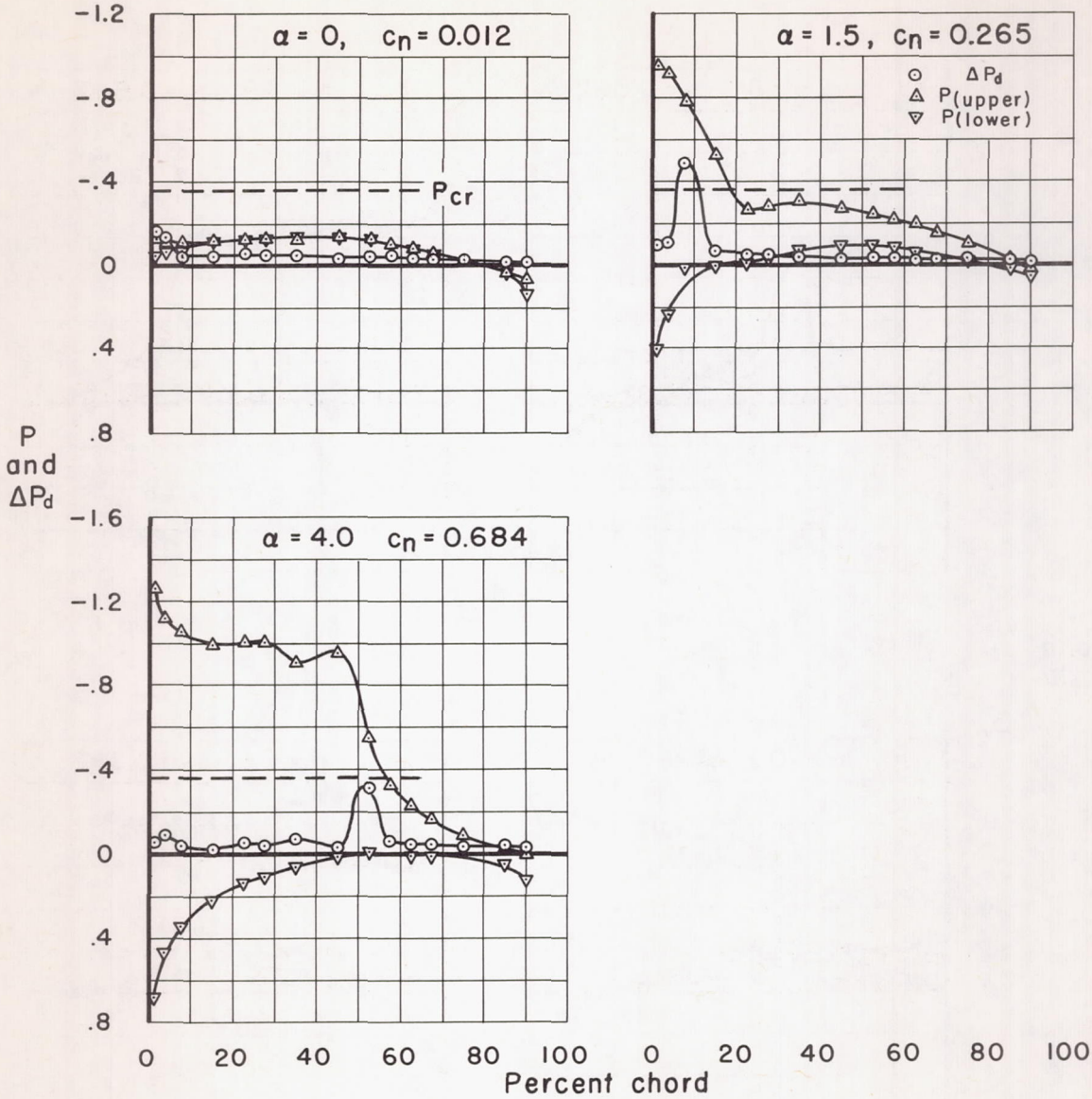

(e) M = 0.83.

Figure 8.- Continued.

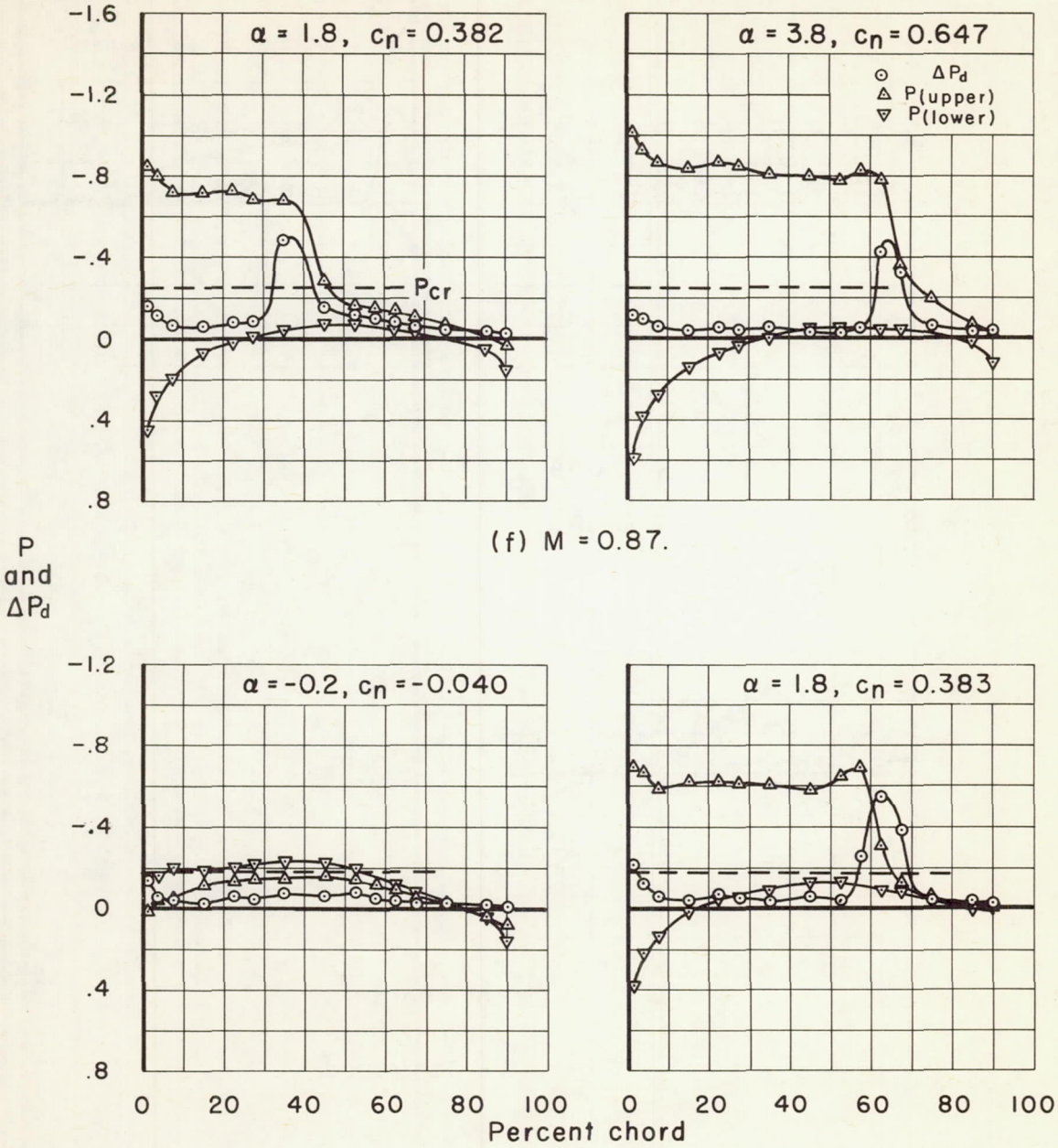

(f) M = 0.87.

(g) M = 0.90.

Figure 8.- Concluded.

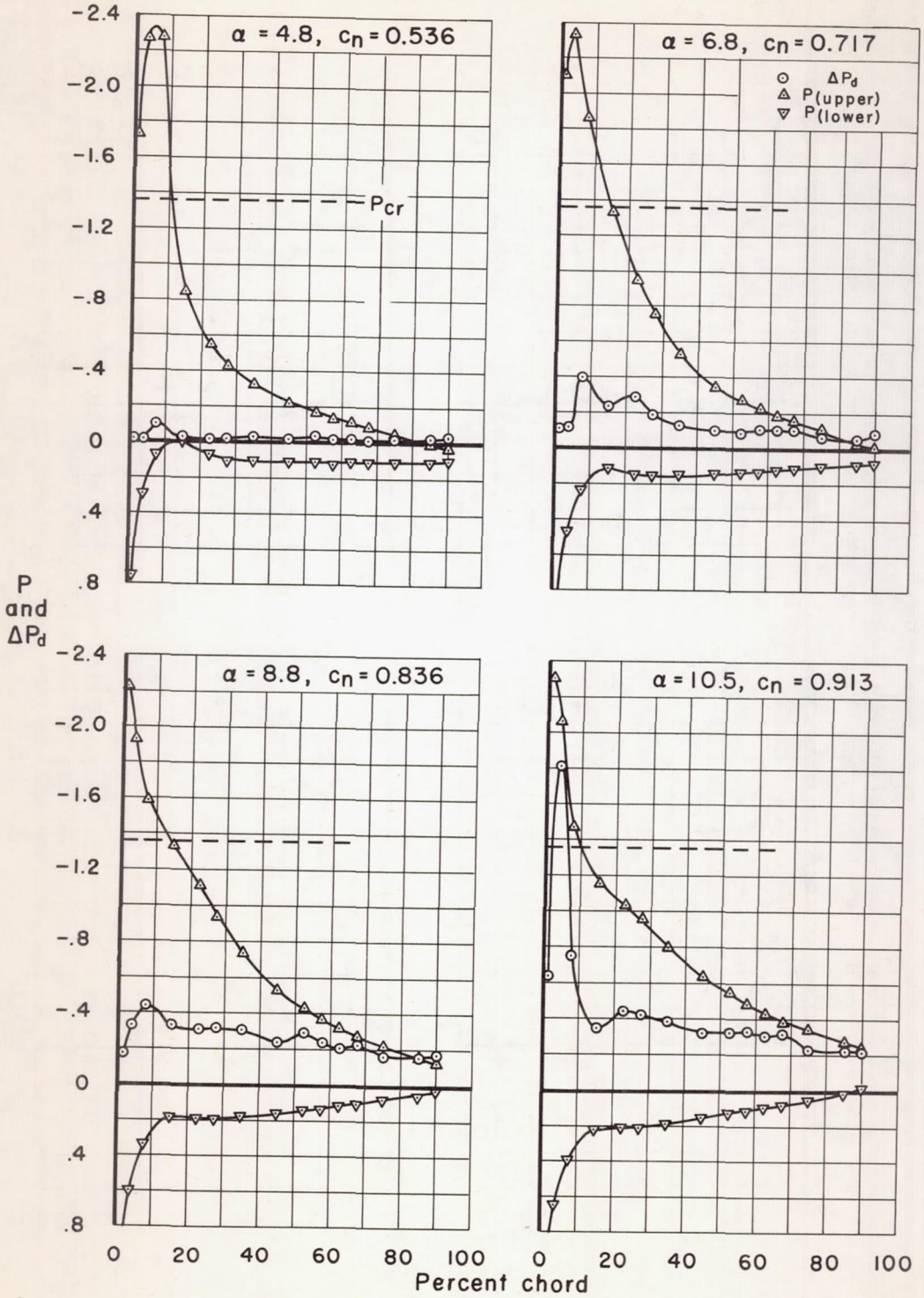

(a) M = 0.59.

Figure 9.- Local-pressure fluctuations and time-average static-pressure distributions for the NACA 2-008 airfoil.

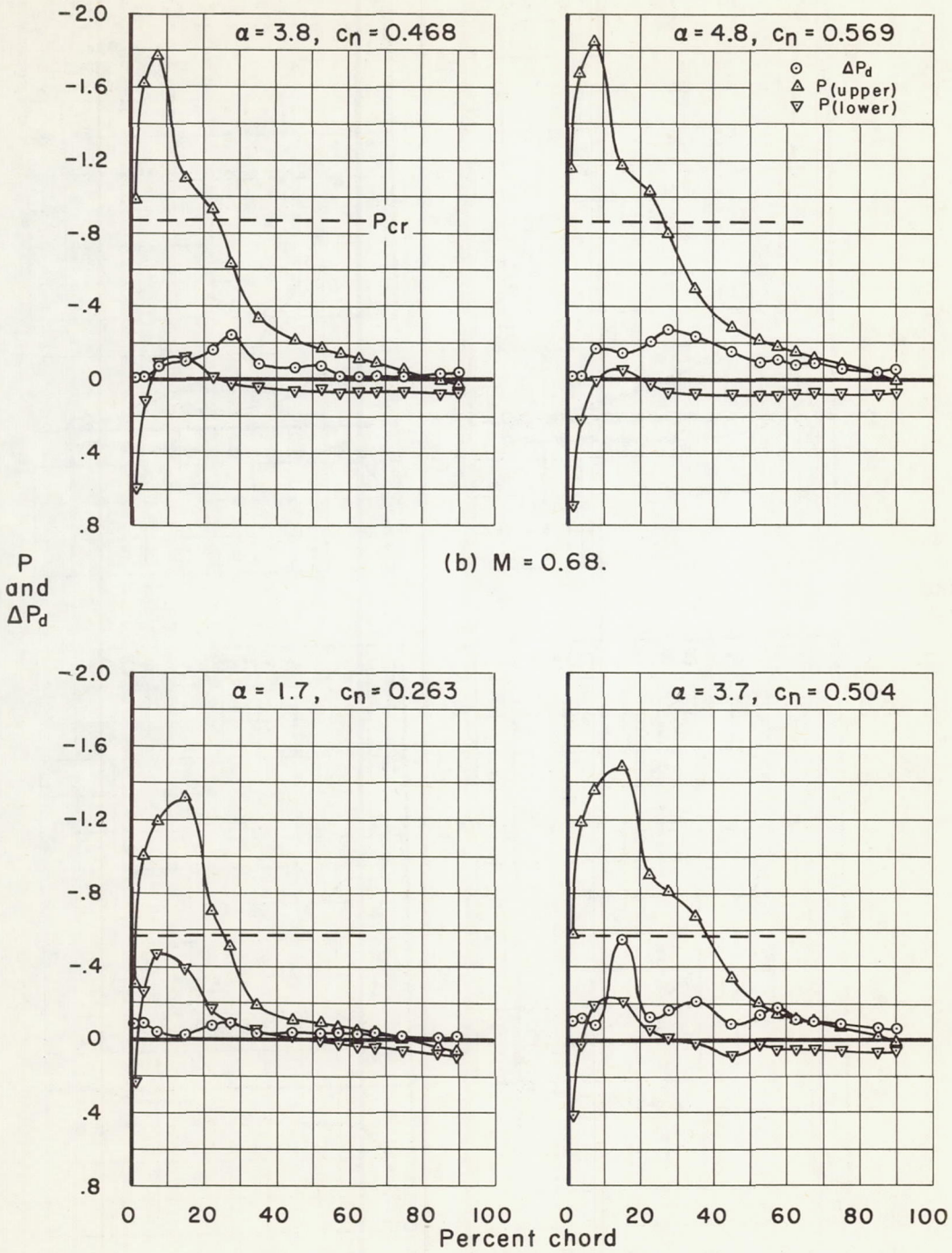

(b) M = 0.68.

(c) M = 0.76.

Figure 9.- Continued.

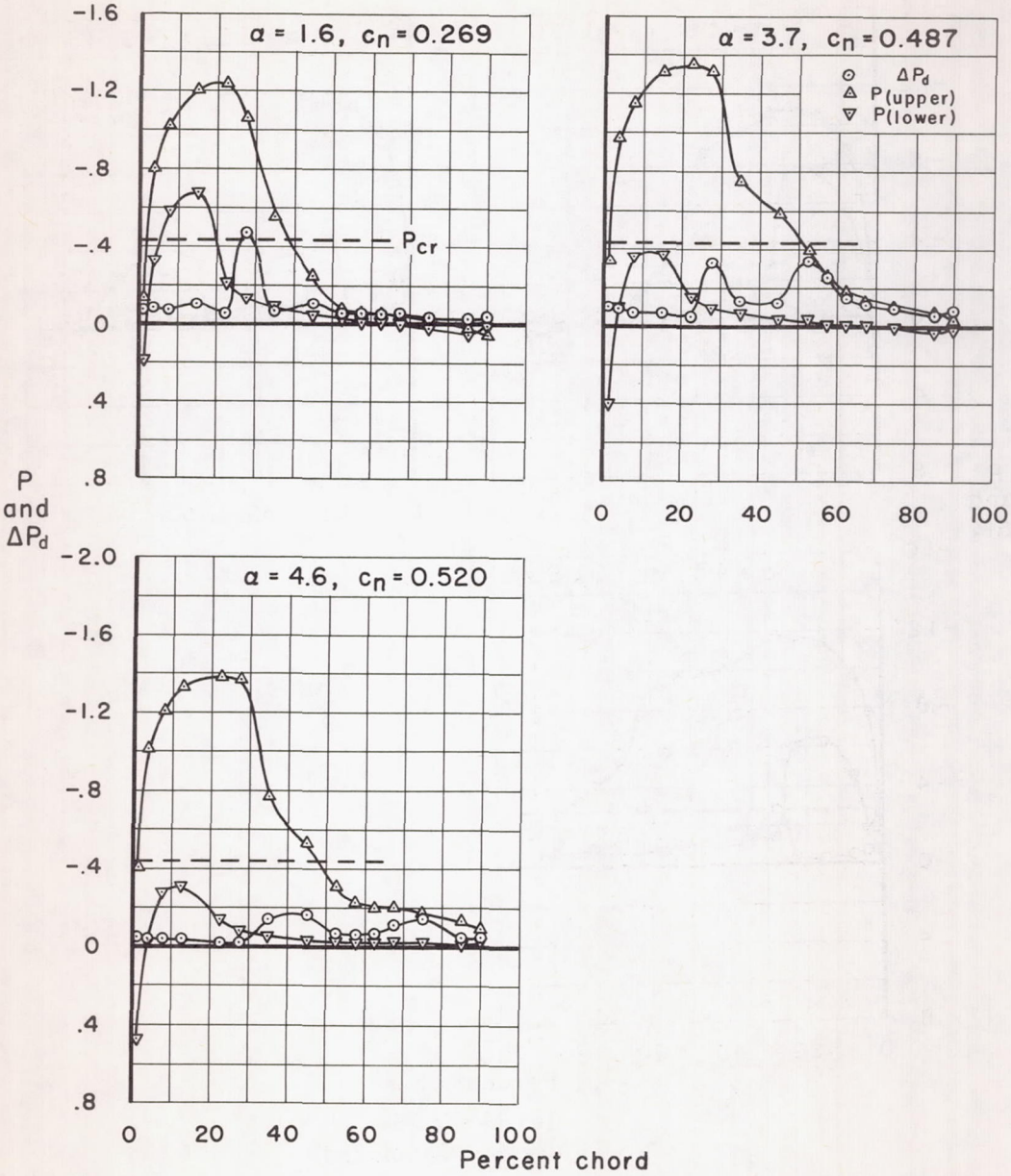

(d) M = 0.80.

Figure 9.- Continued.

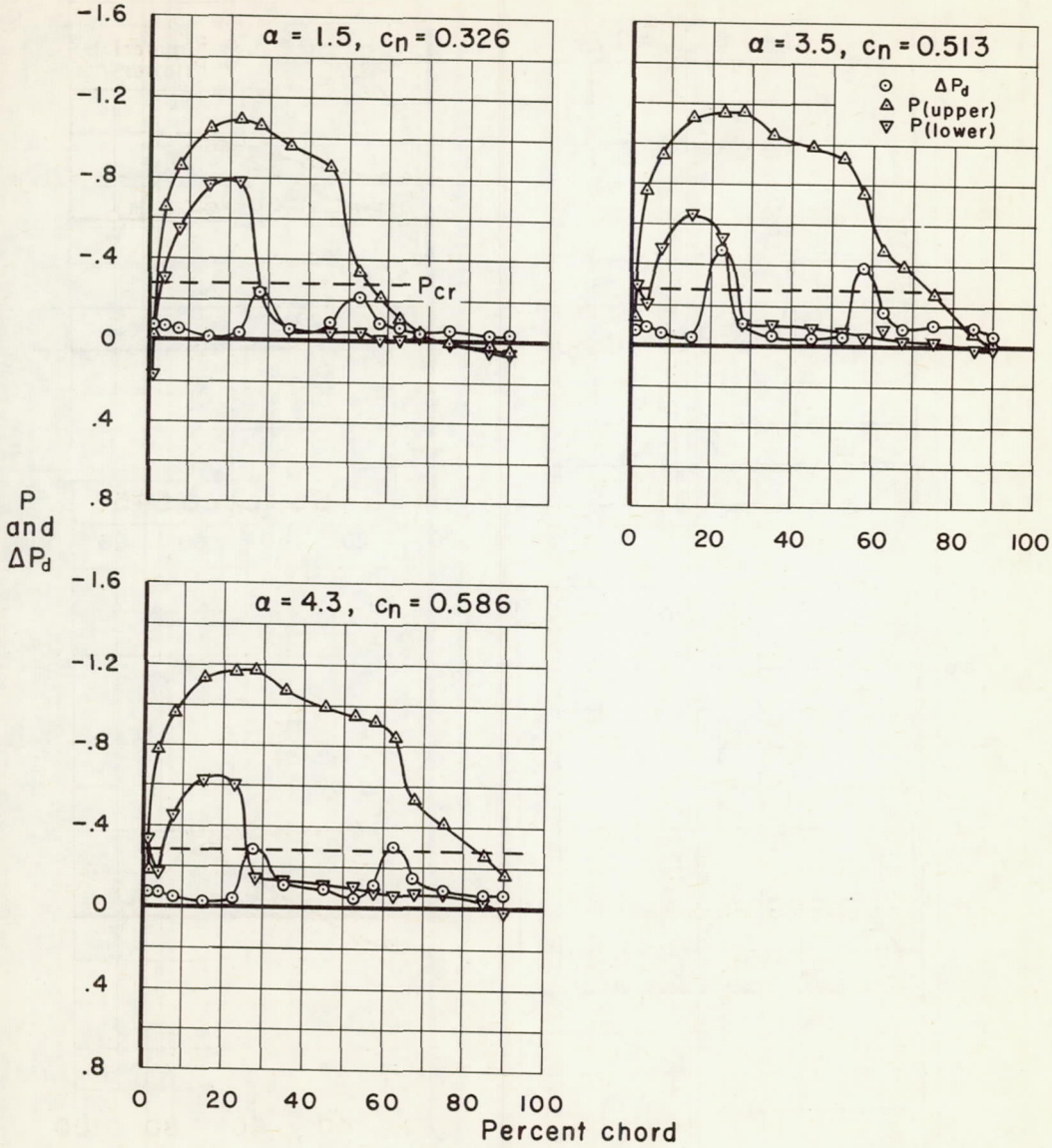

(e) M = 0.86.

Figure 9.- Concluded.

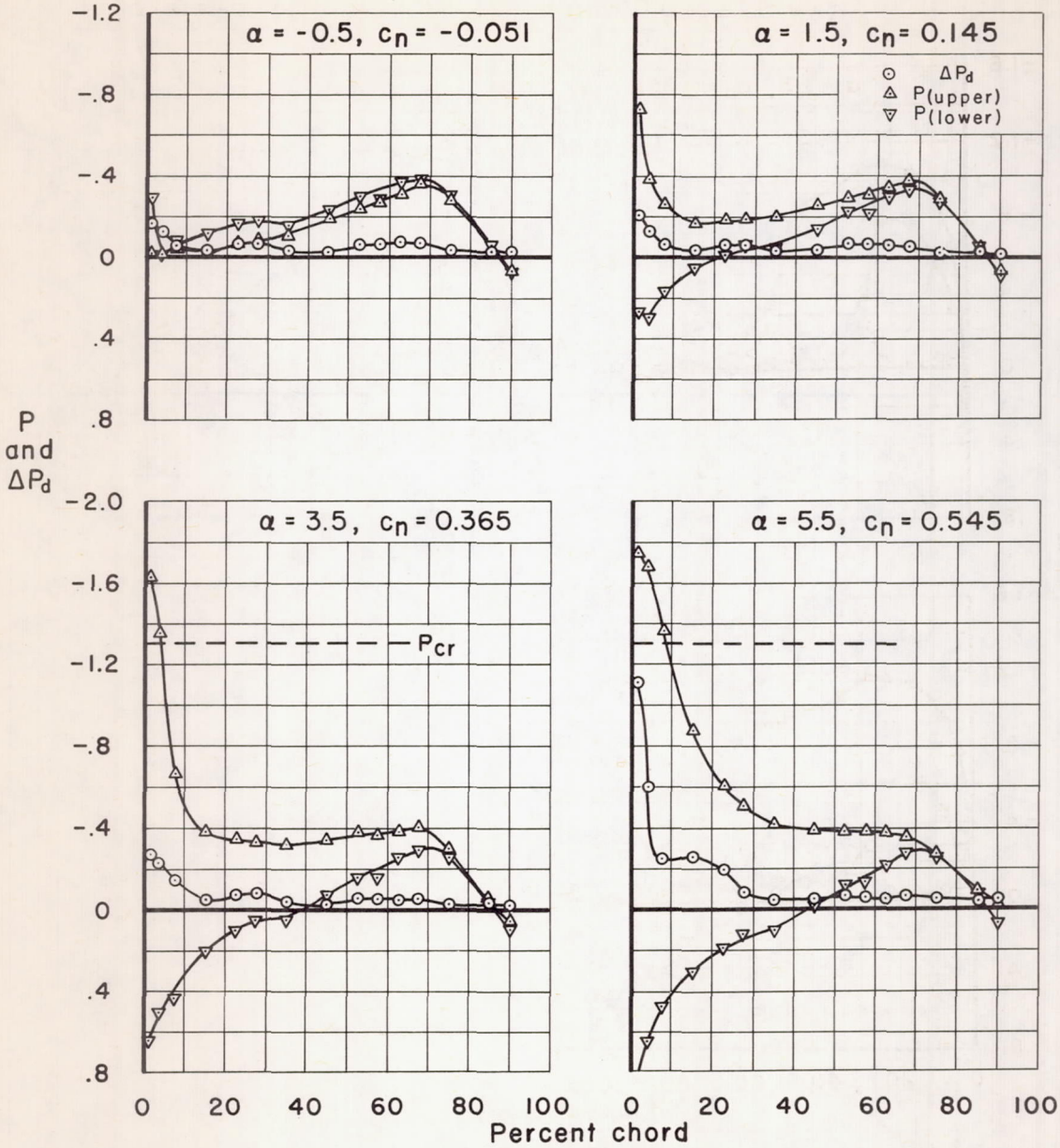

(a) M = 0.60.

Figure 10.- Local-pressure fluctuations and time-average static-pressure distributions for the NACA 877A008 airfoil.

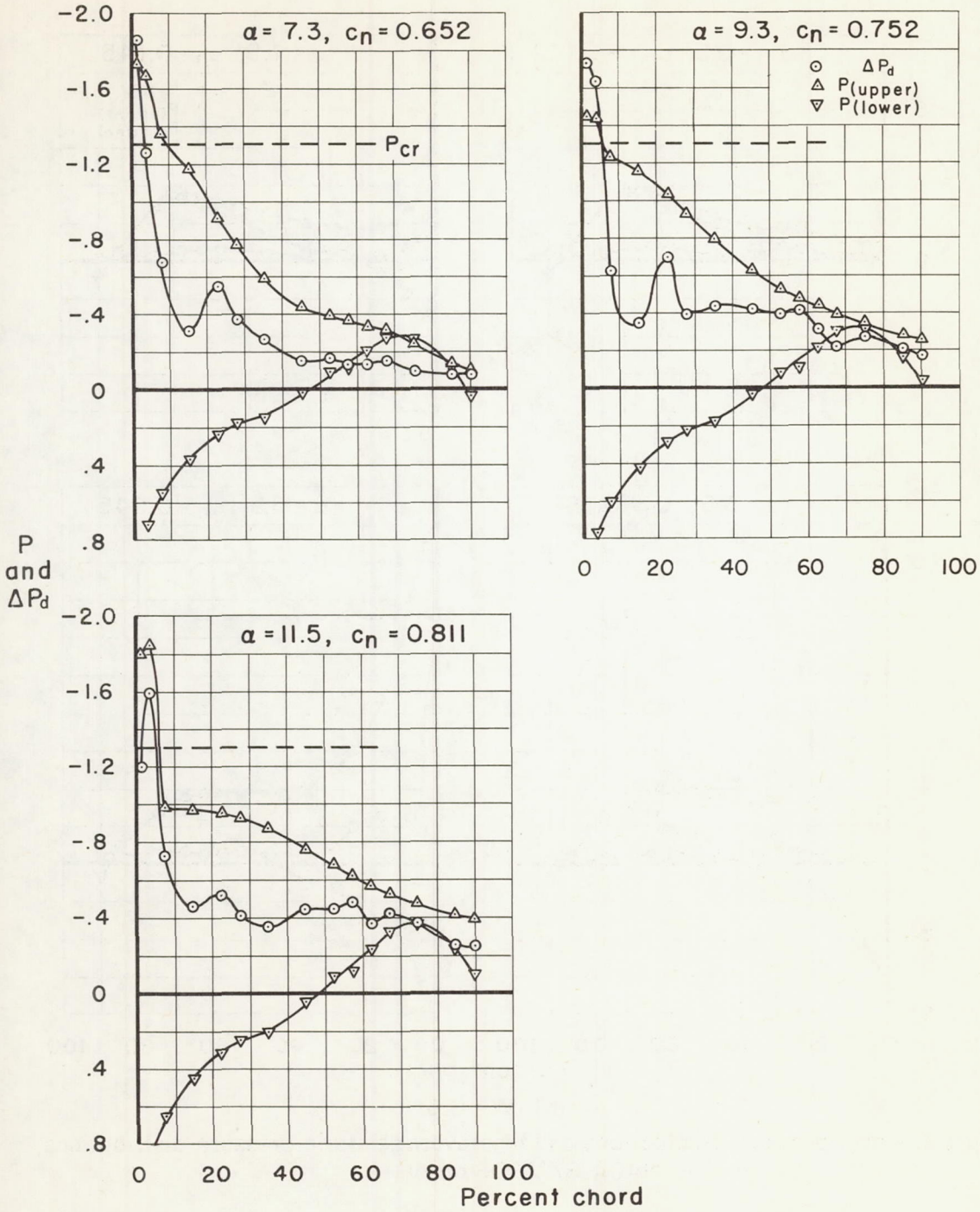

(a) M = 0.60 concluded.
Figure 10.- Continued.

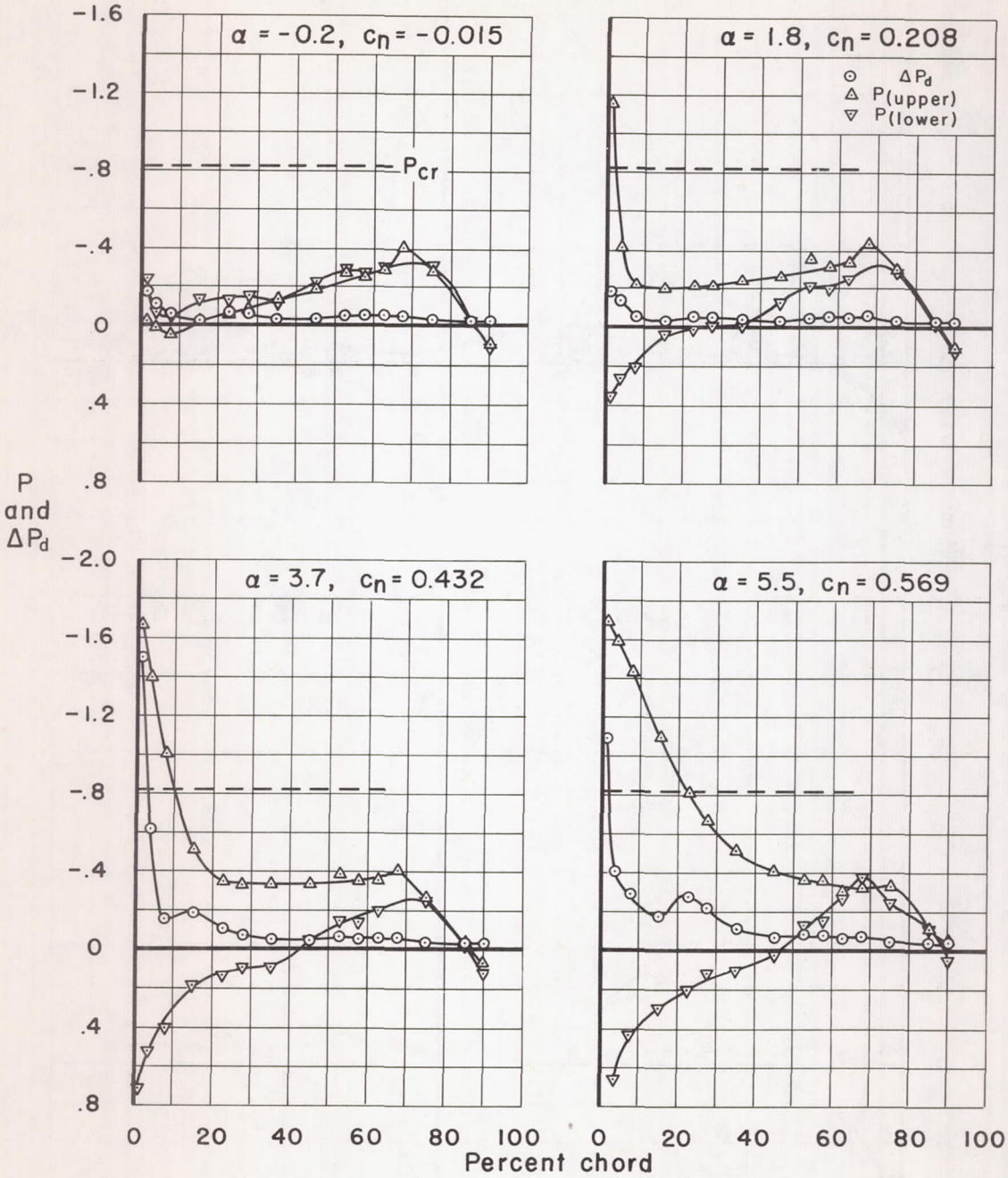

(b) M = 0.69.

Figure 10.- Continued.

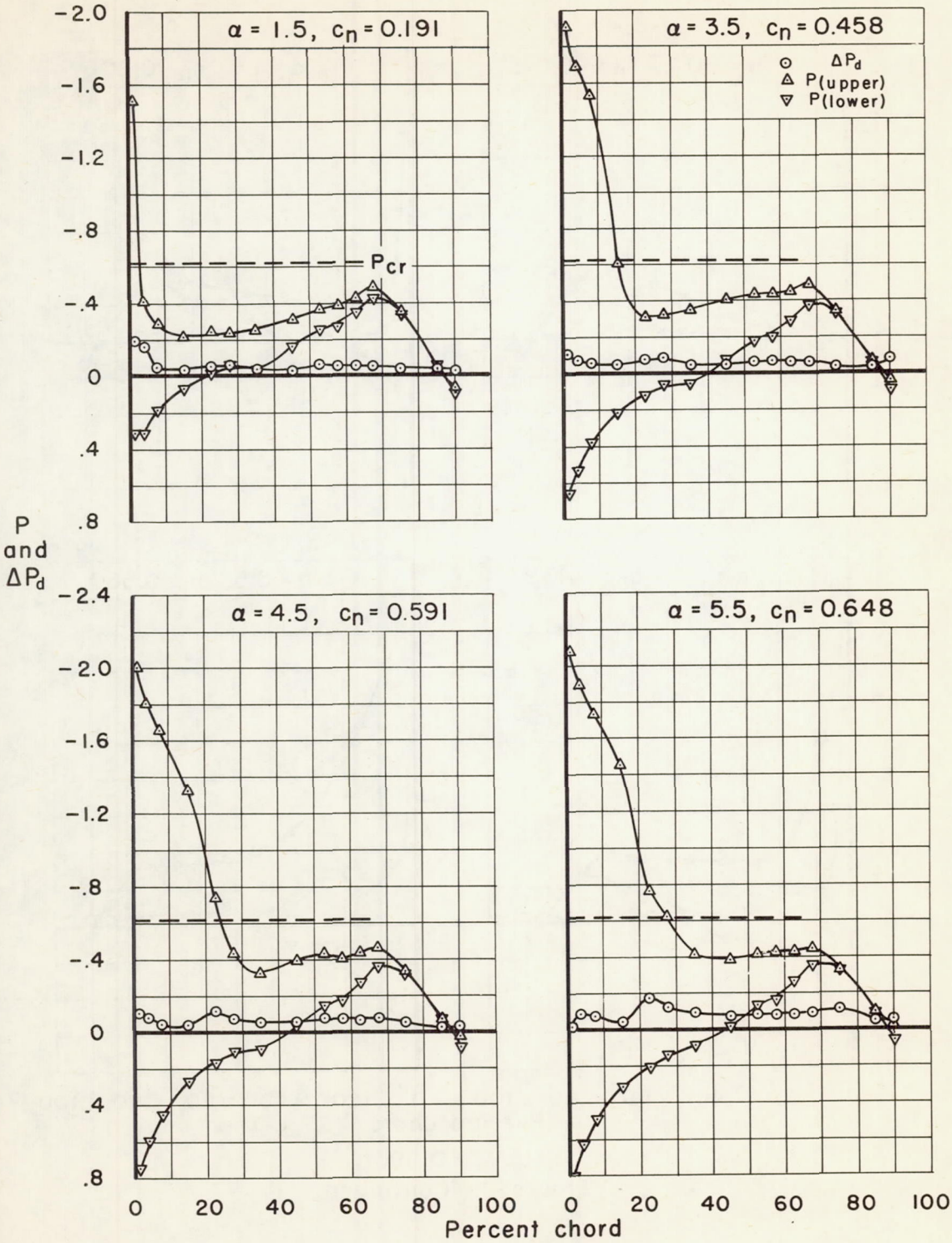

(c) M = 0.74.

Figure 10.- Continued.

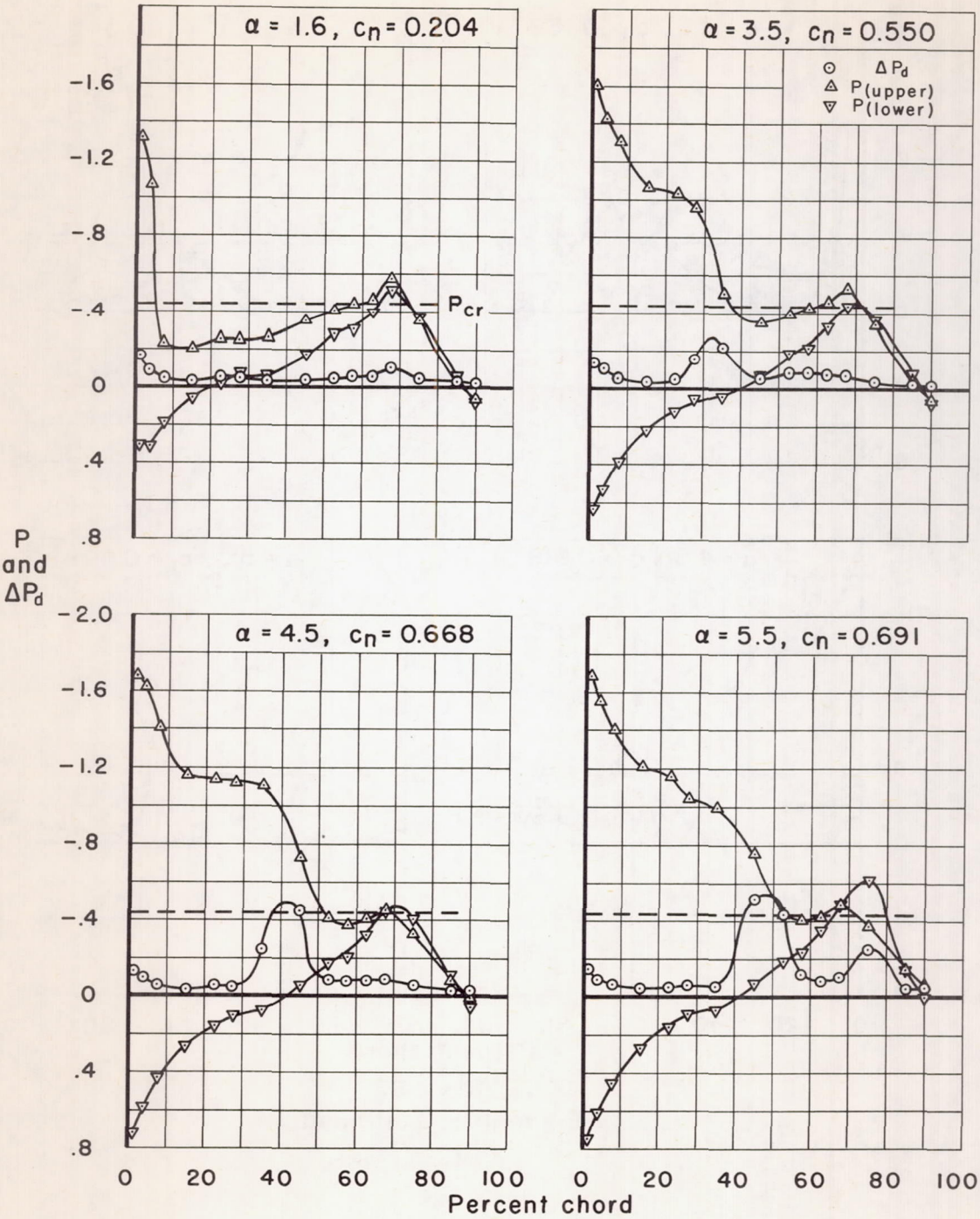

(d) M = 0.80.

Figure 10.- Continued.

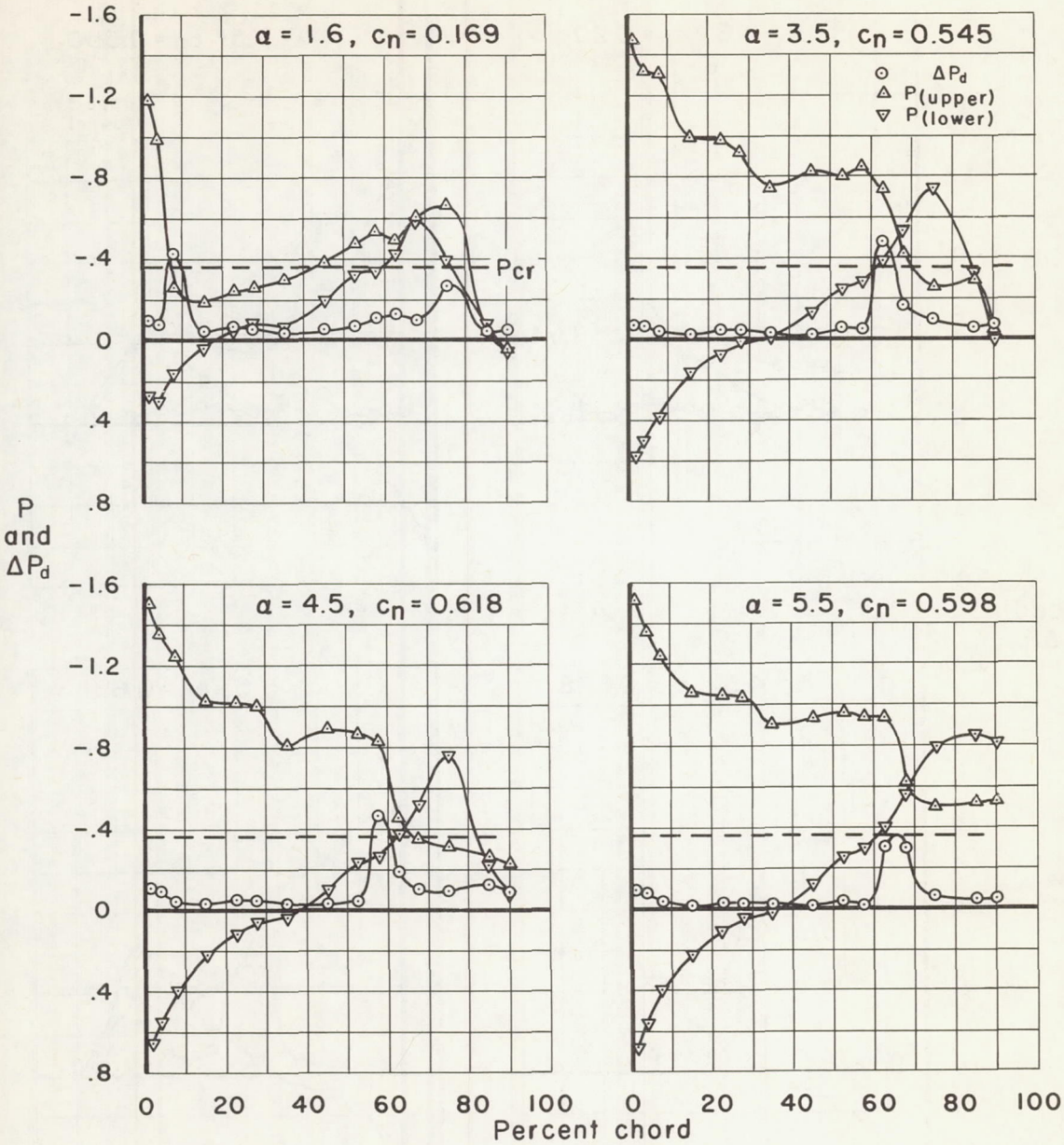

(e) M = 0.83.

Figure 10.- Continued.

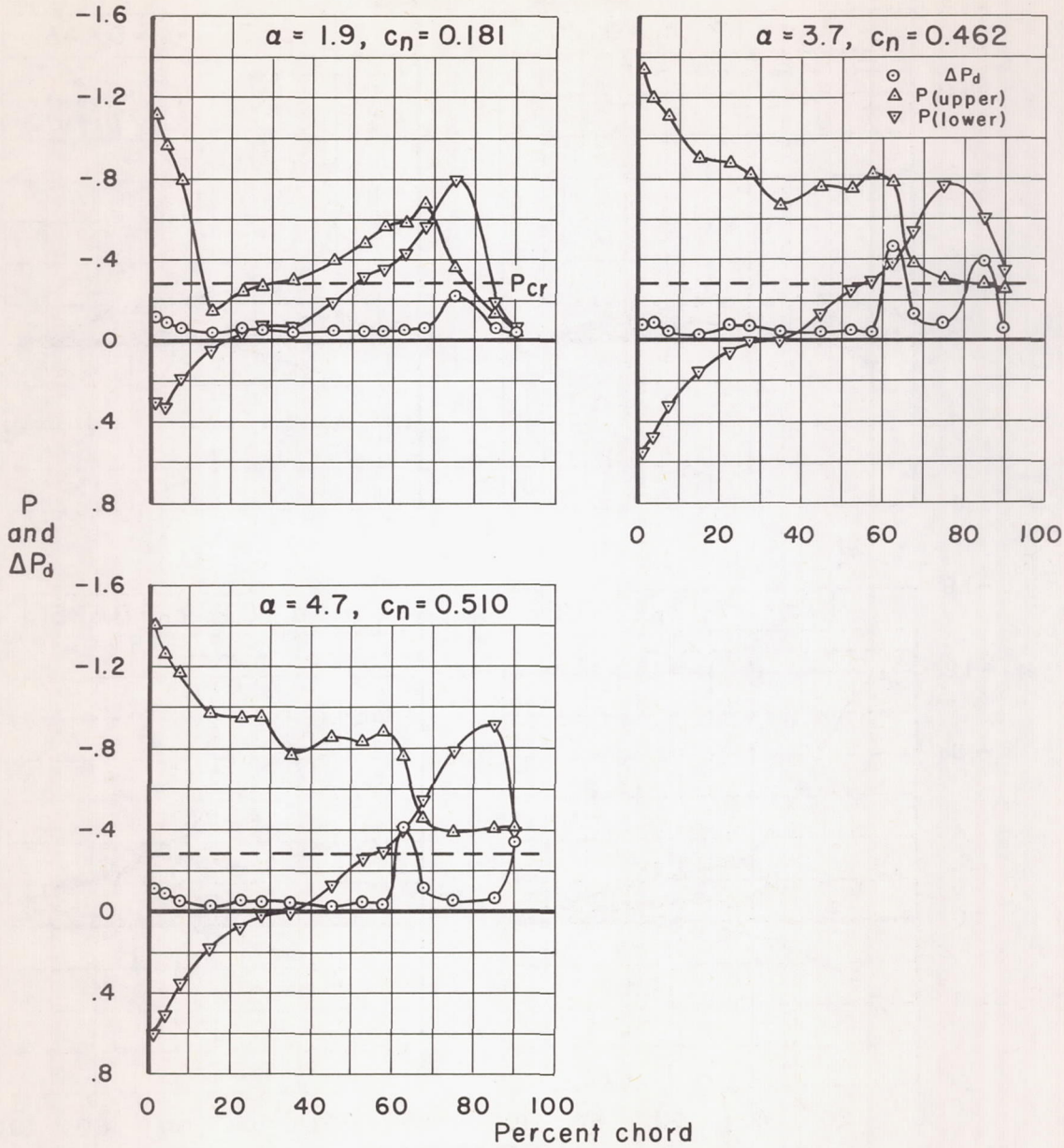

(f) M = 0.86.

Figure 10.- Concluded.

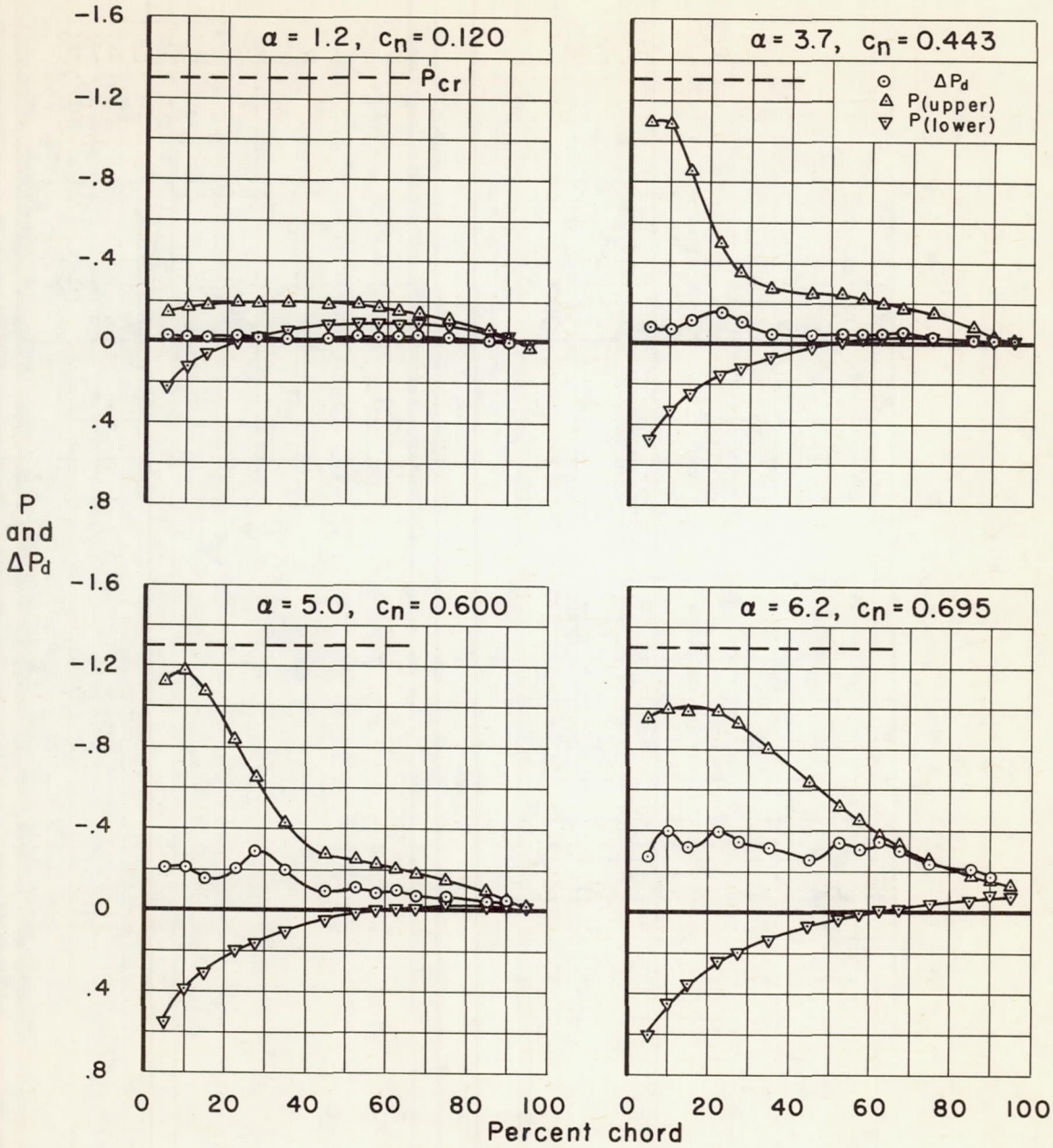

(a) M = 0.60.

Figure 11.- Local-pressure fluctuations and time-average static-pressure distributions for the 4-percent circular-arc airfoil.

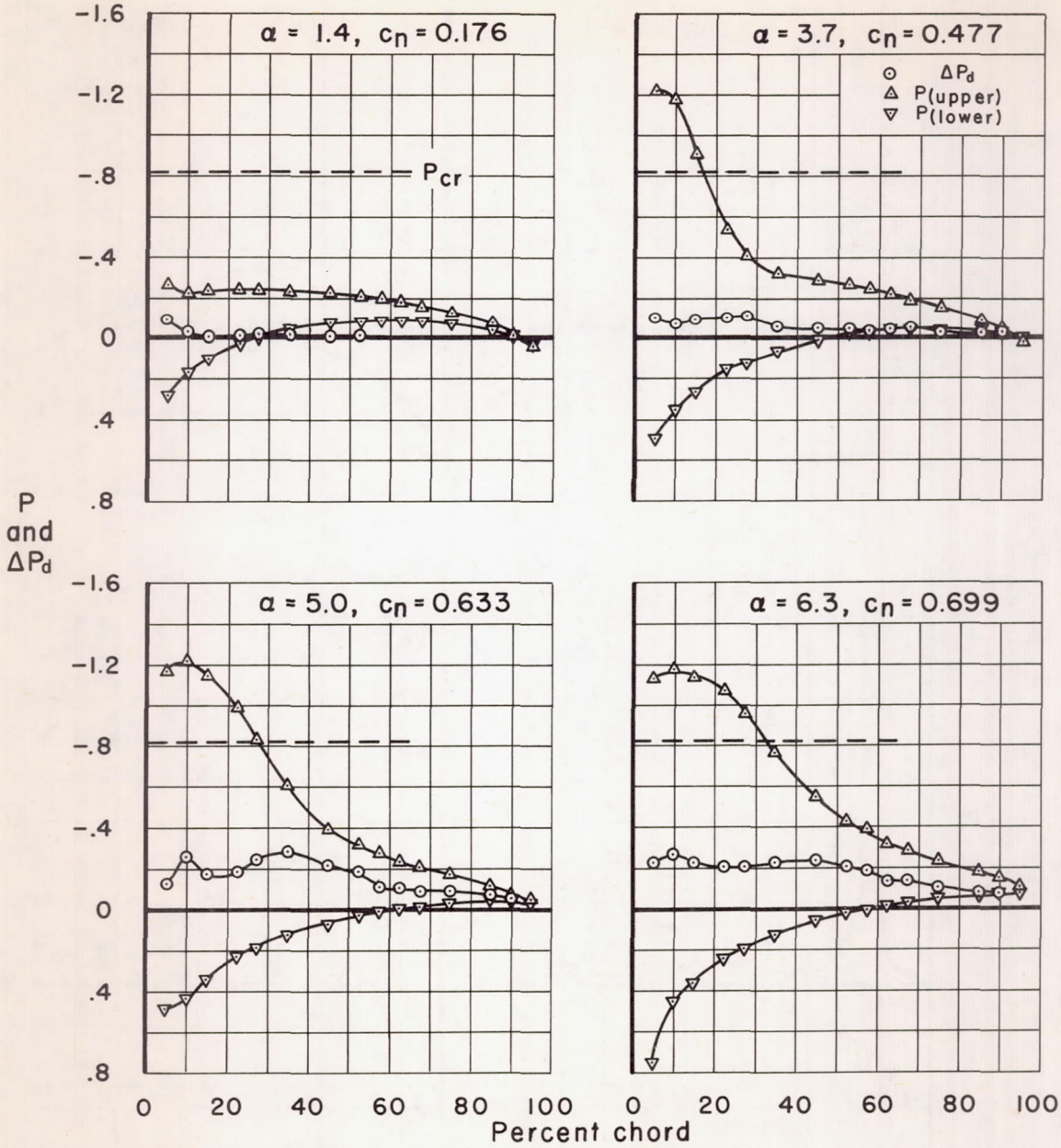

(b) M = 0.69.

Figure 11.- Continued.

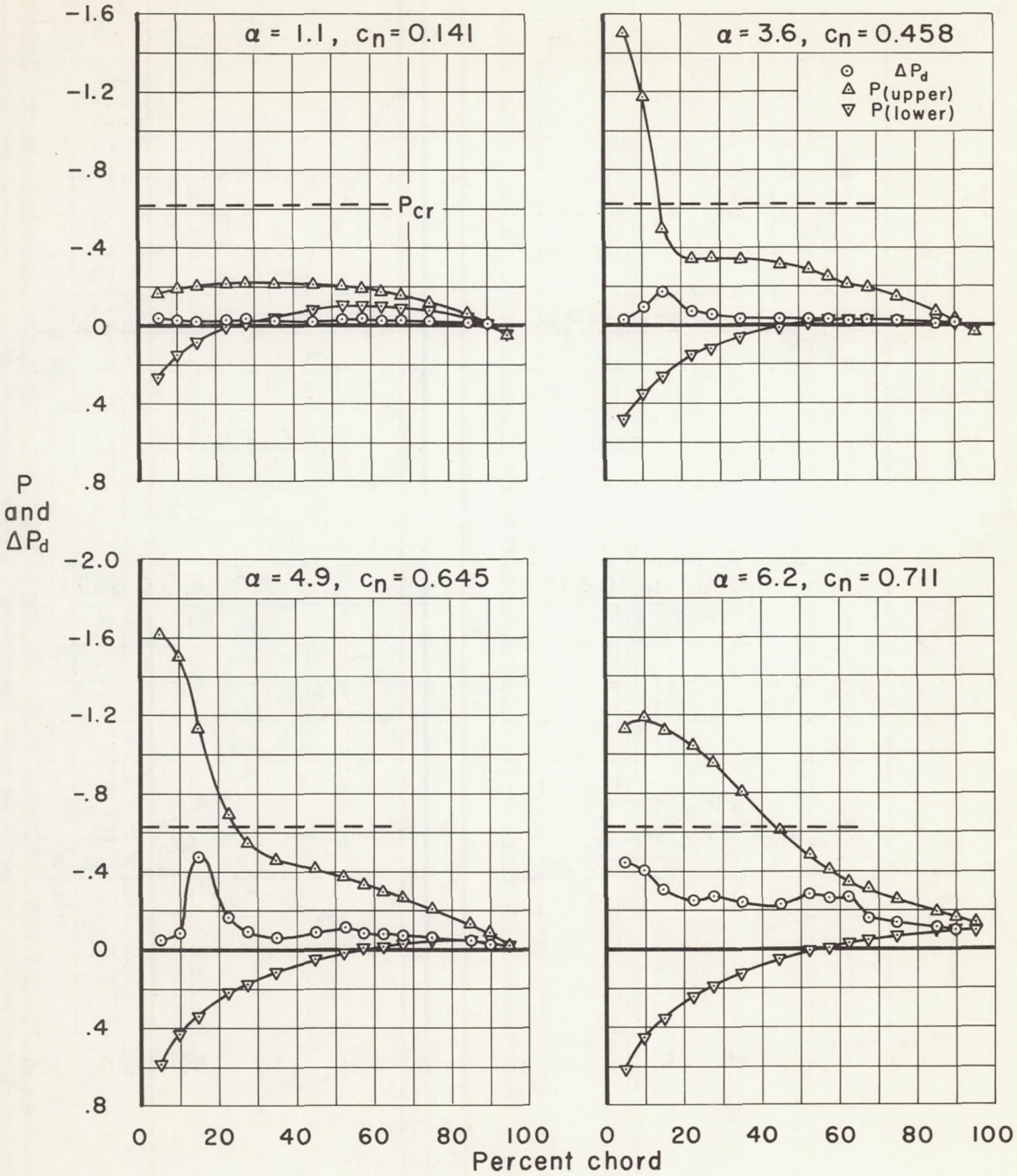

(c) M = 0.74.

Figure 11.- Continued.

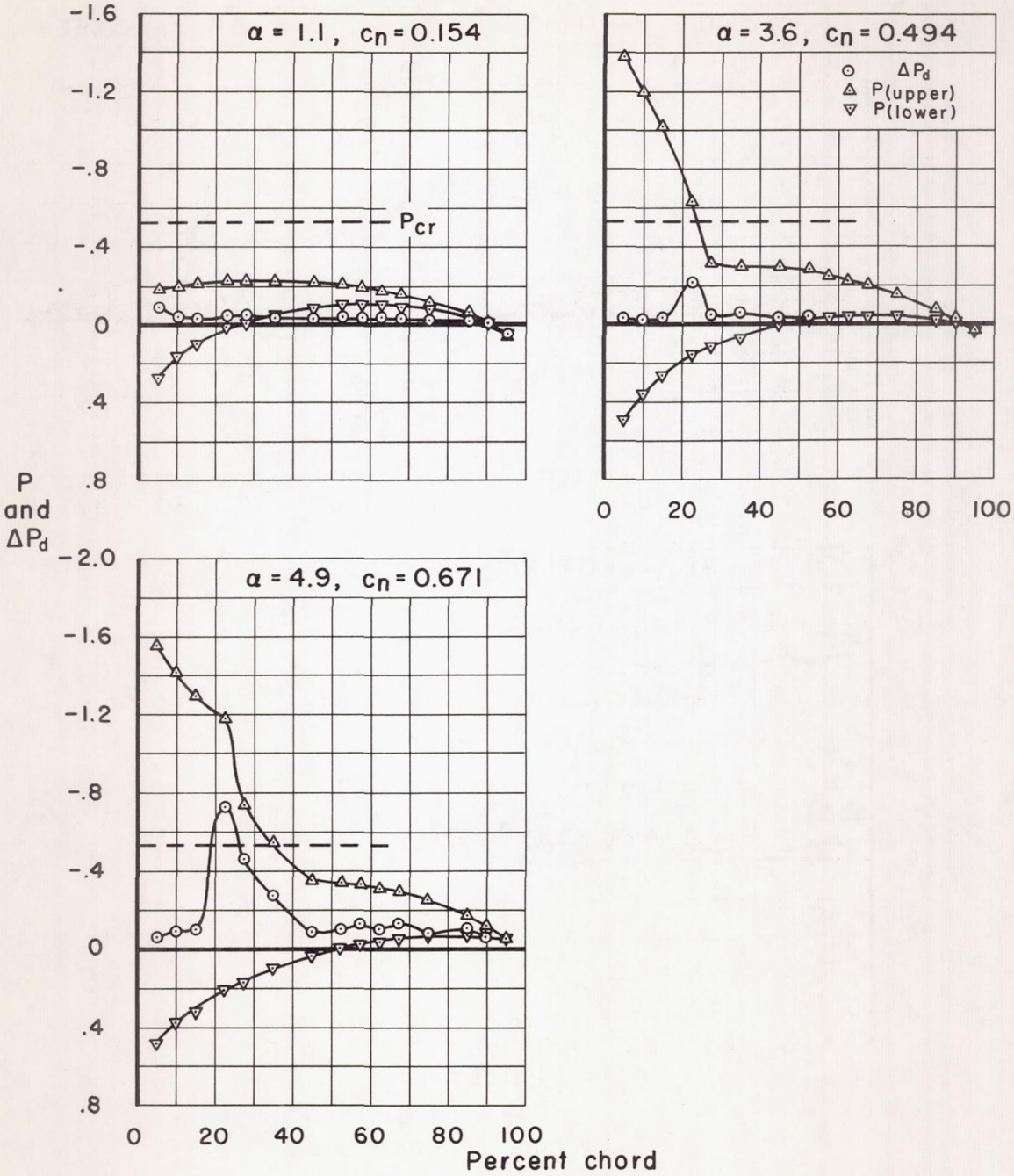

(d) M = 0.77.

Figure 11.- Continued.

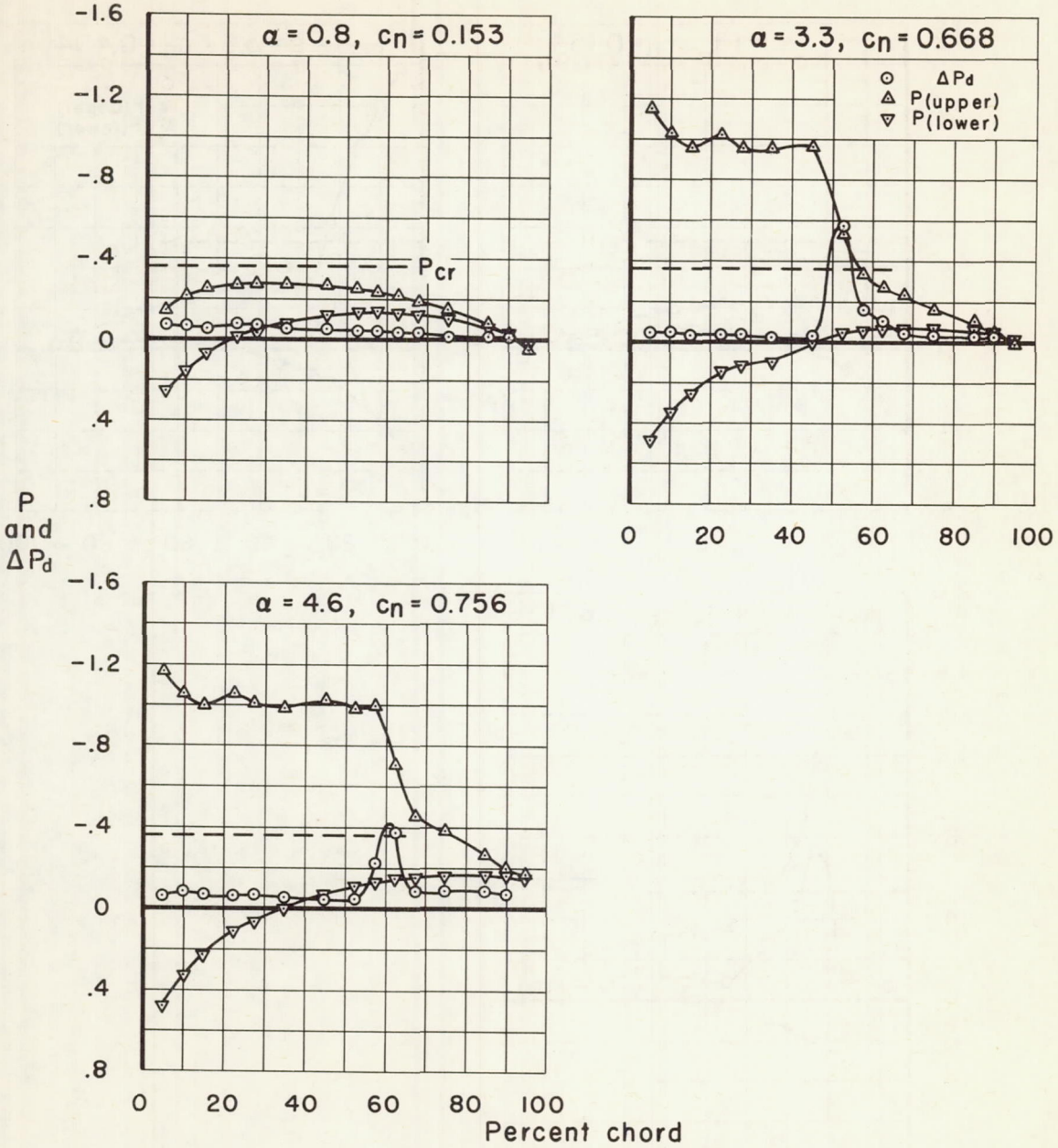

(e) M = 0.83.

Figure 11.- Continued.

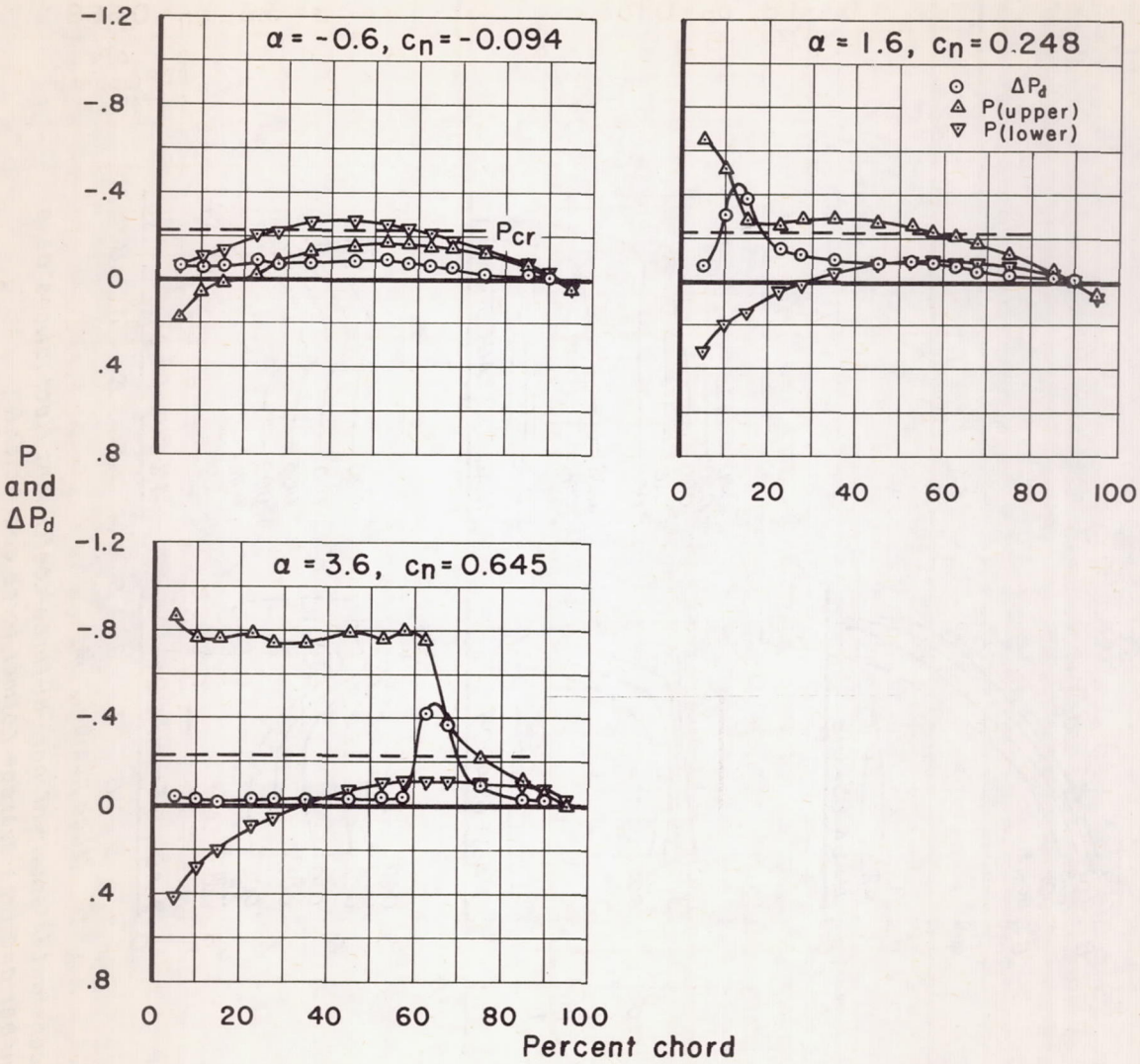

(f) M = 0.88.

Figure 11.- Concluded.

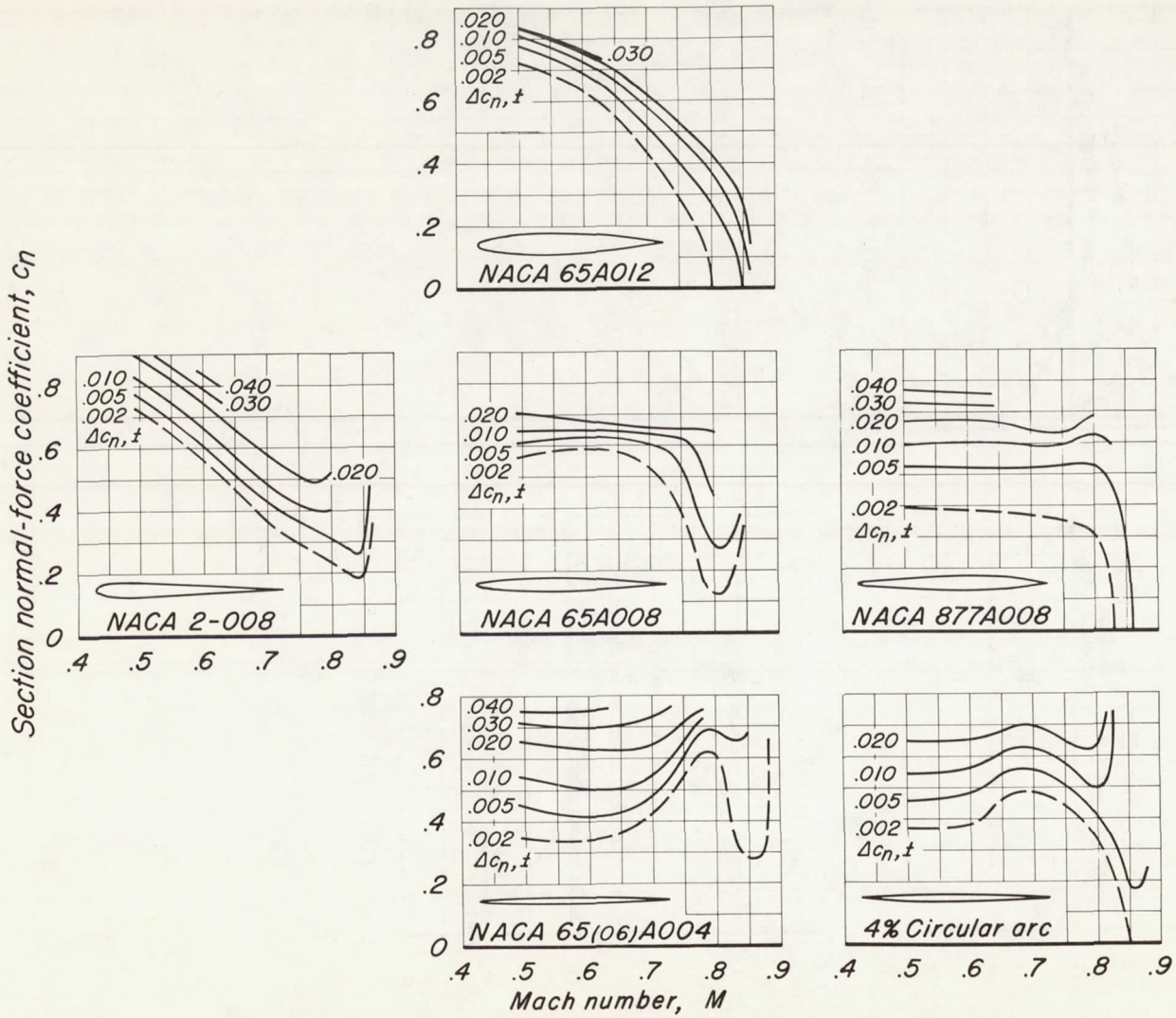

Figure 12.- Contours of constant intensity of normal-force-coefficient fluctuations as a function of Mach number and time-average normal-force coefficient.

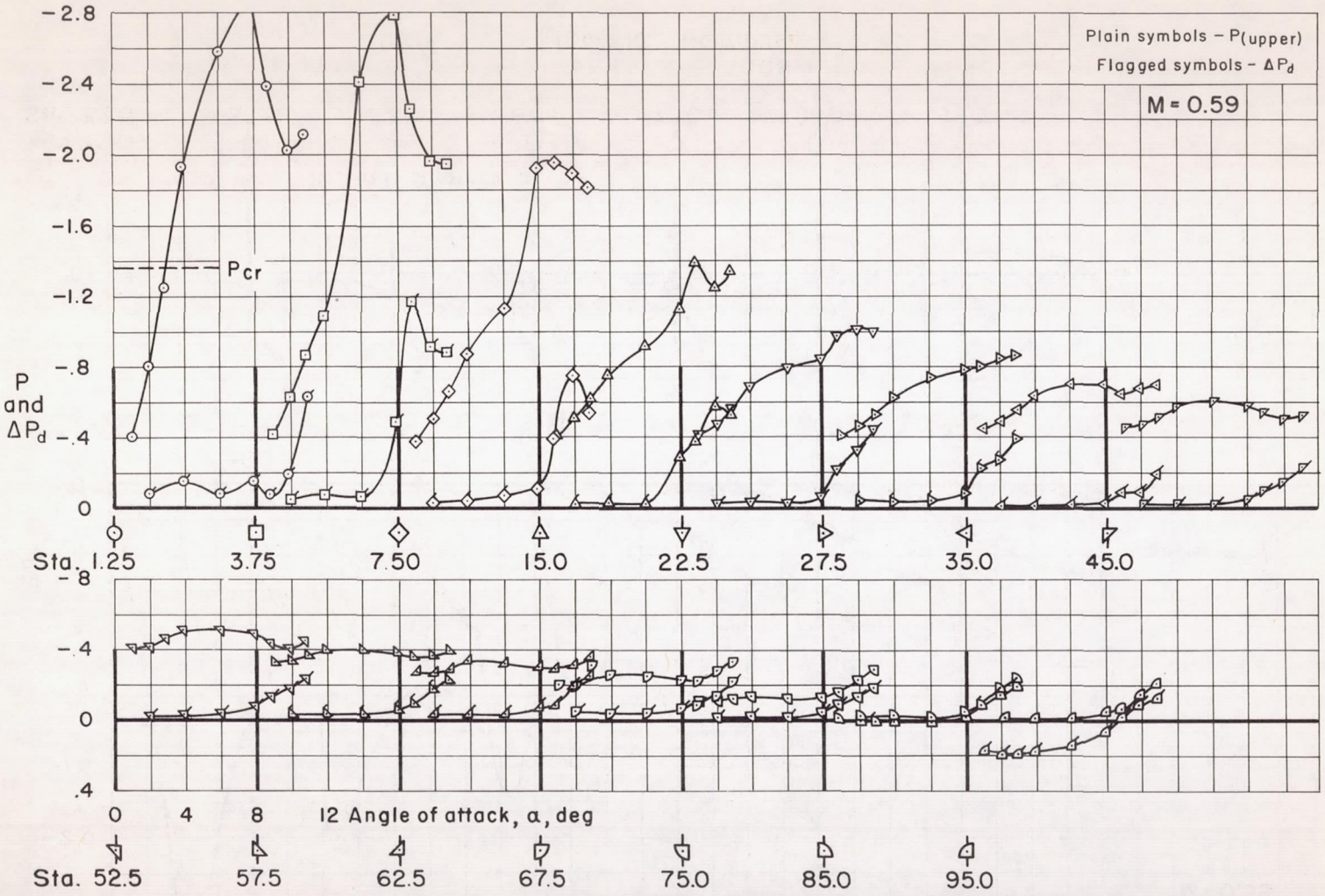

(a) NACA 65A012.

Figure 13.- Pressure fluctuations and time-average static pressures on the upper surface at each station on the airfoil as a function of angle of attack near M=0.60.

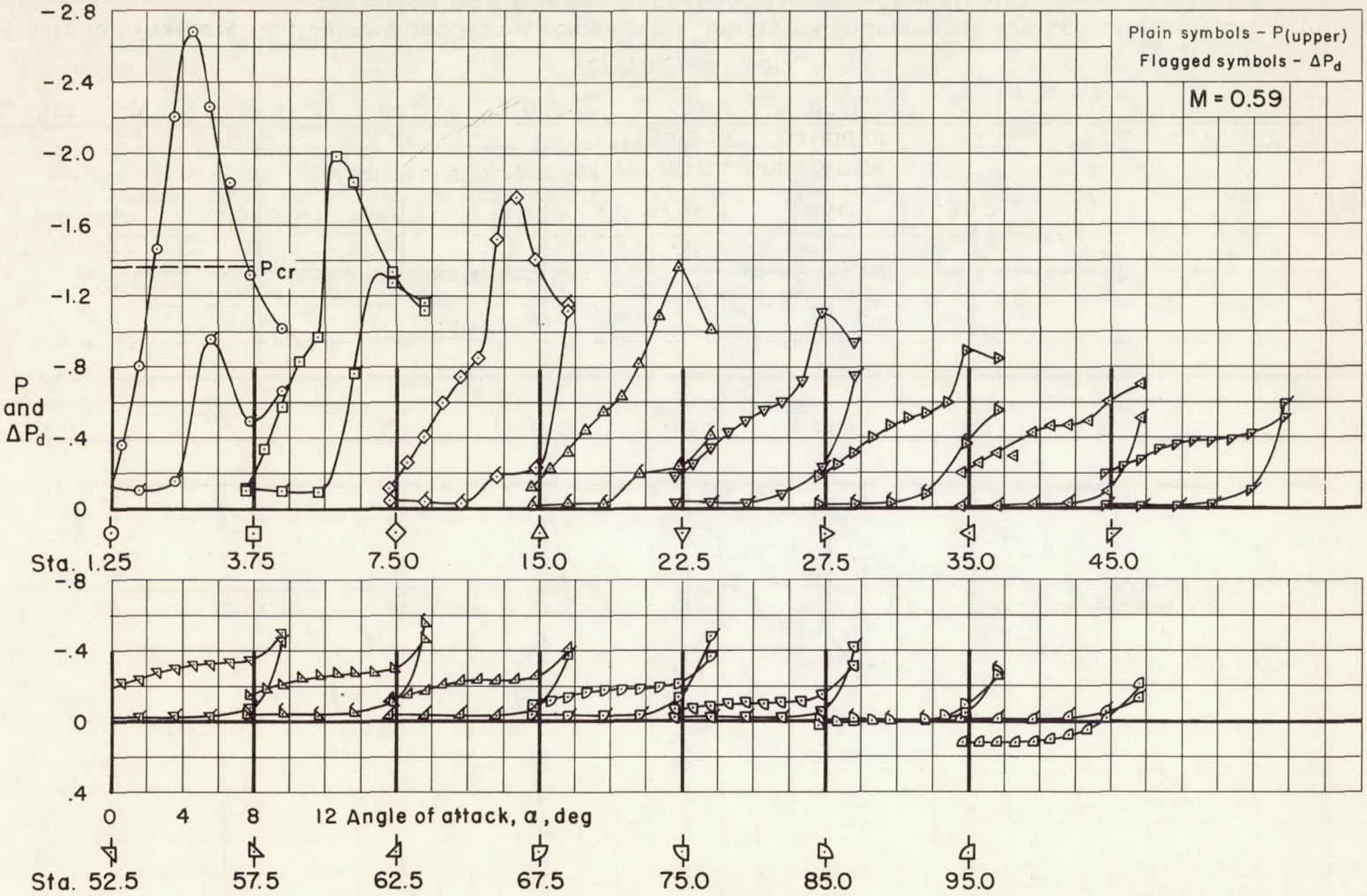

(b) NACA 65A008.
Figure 13.- Continued.

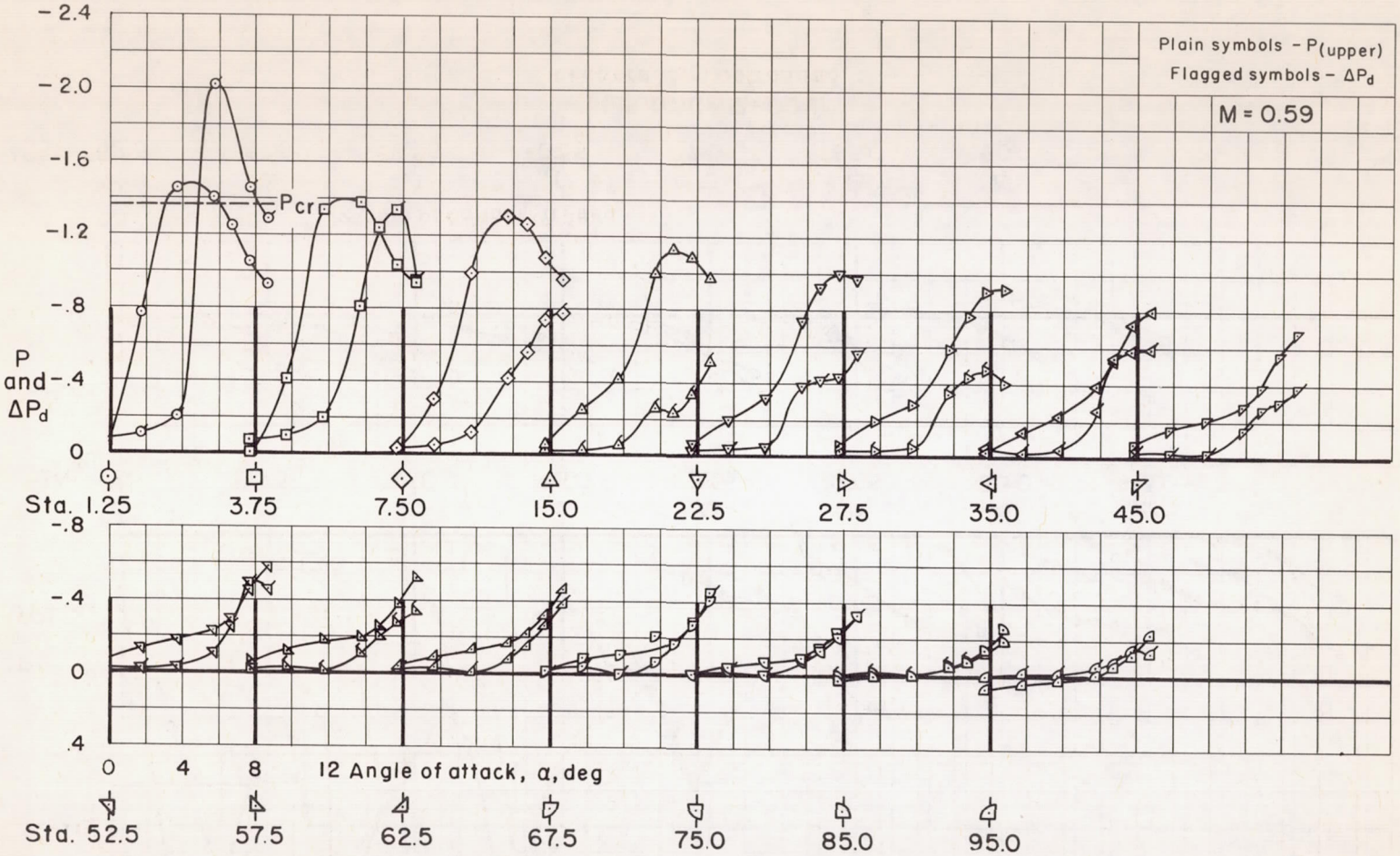

(c) NACA 65(06)A004.
Figure 13.- Continued.

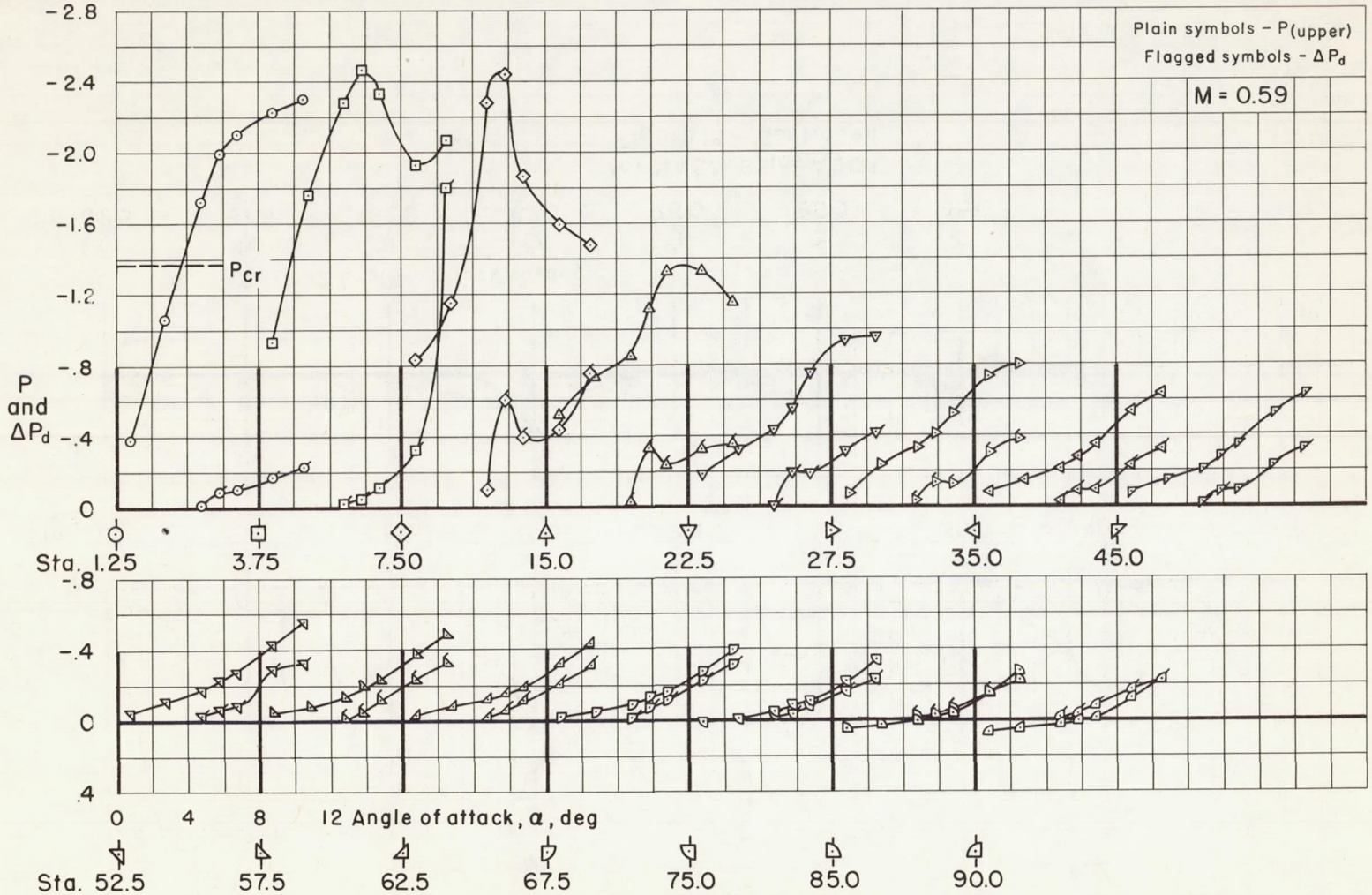

(d) NACA 2-008.
Figure 13.- Continued.

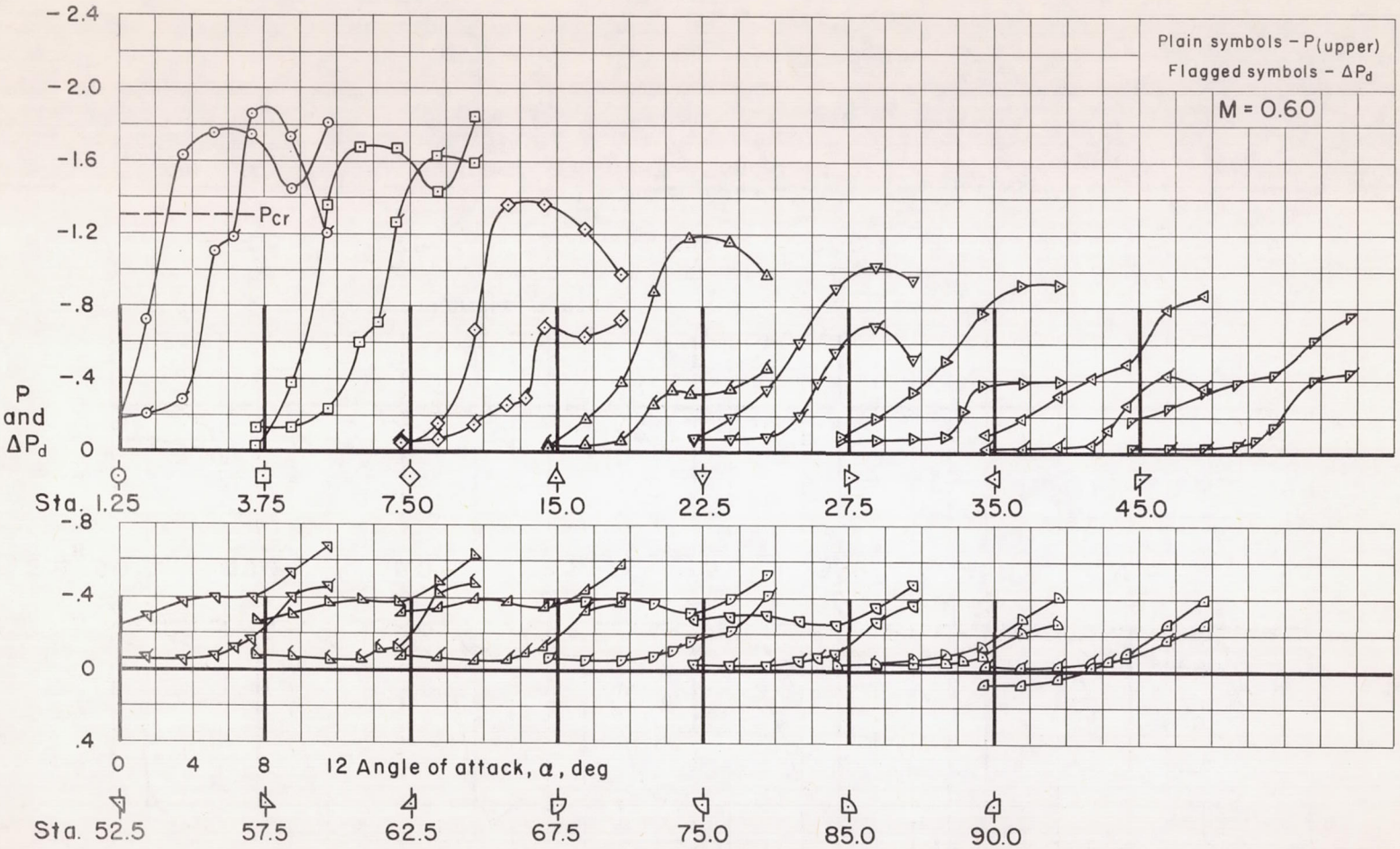

(e) NACA 877A008.
Figure 13.- Continued.

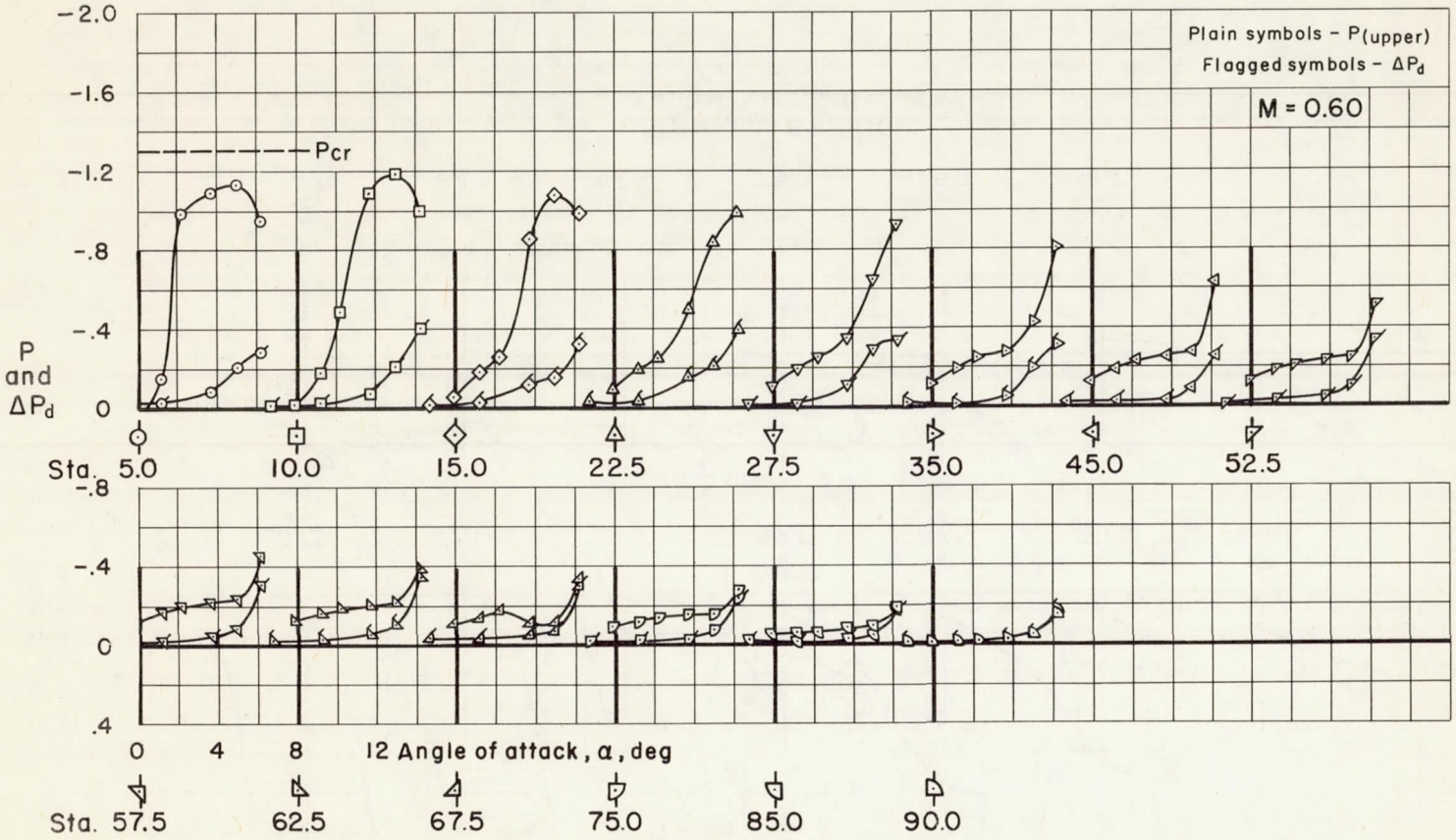

(f) 4-percent circular arc.
Figure 13.- Concluded.

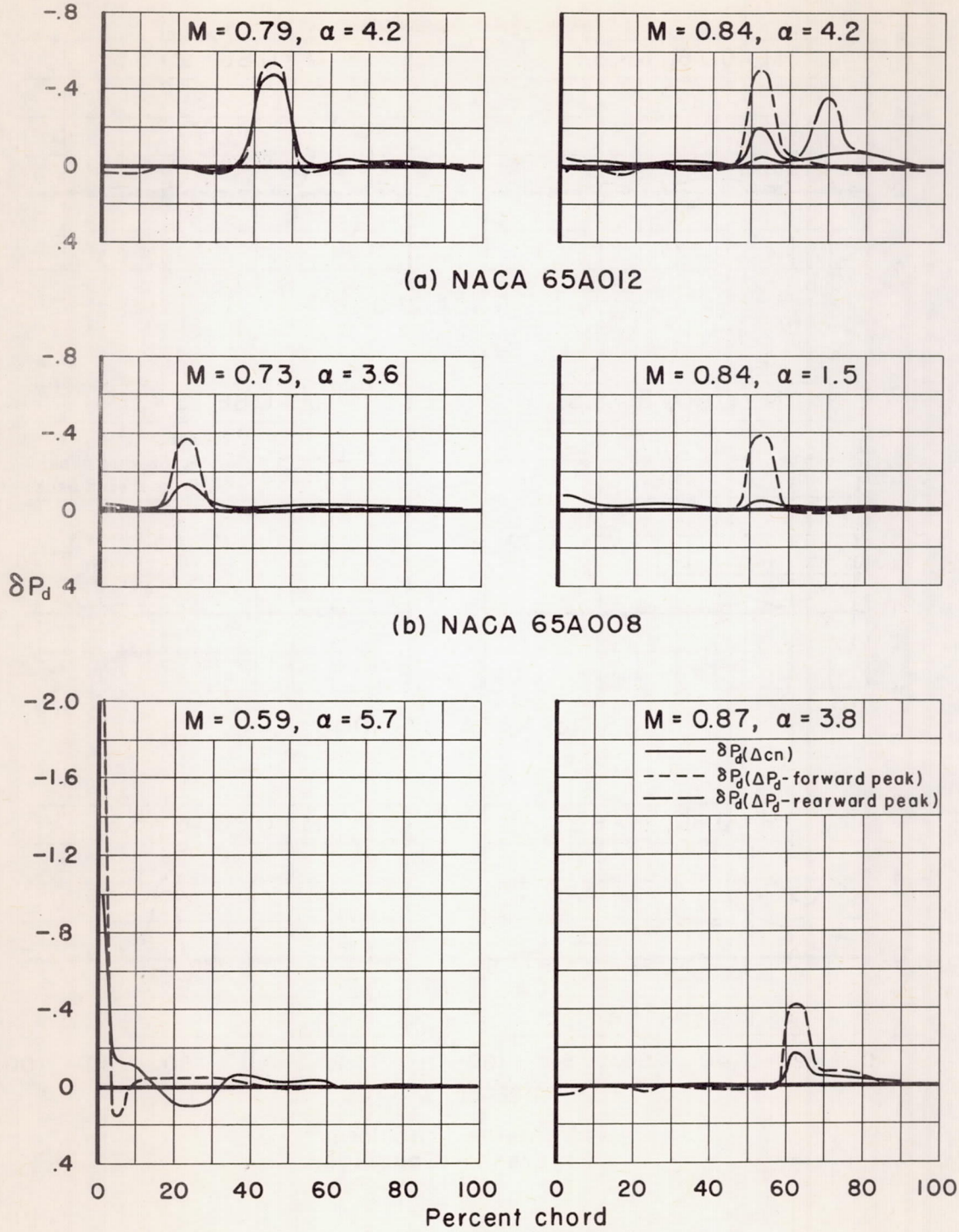

Figure 14.- Influence of peak pressure fluctuations on summed fluctuations of normal-force coefficient.

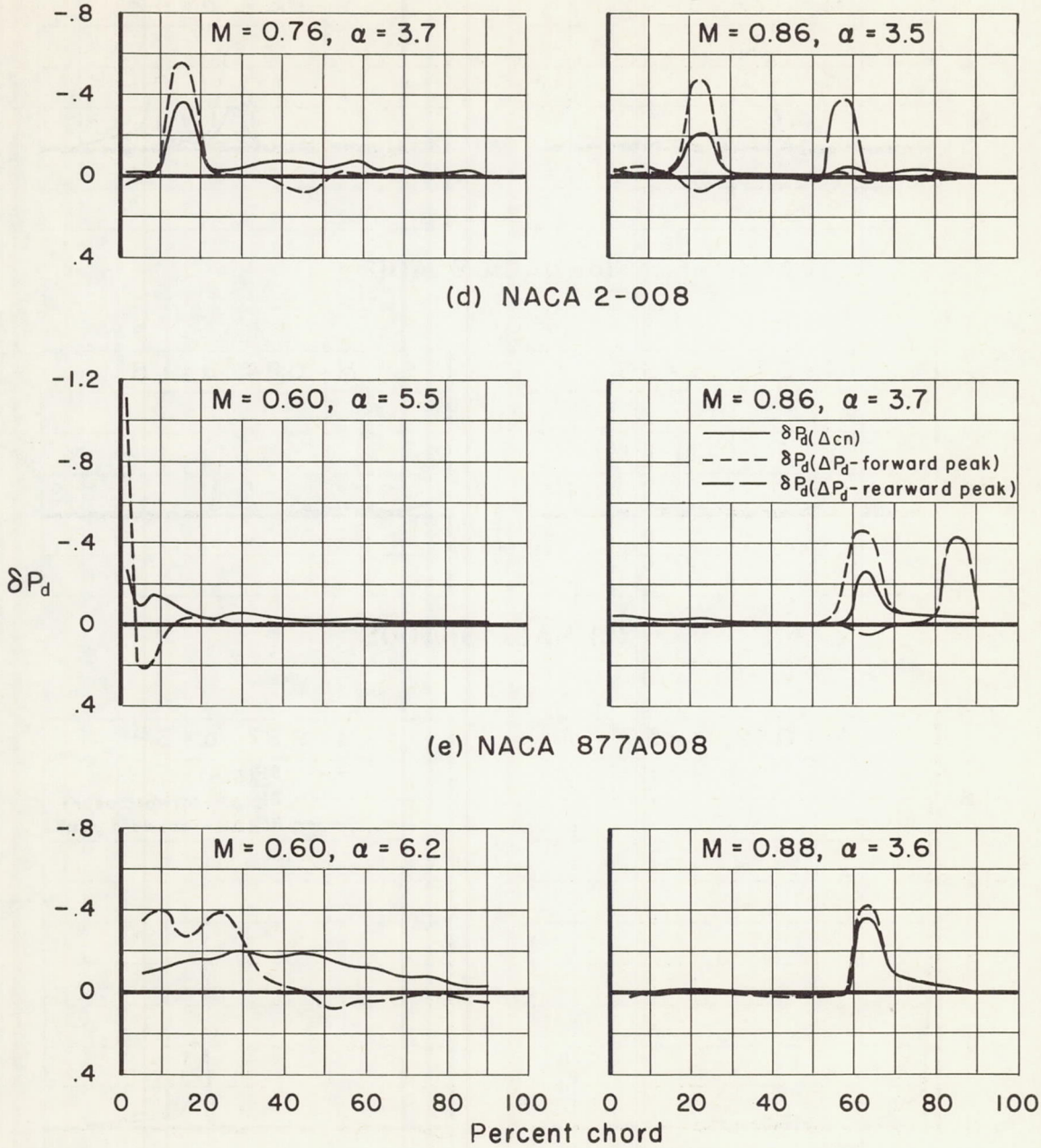

(f) 4-percent circular arc.
Figure 14.- Concluded.

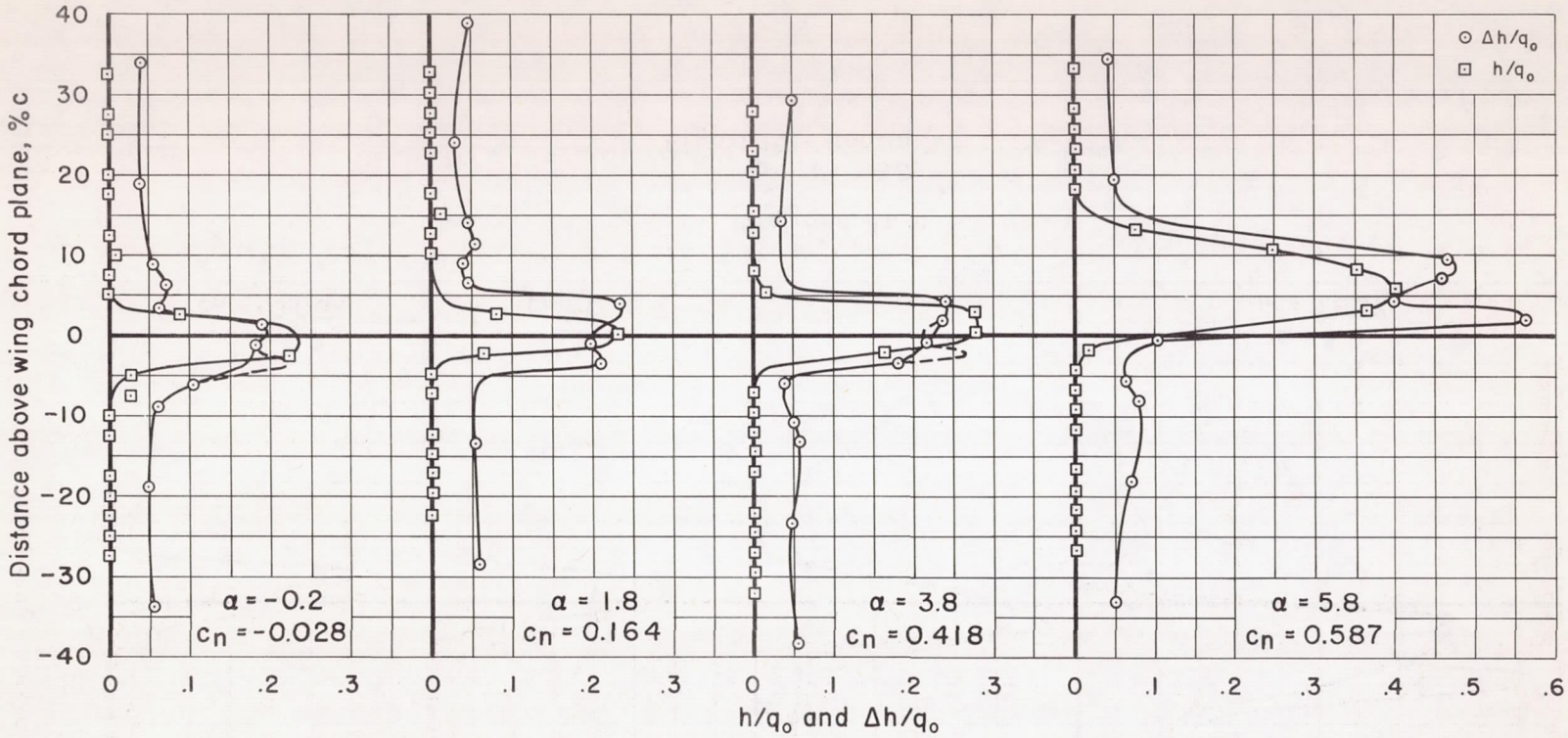

(a) M = 0.59.

Figure 15.- Fluctuations of the total-pressure and the time-average total-pressure loss in the wake of the NACA 65A008 airfoil.

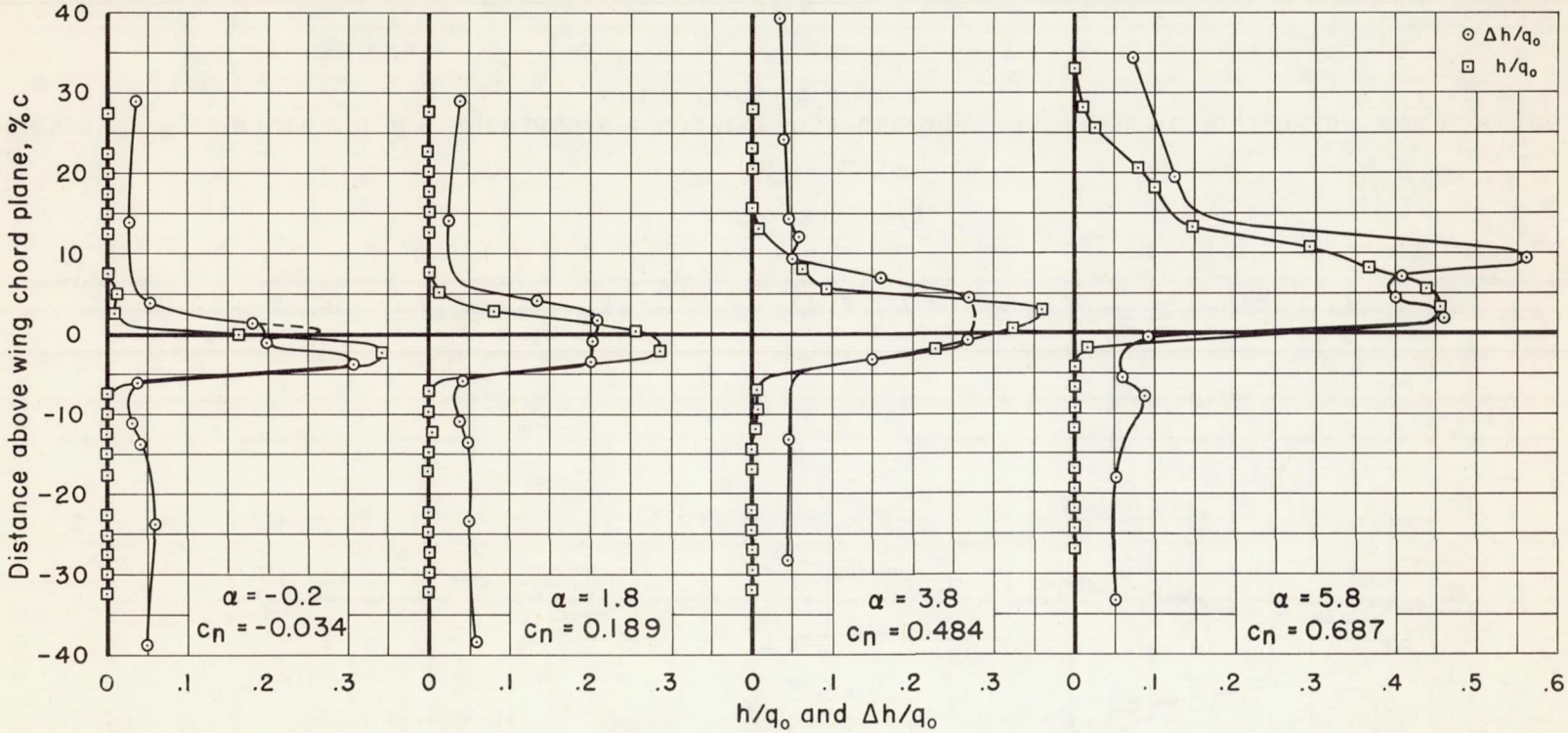

(b) M = 0.68.
Figure 15.- Continued.

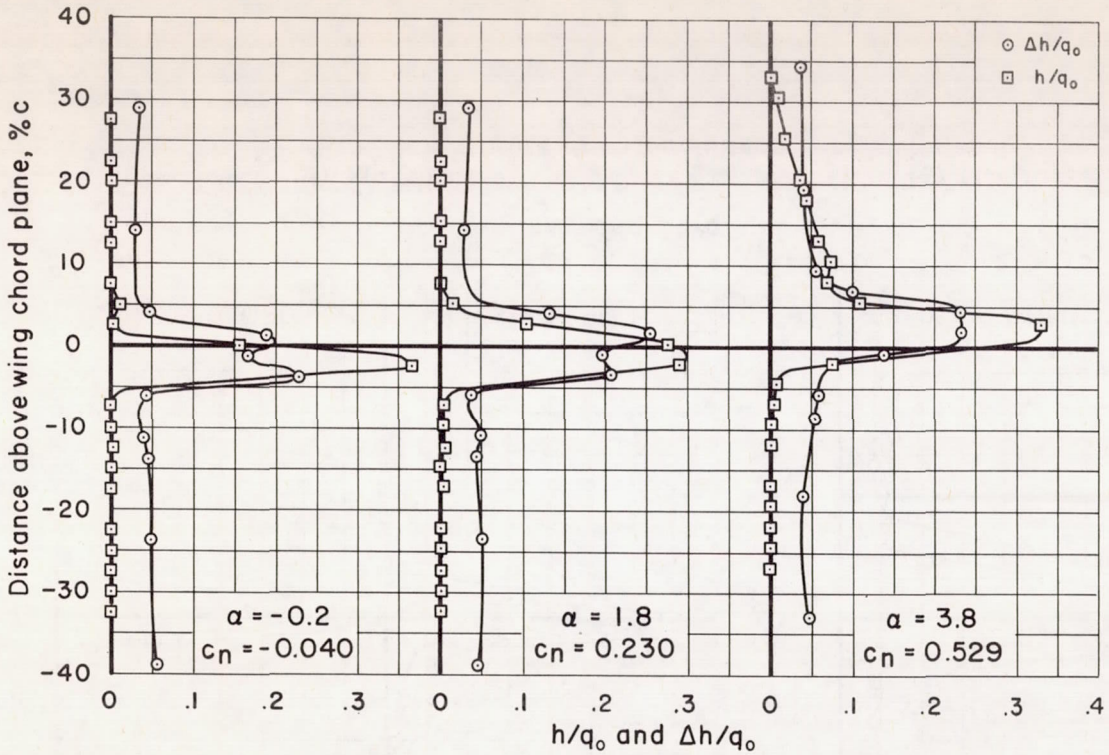

(c) M = 0.73.
Figure 15.- Continued

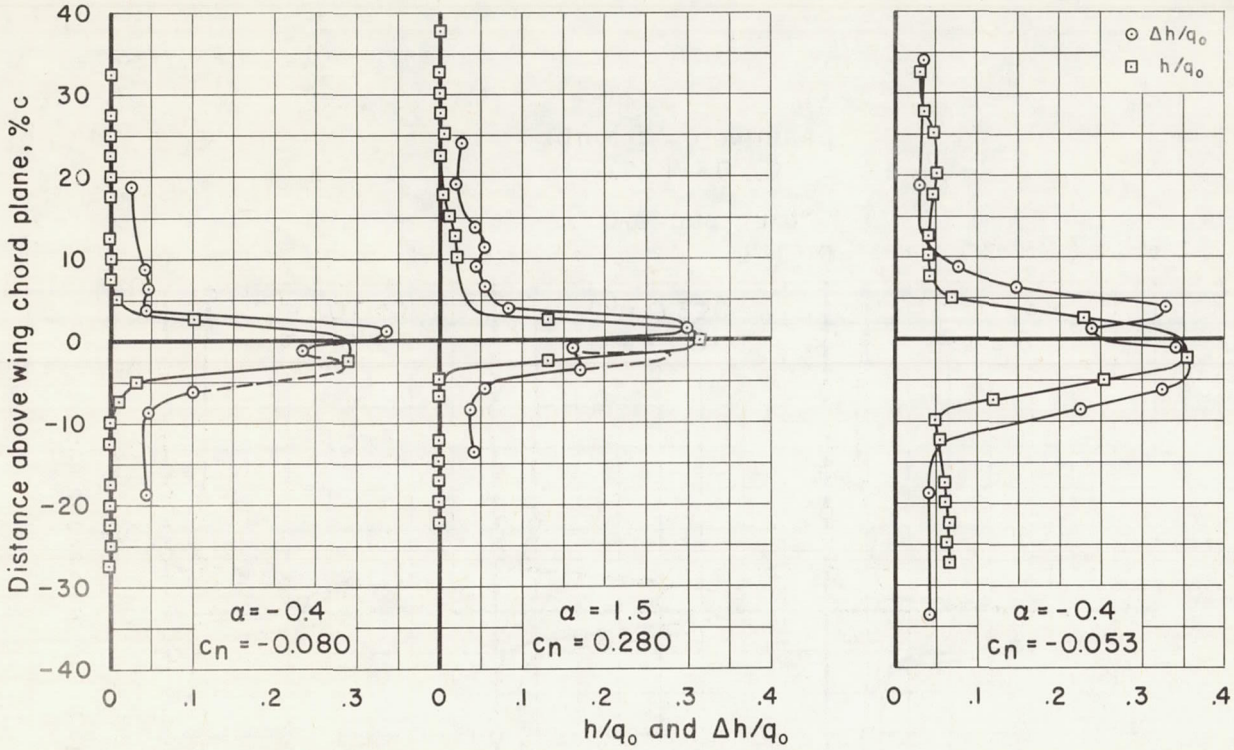

(d) M = 0.84.

(e) M = 0.88.

Figure 15.- Concluded.

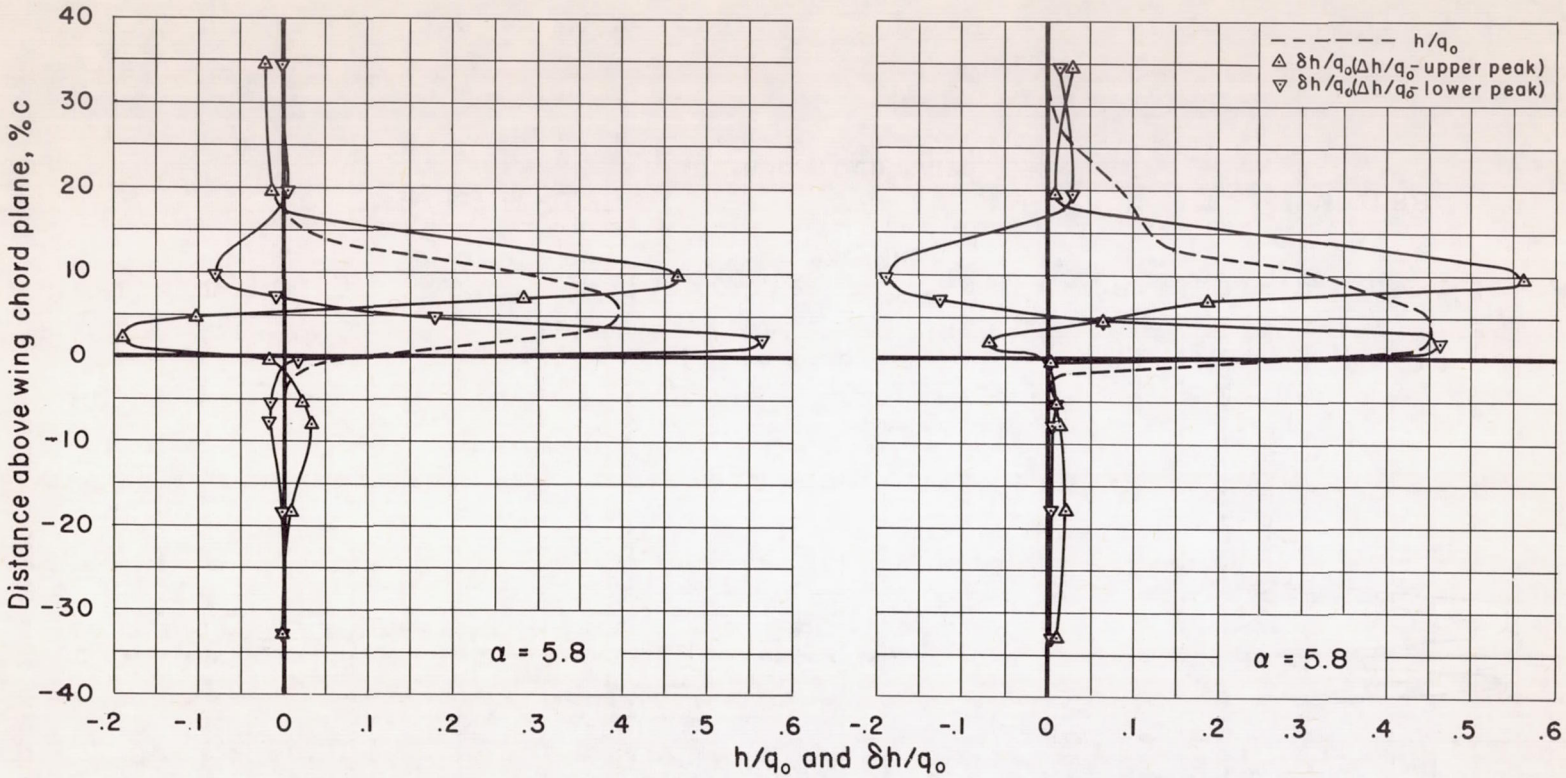

(a) M = 0.59.

(b) M = 0.68.

Figure 16.- Total-pressure differences measured in the wake of an NACA 65A008 airfoil where the total-pressure fluctuations were maximum.

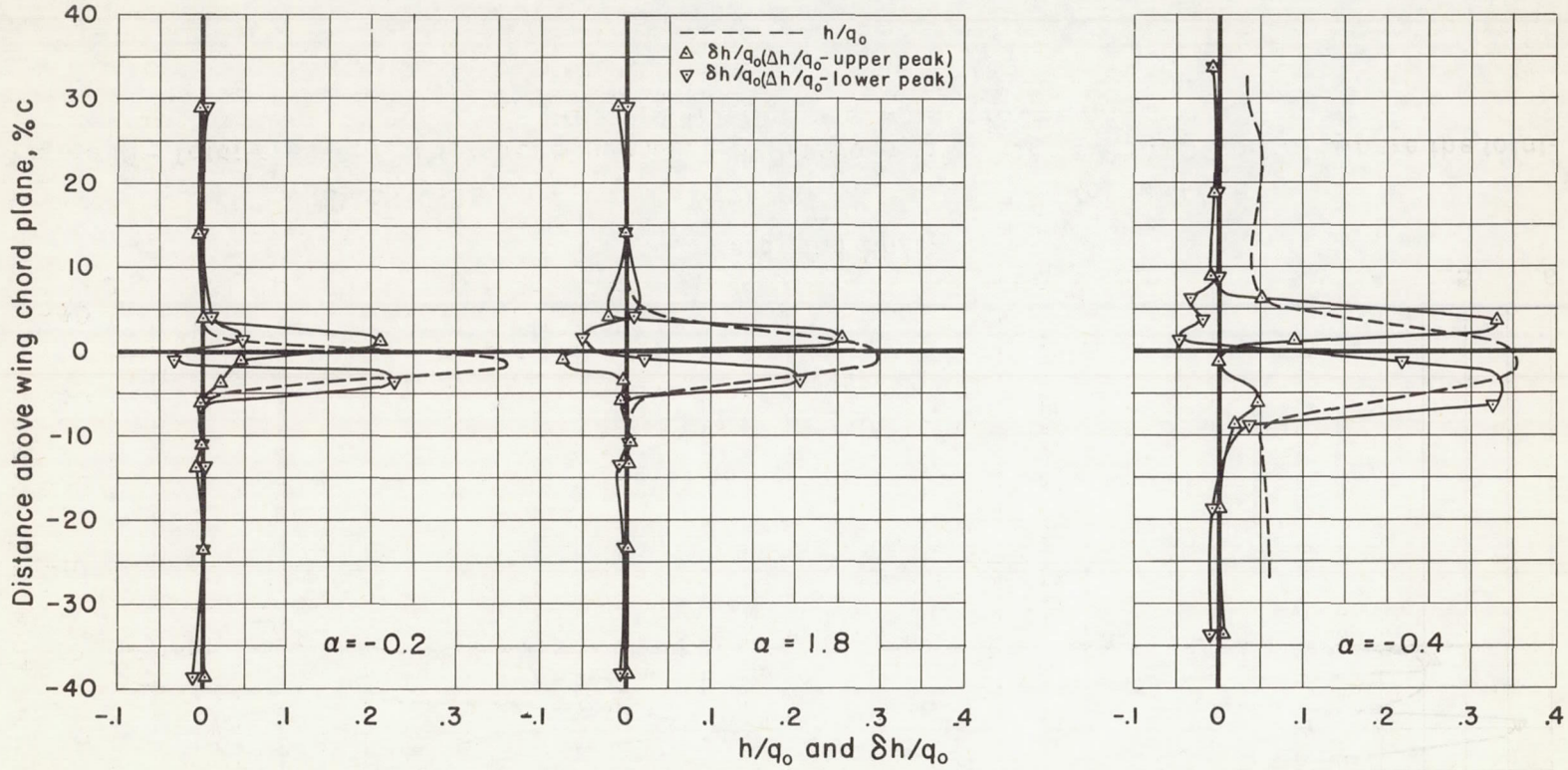

(c) M = 0.73.

(d) M = 0.88.

Figure 16.- Concluded.